НАЦІОНАЛЬНИЙ ТЕХНІЧНИЙ УНІВЕРСИТЕТ УКРАЇНИ
«КИЇВСЬКИЙ ПОЛІТЕХНІЧНИЙ ІНСТИТУТ
імені ІГОРЯ СІКОРСЬКОГО»
Факультет електроніки
Кафедра мікроелектроніки

«На правах рукопису»
УДК _____

«До захисту допущено»
Завідувач кафедри
_____ _____
(підпис) (ініціали, прізвище)
“___”_____20__ р.

Магістерська дисертація

на здобуття ступеня магістра

зі спеціальності: 153 Мікро- та наносистемна техніка

на тему: Гібридні сонячні елементи на основі кремній-полімерних структур

Виконав (-ла): студент (-ка) 2 курсу, групи __ДП-81мп
(шифр групи)

Матяш Олександр Сергійович _____ _____
(прізвище, ім’я, по батькові) (підпис)

Науковий керівник доц., к. т. н., Коваль В. М._____ _____
(посада, науковий ступінь, вчене звання, прізвище та ініціали) (підпис)

Консультант з нормоконтролю Орлов А. Т._____ _____
(підпис)

Консультант з інформаційних питань Діденко Ю. В._____ _____
(підпис)

Рецензент доц., к. т. н., Іванько К. О._____ _____
(посада, науковий ступінь, вчене звання, прізвище та ініціали) (підпис)

Засвідчую, що у цій магістерській дисертації немає запозичень з праць інших авторів без відповідних посилань. Студент _____
(підпис)

Київ – 2019 року

РЕФЕРАТ

Структура і обсяг роботи: 125 сторінок, 80 ілюстрацій, 26 таблиць, 32 джерел за переліком посилань.

Мета роботи: дослідити вплив полімерних шарів різного складу та морфології на електрофізичні параметри гібридних кремній-полімерних сонячних панелей.

Рекомендації щодо використання результатів даних досліджень: впровадження нового класу пристроїв для фотовольтаїки – гібридних сонячних панелей, відкриває шляхи для спрощення технології виробництва пристроїв, дає можливість виключити високотемпературні процеси обробки пластин, а також дає змогу повторно використовувати та переробляти відпрацьовані сонячні панелі, без додаткового збільшення вартості переробки. Органічні молекули, що досліджуються у даній роботі, мають неймовірно низьку вартість, є комерційно доступними(у формі медичних ліків), а також дозволяють проводити технологічні процеси за низьких температур(включно з кімнатною) та є розчинними у більшості стандартних органічних розчинників(а деякі – навіть у воді). Разом з перевагами, які дає використання кремнію у структурі сонячної панелі, введення цих сполук відкриває велику кількість можливостей для розробки та оптимізації нового класу сонячних панелей.

Ключові слова: гібридні сонячні панелі, кремній, клонідин, сульфацил, HOMO, LUMO, fill factor, коефіцієнт корисної дії.

ABSTRACT

Structure and scope of the work: 125 pages, 80 illustrations, 26 tables, 32 sources under the list of references.

Purpose: to study the influence of the polymer layers of different morphologies and compositions on the electrophysical parameters of silicon-polymer hybrid solar cells.

Recommendations on the use of the results of research data: introduction of a new class of photovoltaic devices – hybrid solar cells, allows to simplify manufacturing process, reuse and recycle broken solar cells without additional cost to the recycling process, get rid of the expensive technological steps in solar cell devices processing. The studied organic molecules are extremely affordable, commercially available(in the form of medical drugs), low-temperature processable and soluble in common organic solvents, some – even in water. This, together with advantages of silicon as photovoltaic material, enables a plethora of opportunities for solar cell devices design and optimization.

Keywords: hybrid solar cells, silicon, clonidine, sulfacetamide, HOMO, LUMO, fill factor, power conversion efficiency.

CONTENTS

ABBREVIATIONS

B – Boron

P – Phosphorus

As – Arsenic

GaAs – Gallium Arsenide

JFET –Junction Field Effect Transistor

I-V characteristics – current-voltage characteristics

EQE – External Quantum Efficiency

FF –Fill Factor

PCE – Power Conversion Efficiency

SRH recombination – Shockley-Read-Hall recombination

AM1.5 – Air Mass 1.5

SQ-limit – Shockley-Quiesser limit

KOH – Potassium Hydrochloride

H2O – water

CVD – Chemical Vapor Deposition

ARC – Anti-Reflective Coating

HOMO – Highest Occupied Molecular Orbital

LUMO – Lowes Unoccupied Molecular Orbital

BHJ – Bulk Heterojunction

HSC – Hybrid Solar Cell

E(H)TL – Electron(Hole) Transport Layer

ITO – Indium Tin Oxide

Al – Aluminum

NaOH – Sodium Hydrochloride

HF – Hydrofluoric acid

HNO3 – Nitric acid

Si – Silicon

CLO – Clonidine

SULF – Sulfacetamide

J-V – current density-voltage characteristics

ADC – Analog-to-Digital Converter

OM – Optical Microscopy

SEM – Scanning Electron Microscopy

rpm – rounds per minute

UV – Ultraviolet

Vis – visible

NIR – Near Infrared

Br – Bromine

INTRODUCTION

Solar energy is one of the major sources of alternative, so-called green energy nowadays. The classical technology manufactures solar cells of crystalline silicon, as its absorption spectrum matches with the visible range of sunlight, present in Earth's atmosphere, thus, one can expect relatively high efficiencies of the devices, and as its manufacturing technology is optimized to obtain maximum performance. However, silicon solar cells are very close to achieving their maximum, so one needs to look for alternatives. There are several drawbacks, characteristic to silicon: life cycle is relatively low (around 30 years), recycling technology is either absent or not affordable terms of cost, relatively complicate processability, because requires high temperatures.

So, one needs to look for the alternatives. And one of the best is, definitely, switch to hybrid solar cells. Being carefully designed, these devices can overcome all the struggles, which silicon experiences. The replacement of one active layer by organic films cancels the necessity of high-temperature equipment utilization and wafer processing. The solubility in common organic solvents makes recycling easy and affordable. The las, but not the least – there are plenty of organic materials around, so one can choose the best performing among it, or improve the material, which is in use by playing with the side chains of the molecule.

Thus, the *purpose* of this work is: to study the influence of the polymer layers of different morphologies and compositions on the photovoltaic parameters of silicon-polymer hybrid solar cells.

Based on this, the following tasks were formulated:

1. Manufacture silicon-polymer structures and make hybrid solar cells on their base.
2. Measure the photovoltaic parameters of the fabricated devices.
3. Make the conclusions about the influence of the composition and morphology of the polymer films on devices' performance.

1. SEMICONDUCTOR PROPERTIES OF MATERIALS

1.1. Energy band structure

According to their electrical properties, all the materials can be classified into three categories: conductors, semiconductors and insulators [1]. This can be clearly seen from the energetic spectrum of material atoms, which is represented by the set of allowed and forbidden energy levels. Together, these levels form energy bands, which determine the properties of material.

These levels and bands appear because the energy of electrons in the material is quantized, according to Bohr's theory [2]. This means that electrons within the material can have only certain energies, thus to be in a certain energy band. One distinguishes three different bands: the valence band, the bandgap and the conduction band. According to the relative displacement of these bands, the material can be considered as one of the types mentioned above (fig. 1.1)[1].

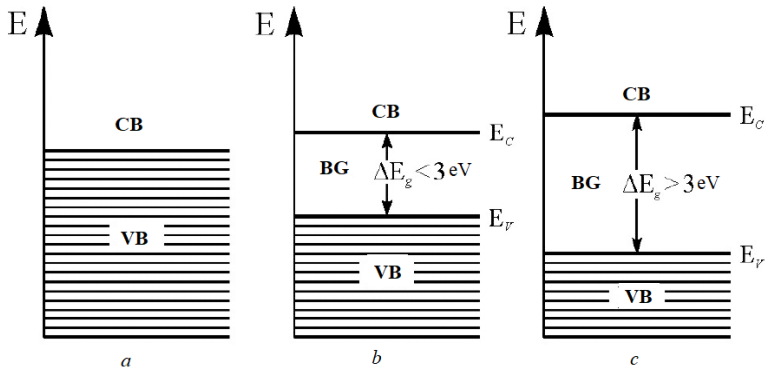

Figure 1.1 – Energy band structure: a) metal; b) semiconductor; c) insulator material [1]

In metals, electrons are not tied to lattice atoms, and the material's structure is composed by the lattice of atoms and an electronic cloud, freely floating within the lattice. This simple model denotes key metal's property – conduction of electrical current. This can also be seen from the energy band structure of the metal (fig.1, a): the valence band overlaps the conduction one, which means that the electrons can freely move to the higher energy levels without gaining the big amount of extra energy.

The valence band corresponds to the set of energies, having which electron will be tied to the atom and won't take part in electrical current conduction. The conduction band, in turn, corresponds to the energy of electrons, which are part of electrical current.

Both semiconductor and insulator materials have a third band in their energy structure. This one is called the bandgap and includes energy levels, occupying which by electrons is forbidden. Presence of the bandgap changes material's properties dramatically, creating unique effects, like polarization of insulators.

By analyzing the band diagram, one can distinguish semiconductor materials from the insulators by looking at the value of the bandgap. It is known, that materials with the bandgap lower than 3 eV have semiconductor properties when the ones with the bandgap higher than 3 eV will behave as insulators [1].

Presence of the bandgap gives an insight into the key property of semiconductor material – to conduct electrical current only when sufficient energy is applied to the device. In this situation, electrons from the valence band can gain energy to overcome the bandgap(if the applied energy is higher than bandgap's value) and appear at the conduction band, which means that they're now contributing to electrical current. The energy required for the transition electrons can gain either from the outside of the material or from the thermal fluctuations within the material (phonon vibrations of atoms).

So, to conclude, all the materials can be divided into 3 groups according to their electrical properties, which is suitable to illustrate by the energy band diagrams. Semiconductor materials have 3 bands in their structure: the valence band, the conduction band and the bandgap. Normally, the valence band is populated by the electrons, and the additional energy needs to be applied to transfer them from the valence to the conduction band. Appearing in the conduction band, electron contributes to the electric current.

1.2 Electric current in semiconductors

Let's imagine that electron from the valence band gained sufficient energy for the transition to the conduction band. Then the level in valence band from which the

electron has left appears to be unoccupied and can be taken by another electron from the valence band. This process will be repeated for this electron's energy level etc. Thus, transferring one electron from the valence band to the conduction one enables the process of the electron movement within the valence band.

However, it is not suitable to analyze the transitions of each electron of the valence band. Thus, a concept of the hole was introduced. The vacant place that electron creates by leaving the valence band is considered as a quasi-particle with a positive charge and the non-zero effective mass. This particle is called "the hole". Then a process of multiple transitions of electrons within the valence band can be modeled as a movement of the hole deeper to the band. This concept is illustrated by fig. 1.2.

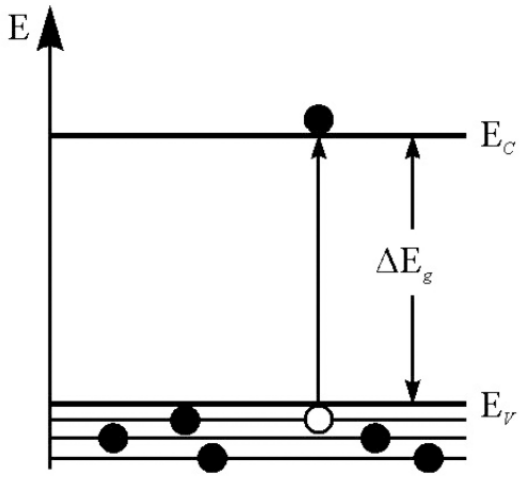

Figure 1.2 – A creation of the hole by the transfer of the electron to the conduction band [1]

The creation of free electron-hole pairs is called *generation* of charge carriers. At some point, the electron in the conduction band will lose its energy and will be transferred back to the valence band. Then the hole, which was occupying the corresponding level, will also disappear. This is called *recombination* of charge carriers. The processes of generation and recombination are key processes for the solar cells, as will be shown later.

Thus, the electric current in semiconductors is caused by the movement of two types of charge carriers: the electron in the conduction band and the hole in the valence band.

1.3 Intrinsic and doped semiconductors

The process, described above, illustrates the behavior of the pure semiconductor material. By pure one means that there are no other atoms instead of the semiconductor material's ones within its structure. For example, this means that silicon sample is composed only of Silicon and doesn't contain any other atoms (in a perfect case). This kind of material is then called *intrinsic* material, and the charge carriers generated are *intrinsic* charge carriers. Those are mostly activated thermally. Thus electron gains the energy needed to overcome the bandgap from the lattice thermal vibrations, and in this case, charge carriers are generated in pairs (electron-hole). Thus, for the intrinsic material:

$$n_i = p_i, \tag{1.1}$$

where n_i, p_i – intrinsic electrons and holes concentration respectively, cm^{-3}.

However, intrinsic semiconductors normally demonstrate poor electrical properties in terms of conduction of electrical current, thus one generally deals with the doped semiconductors. Doping means inserting the atoms of different chemical group than semiconductor's one into the material in order to enhance its electrical properties. For Silicon, the major dopants are Phosphorus and Boron.

Inserting those dopants creates additional unbonded charges within the semiconductor material, thus creates additional charge generation events, which results in a higher contribution of the charge carriers of the particular type into the electric current.

Let's consider an example of doping Silicon with Boron. Silicon is an element of the IV group of the periodic system, which means that it has 4 valent electrons on its outer orbital. By doping the material, one replaces a part of Silicon atoms in the lattice with the dopant atoms. Boron is the element of the III group, which means it has only 3 valent electrons. Bonding Boron atom to Silicon one leads to appearing of one unpaired valent bond. In case of the thermal excitation, one of the electrons of the bonded state can be transferred to the unpaired bond, and Boron will become a negative ion. In the

bond, from which electron has left, a vacancy will appear, which is equivalent to the appearance of the hole. Thus, an additional charge carrier is created by inserting a dopant atom to the system. From the energy band diagram standpoint, this will lead to the appearance of an extra energy level in the bandgap, close to the highest occupied level of the valence band. This level will contain the hole created by the dopant atom. Thus it could accept the electron from the valence band (fig. 1.3). That's why this type of dopant is called the *acceptor* dopant.

The same can be said for doping Silicon with Phosphorus. The addition of the atom of the V group leads to the appearance of the additional unbonded electron, thus to the creation of the energy level within the bandgap, close to the lowest unoccupied level of the conduction band. This level will contain the electron, which can be easily transferred to the conduction band by, for instance, thermal excitation. That's why this type of dopant is called the *donor* dopant.

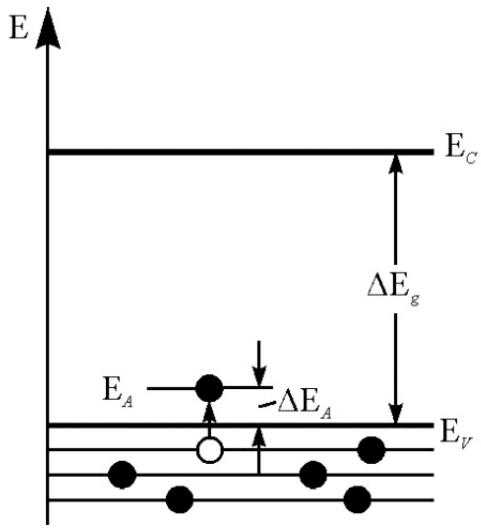

Figure 1.3 – The acceptor energy level can accept an electron from the valence band [1]

It is remarkable that by doping the semiconductor, one increases the number of the charge carriers of particular sign (either electrons or holes), without increasing the concentration of the carriers of the opposite sign. At a certain level of doping, when the concentration of one of the charge carriers is much larger than the intrinsic concentration of another one, the electric properties of the material are mainly

determined by the carriers with larger concentration. Then one will call this semiconductor either

n-type (if the concentration of electrons is much greater than of holes) or *p-type* (if the concentration of holes is much greater than one of the electrons).

To summarize, doping the semiconductor leads to the creation of extra charge carriers. This results in the appearance of the additional energy levels within the bandgap. Semiconductors of IV group are normally doped with atoms of III and V groups. The most general dopants are B, P and As.

1.4 Generation and recombination of charge carriers in semiconductors

In the semiconductor material, under thermal equilibrium, charge carrier concentrations are related to each other with the mass-action law, which shows that the product of electrons and holes equals the square of the intrinsic concentration (eq.1.2). This shows, that, for instance, if the concentration of electrons will increase, this will decrease the concentration of holes, because the probability of hole to recombine with the electron becomes higher.

$$np = {n_i}^2, \tag{1.2}$$

where n , p – electrons and holes concentration respectively, cm^{-3};

n_i – intrinsic electrons concentration, cm^{-3}.

The cases when the situation differs from this relation correspond to the appearance of the processes, which are trying to return the system to equilibrium[3].

The process which takes place is either generation (eq. 1.3) or recombination (eq. 1.4):

$$np < {n_i}^2, \tag{1.3}$$

$$np > {n_i}^2, \tag{1.4}$$

Recombination processes in inorganic semiconductor can be divided into four types:

1. Direct recombination – mainly occurs in direct bandgap semiconductors [4], like GaAs. In this case, recombination rate will be proportional to the concentration of

electrons in the conduction band and to the concentration of holes in the valence band, available for recombination.

2. Shockley-Read-Hall recombination – the recombination through a trap state, which means that recombination occurs, when the electron and the hole are absorbed by the trap state, where they recombine with each other.
3. Auger recombination – or three-particle recombination, which is mainly observed for indirect bandgap materials [4]. In this case, the excess energy and momentum of the particles, which recombine, is transferred to the third particle, either electron or hole.
4. Surface recombination – recombination on the trap states, created by unbonded surface states, by the impurities, etc.

We will discuss recombination processes for solar cells in detail later.

Generation rate is related to the recombination one through:

$$R = \frac{G}{n_i^2}, \tag{1.5}$$

In thermal equilibrium:

$$R = G, \tag{1.6}$$

where R – recombination rate;

G – generation rate;

n_i – intrinsic electrons concentration, cm^{-3}.

Generation and recombination processes determine the charge carrier's lifetime, which is an effective measure of how fast the carriers need to be extracted from the solar cell, for them to contribute to the generated current. This will also be discussed later on.

To conclude, under the thermal equilibrium, the charge carrier's concentrations are determined by mass-action law. In this case, generation of carriers equals recombination. There are different processes of recombination involved depending on the material's properties. The situation, when there is an excess concentration of carriers, will lead to recombination to occur. If the deviation from mass-action law to

the opposite side occurs (eq. 1.3), then the generation process will be involved, in order to return the system to the equilibrium.

1.5 Mobility and drift of charge carriers

Mobility is the measure of how fast charge carriers propagate through the medium under the electric field applied. Speaking about math, it's the proportionality constant between drift velocity, which is the actual speed of a charge carrier moving under the electric field, and the value of this field [3]:

$$\boldsymbol{v_{dr}} = \mu \boldsymbol{E}, \tag{1.7}$$

where $\boldsymbol{v_{dr}}$ – drift velocity, $\frac{cm}{s}$;

μ – mobility, $\frac{cm^2}{V \cdot s}$;

$\boldsymbol{E}$ – electric field, $\frac{V}{cm}$.

Achieving high values of mobility in the solar cells is crucial since the carriers with higher mobility have a higher probability of being extracted before they recombine, thus they contribute to the generated electrical power.

Mobility of charge carriers strongly depends on the carrier concentration (fig. 1.4) and on temperature (fig. 1.5). The first dependency is explained by the fact that in the materials with higher charge carriers concentration, there are more scattering events than in ones with the lower concentration. This is due to the higher probability of particle-particle interaction due to the larger number of particles. With the increase of the temperature, mobility first goes up due to the extra thermal energy, gained by charge carriers, but after a certain value goes down, due to the bigger influence of electron-phonon scattering.

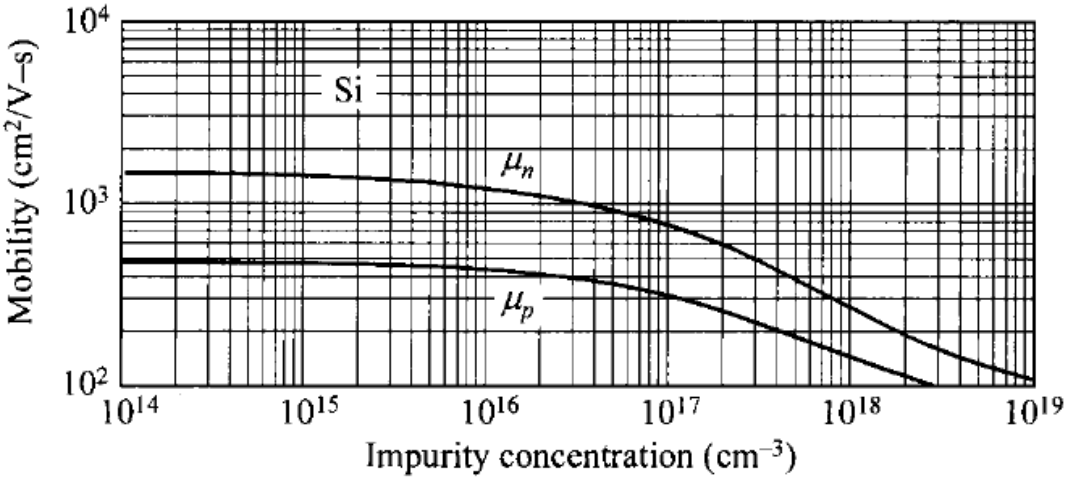

Figure 1.4 – Mobility dependence on impurity concentration [3]

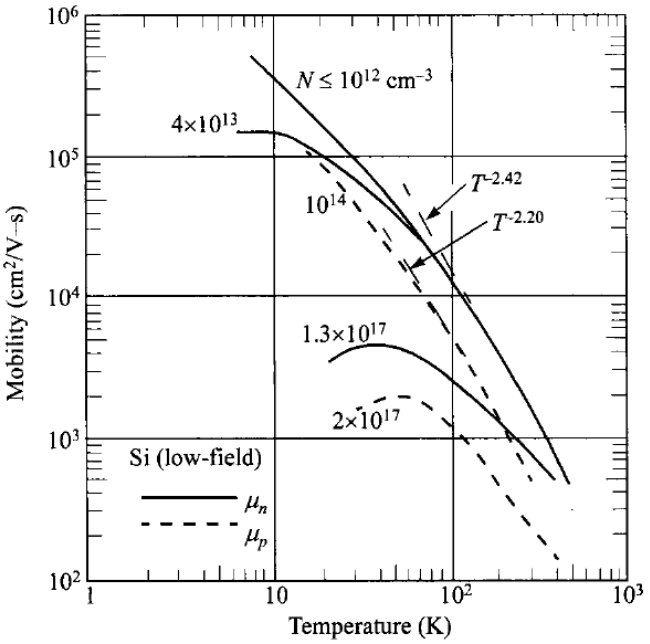

Figure 1.5 – Mobility dependence on the temperature for different impurity concentration [3]

Mobility also determines the key parameter, which characterizes the ability of the semiconductor to conduct electrical current – the conductivity.

In inorganic crystalline semiconductors, conductivity is derived as the product of the charge carrier mobility, the concentration of the carriers, multiplied by the elementary charge q.

In a doped semiconductor, conductivity is mostly derived by the impurity inserted during the doping process. However, in general case, conductivity depends on both electron's and hole's charge carrier concentrations and it's mobilities:

$$\sigma = q(\mu_n n + \mu_p p), \tag{1.8}$$

where σ – conductivity, $Sm \cdot m$;

q – electric charge, C;

$\mu_{n,p}$ – electrons, holes mobility, $\frac{cm^2}{V \cdot s}$;

n,p – electrons, holes concentration, cm^{-3}.

To summarize, mobility is the measure of how fast the charge carriers move under the electric field applied. It strongly depends on the charge carriers' concentration, as well, as on temperature. Mobility determines one of the key parameters of the semiconductor material – conductivity.

1.6 Diffusion

Whenever there's a locally introduced charge within the system, it will be out of the equilibrium state. The typical effects which create this situation are local injection and non-uniform illumination[3]. In this case, a gradient of concentration of charge carriers exist. To bring the system back to the equilibrium, the process of redistribution of charge carriers occurs – charges are moving from the areas with high concentration to the ones with low concentration. This process is called *diffusion*. The flux of these carriers is described by Fick's law [3]. For electrons:

$$\frac{d\Delta n}{dt} = -D_n \frac{d\Delta n}{dx} \tag{1.9}$$

The flux of carriers forms the diffusion current [3]:

$$J_n = qD_n \frac{d\Delta n}{dx} \tag{1.10}$$

$$J_p = -qD_p \frac{d\Delta p}{dx} \tag{1.11}$$

where $\Delta n, p$ – concentration of excess carriers, cm^{-3}; q – electric charge, C; $D_{n,p}$ – diffusion constant for electrons, holes, $\frac{cm^2}{s}$; $J_{n,p}$ – electron, hole current density, $\frac{A}{cm}$.

Diffusion is also related to mobility. To illustrate this, imagine the n-type semiconductor with non-uniform distribution of charge carriers[3]. Without the external field, the net current through the system is zero. Thus, the internal electric field will create drift current to equalize the diffusion one:

$$qn\mu_n E = -qD_n \frac{dn}{dx} \tag{1.12}$$

If the semiconductor can be described by Boltzmann statistics, we get:

$$D_n = \frac{kT}{q}\mu_n \tag{1.13}$$

where q – electric charge, C;$D_{n,p}$ – diffusion constant for electrons, holes, $\frac{cm^2}{s}$; $J_{n,p}$ – electron, hole current density, $\frac{A}{cm}$; n – concentration of electrons, cm^{-3}; E – electric field, $\frac{V}{cm}$; $\mu_{n,p}$ – electron, hole mobility, $\frac{cm^2}{V \cdot s}$;T – temperature, K; k – Boltzmann constant, $\frac{J}{K}$.

Another important parameter, which arises from the diffusion process, is diffusion length, which can be taken as an average path that the charge carrier makes before its annihilation:

$$L_{n,p} = \sqrt{D_{n,p}\tau_{n,p}}, \tag{1.14}$$

where $L_{n,p}$ – diffusion length for electrons, holes, cm; $D_{n,p}$ – diffusion constant for electrons, holes, $\frac{cm^2}{s}$; $\tau_{n,p}$ – electron, hole lifetime, s.

So, diffusion is a process which happens when a non-uniform distribution of parameter within the system exists. Then such a system will experience the relaxation process, the goal of which is to vanish the non-uniformity. The most relevant case for semiconductors is the existence of the gradient of charge concentration. Then diffusion current occurs. With an absence of the external field applied, diffusion current will be equalized by the drift one, created by the internal field, so the net current through the device is zero.

1.7 The p-n junction

A p-n junction is the most important structure of semiconductor devices. The unique properties of this structure are used to create a great variety of components, such as diodes, bipolar and JFET(Junction Field Effect Transistors), solid-state switches, and many more. The p-n junction is also the key element of the solar cell. So let's take a look into the structure of this element.

Consider the structure composed of two semiconductor materials: one of n-type and another of p-type – connected together and the reverse bias voltage is applied to the system (fig 1.6, a). Under the reverse bias, one should assume the higher potential at the electrode, connected to the n-type material. Also assume, that both materials are uniformly doped and the concentration of acceptor dopant N_A is much higher than the concentration of the donor N_D.

$$N_A \gg N_D \tag{1.15}$$

where N_A, N_D – acceptors, donors concentration, cm^{-3}.

Whenever there's a physical connection, the electrons from the n-type side will start flowing towards the p-type side, because of the gradient of concentration from n- to p-side. In turn, holes will behave in the same way, diffusing in the opposite direction, towards n-type material. Atoms, from which the charge carriers have left for diffusion, will become charged ions, creating the electric field around. The value of the field is defined by the contact difference of potentials created by the charged ions. This difference is often called *built-in* potential and this is an internal difference of potentials under the zero bias condition:

$$\varphi_0 = \frac{kT}{q} \ln\left(\frac{N_A N_D}{n_i^2}\right) \tag{1.16}$$

where φ_0 – built-in potential, V; q – electric charge, C; T – temperature, K; k – Boltzmann constant, $\frac{J}{K}$; N_A, N_D – acceptors, donors concentration, cm^{-3}, n_i – intrinsic electrons concentration, cm^{-3}.

This field will create drift currents in directions, opposite to the diffusion. At some point, drift currents will equalize diffusion ones and the movement of charge carriers across the border between two materials will stop. The internal field slows down the major charge carriers (electrons for n-type, holes for p-type), and speeds up the minor ones, so if the hole of the n-type region or the electron of the p-type region will appear under the influence of the electrical field, they will be immediately swept to the opposite region.

This process occurs only around the border of two materials. In the depth of each layer, lattice atoms stay neutral because the carriers leaving the atoms will be replaced by the free carriers around.

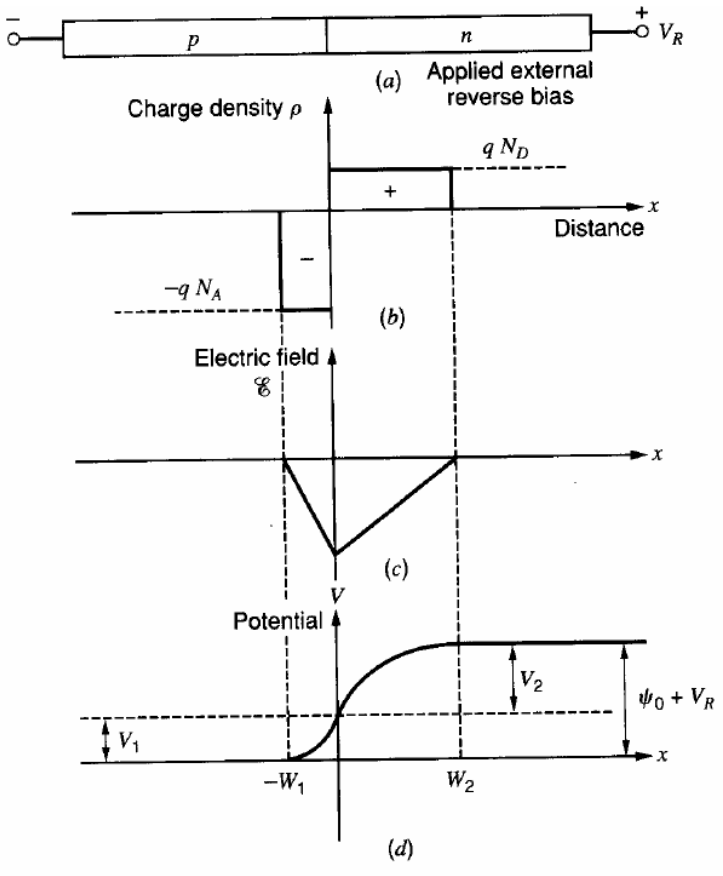

Figure 1.6 – The p-n junction: a) two materials of different conductivity type, connected together. The reverse bias is applied to the structure; b) the ionized areas around the border of two materials connection; c) distribution of the electrical field within the structure; d) distribution of the potential within the structure [5]

The situation described above occurs only within the region, called *the depletion region*. The width of the depletion region depends on the doping concentrations and related to it as:

$$\frac{N_A}{N_D} = \frac{W_2}{W_1} \tag{1.17}$$

Using Poisson's equation and the boundary conditions, one can derive the expressions for the width of the depletion region. The whole derivation is presented in [5]. Here only the result will be displayed:

$$W_1 = \sqrt{\frac{2\varepsilon\varepsilon_0(\varphi_0 + V_R)}{qN_A(1 + \frac{N_A}{N_D})}} \tag{1.18}$$

$$W_2 = \sqrt{\frac{2\varepsilon\varepsilon_0(\varphi_0 + V_R)}{qN_D(1 + \frac{N_D}{N_A})}} \tag{1.19}$$

where $W_{1,2}$ – width of depletion regions, cm; φ_0 – built-in potential, V; q – electric charge, C; N_A, N_D – acceptors, donors concentration, cm^{-3}; ε – dielectric permittivity; ε0 – dielectric constant, $\frac{F}{cm}$.

From these equations, one can see, that depletion region is in inverse proportion with the dopant concentration and extends deeper into the material when the reverse bias is applied. Another remarkable thing is that in case of one doping concentration bigger than another, the depletion region exists almost entirely in the lightly doped region [6].

To summarize, in this chapter, the basic properties of inorganic semiconductor materials were described. The insight into the key parameters and processes in semiconductor materials and devices, as p-n junctions, was given. The relations between these parameters were shown.

2. SILICON SOLAR CELLS

Before going deep into the working principles and designs of the solar cells, one should get an insight into the very basic effect, which causes the cell to generate electrical power out of solar energy. This effect is called photogeneration and will be briefly discussed in the next section.

2.1 Photogeneration in semiconductors

Photogeneration is the process of generating free charge carriers by absorbing a photon and transferring its energy to the bonded carriers in order to excite it to the higher energy state where they could become free carriers.

Photogeneration in semiconductors is generally called photovoltaic effect. Let's have a closer look at it. One considers three basic processes, which occur when the effect is observed[4]:

1. Absorption of the photon and generation of the charge carrier (fig. 2.1a,b): semiconductor material can absorb only certain photons with the respective energies. If one recalls in memory semiconductor's energy band diagram, one realizes that to generate charge carriers, thus to excite the electron from valence band to the conduction band, one should supply the energy, larger than the bandgap value. Thus, only those photons with energies equal or greater than bandgap's value can be absorbed by the material and generate charge carriers:

$$E_{ph} = hf, \quad (2.1)$$

$$E_g \leq hf, \quad (2.2)$$

where E_{ph} - energy of the photon, eV; E_g – bandgap, eV; h – Planck's constant, J·s; f – frequency, Hz.

When the electron is excited to the higher state, which means it is transferred to the conduction band, it leaves the hole in the valence band, which can also be

treated as the free charge carrier. Thus, one photon generates one pair of charge carriers – the electron and the hole.

But this is not enough to generate electrical power. After some time, the electron will lose its energy and will fall back to the valence band, where it will recombine with the hole. Thus, an additional step is needed for power generation.

2. Separation of generated carriers (fig. 2.1c): fortunately, the p-n junction exists in the interface of two semiconductors with different conductivity types. As was described before, charge transfer processes in the p-n junction result in the internal electric field existence. This field separates generated charge carriers, forcing them to drift towards the electrodes of the device.

   So far, the charge carriers have been generated and separated. However, they're still located within the semiconductor material; thus, they're not performing any work for the external circuit. In order to swipe it to the external circuit, one must collect those carriers.

3. Collection of the charge carriers (fig. 2.2): if the electrodes, attached to the semiconductor, have the respective work functions, then generated carriers will be collected to the electrodes, from where they will flow through the external circuit, where they can be collected into the battery, for example.

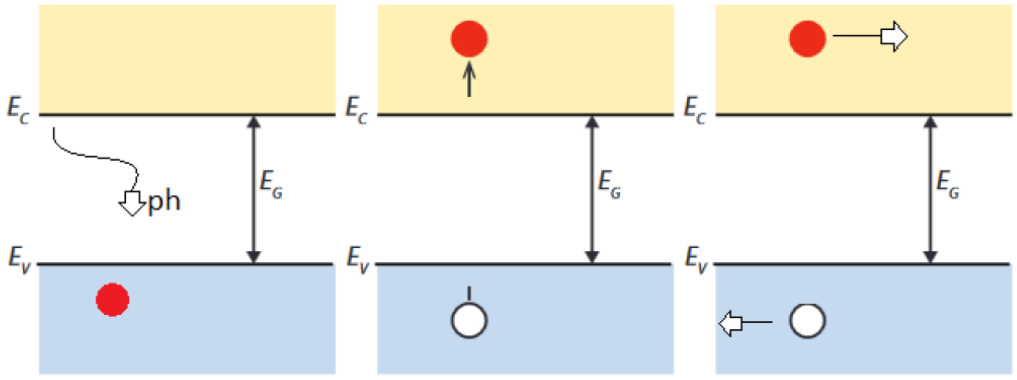

a) b) c)

Figure 2.1 – The process of: a) absorption of the photon; b) charge carriers generation; c) carriers separation [4]

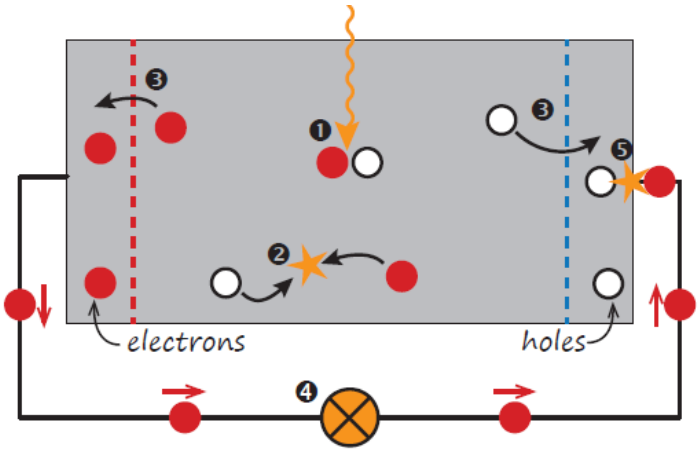

Fig. 2.2 – The working principle of the solar cell [4]

The photogeneration process can be easily seen while studying I-Vs of the device. By illuminating the sample, one will observe the shift of the characteristics down along the current axis (fig. 2.3). This can be clearly explained if one will consider the change in the net current of the cell under the zero-bias condition. As can be seen from the graph, in the dark, the characteristics of the cell show, in fact, a diode behavior. Thus, without any voltage applied, the current flowing through the sample is zero. However, under illumination, one will observe a significant rise of the power generated by the cell. This is due to the electrical current generated by absorbed photons.

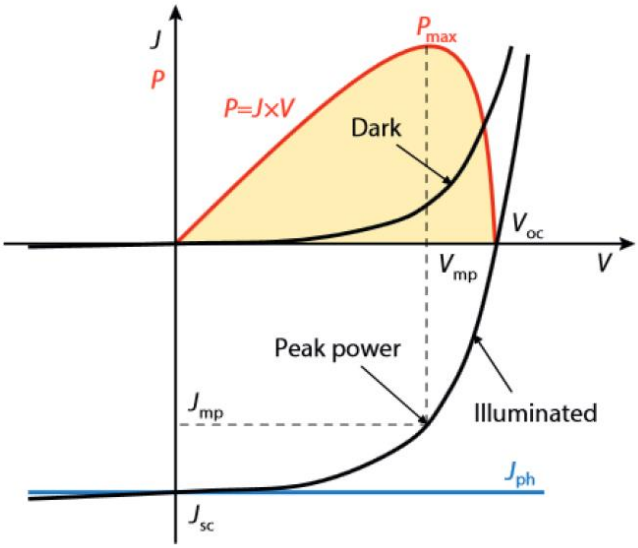

Figure 2.3 – The J-V characteristics of the solar cell under the dark condition and the illumination [4]

To conclude, photogeneration is the process of creation of free charge carriers within the material by absorbing the photon with energy, higher than the bandgap value of the semiconductor. Three main steps of this process include photon absorption and charge carriers generation, charge carriers separation and collection.

2.2 I-V characteristics and key electrical parameters of the solar cell

Consider a circuit in the fig. 2.4. This one represents the equivalent circuit of the ideal solar cell under illumination. As can be seen from the graph in fig. 2.3, silicon solar cell, in fact, behaves as a semiconductor diode. Under illumination, its characteristic is shifted due to the appearance of the net current, created by the absorbed photons.

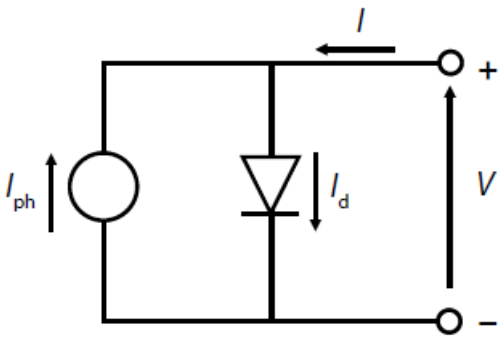

Fig. 2.4 – The equivalent circuit of the ideal solar cell under illumination [4]

The key parameters of the solar cell can be extracted from the graph in fig. 2.3 if one considers the I-V curve, which corresponds to the cell under illumination. They are:

J_{sc} – short-circuit current density, $\frac{A}{m^2}$. This is the maximum current that can be generated by the solar cell. Note that this current is measured under zero-bias condition. The value of this current is strongly related to photon flux and EQE(external quantum efficiency) of the cell;

V_{oc} – open-circuit voltage, V. This is the maximum voltage that solar cell can draw on its output terminals, while the load is disconnected. Note that it's is measured under zero-current condition.

The point noted as Peak Power corresponds to the working point of the solar cell, in which power, generated by the device, is maximized, thus, this is the optimal working point for any solar cell device. It's characterized by the next parameters:

$J_{mp} - \text{peak current}, \frac{A}{m^2}$;

$V_{mp} - \text{peak voltage}, \text{V}$;

$P_{max} - \text{maximum power, drawn from the output of the solar cell}, \frac{\text{W}}{\text{m}^2}$.

The maximum power is calculated:

$$P_{max} = J_{mp} \cdot V_{mp} \tag{2.3}$$

Another important parameter of the solar cell is FF (fill factor). This one is calculated as the relation of the peak power to the theoretical maximum of power output from the cell. Fill factor quantitatively characterizes losses in the cell:

$$FF = \frac{P_{max}}{J_{sc} \cdot V_{oc}} \tag{2.4}$$

where $J_{sc} -$ short-circuit current density, $\frac{A}{m^2}$; $V_{oc} - \text{open} - \text{circuit voltage}, \text{V}$; $P_{max} -$ maximum output power, $\frac{\text{W}}{\text{m}^2}$; FF – fill factor;

The most important parameter of the solar cell is PCE – the power conversion efficiency, which shows, how much of the input power is converted into electrical one:

$$PCE = \frac{J_{sc} \cdot V_{oc} \cdot FF}{P_I} \tag{2.5}$$

here P_I – the input power, $\frac{W}{m^2}$. The input power is an integral characteristic of the photon energy of the beam, incident to the cell's surface. The standard test conditions denote the maximum power as 1000 $\frac{W}{m^2}$.

For the silicon technology of solar cell fabrication nowadays, the PCE value is around 23-25%.

This is the perfect model of the solar cell. However, nothing in this world is perfect; that's why one should be aware of the existing losses, related to the cell's design and physical effects within the cell.

2.3 Recombination in the solar cell

The case, described above, corresponds to the ideal situation when no recombination is taken into account, and all generated charge carriers contribute to the current. Reality is different. There no way to make a perfect lossless cell. There are always trap states, lattice acoustic vibrations, and impurities within your material. So the good way is to know your enemy – to be able to determine and quantize the losses in your device in order to minimize it.

In the previous chapter, we've introduced some basic models for losses, so now we're going to expand those to provide insight into the mechanisms discussed.

So let's go through the types of losses one by one:

1. Direct recombination occurs mostly in direct bandgap semiconductors. This means that there's only energy transfer occurs during the process, and the momentum conservation is observed.

   Let's assume that direct recombination rate is proportional to the concentration of electrons in the conduction band and to the holes in the valence band, available to recombine with. Then the equation for the recombination rate is:

$$R = \beta np \tag{2.5}$$

where R – recombination rate, $\frac{1}{cm^3 \cdot s}$; β – proportionality factor, cm^3; n, p – concentration of electrons, holes, cm^{-3};

Under the condition of thermal equilibrium generation of carriers is equalized by recombination:

$$R_{th} = G_{th} = \beta n_0 p_0 \tag{2.6}$$

where $R(G)_{th}$ – recombination(generation) rate, $\frac{1}{cm^3 \cdot s}$; β – proportionality factor, $\frac{cm^3}{s}$; n_0, p_0 – equilibrium concentration of electrons, holes, cm^{-3}.

Now consider the sample under illumination. The excess charge carriers are produced, so:

$$\Delta n = n - n_0 \tag{2.7}$$

$$\Delta p = p - p_0 \tag{2.8}$$

where n, p – concentration of electrons, holes, cm^{-3}; n_0, p_0 – equilibrium concentration of electrons, holes, cm^{-3}; $\Delta n, \Delta p$ – excess concentration of electrons, holes, cm^{-3};

Then the equation for the generation must include photogeneration component:

$$G = G_{th} + G_L \tag{2.9}$$

where G_L – photogeneration rate, $\frac{1}{cm^3 \cdot s}$.

Then in the steady-state, recombination equals to generation, then:

$$R_d = G_L = G - G_{th} = \beta(np - n_0 p_0) \tag{2.10}$$

Here R_d stands for radiative, or direct recombination. Fig. 2.5 illustrates the mechanism of such type of recombination. The last thing to notice is that this type of recombination almost never occurs in Silicon cells, as Silicon is indirect bandgap material.

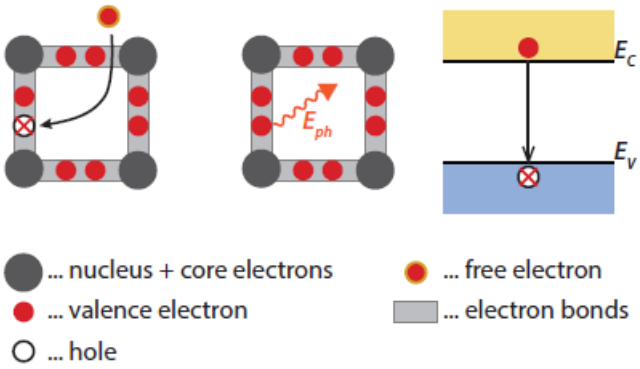

Figure 2.5 – The illustration of direct, or radiative recombination [4]

2. Shockley-Read-Hall (SRH) recombination or recombination on the trap states is one of the types of recombination present in Silicon solar cells. This one occurs when there is a defect or impurity in the crystal structure. This results in the appearance of the allowed energy level within the bandgap. Then the electron from the conduction band can be trapped at such level. Then the hole from the valence band will be attracted by the electron and will recombine with it. The derivation of the recombination rate equation can be found in [4], here only the final formula will be presented:

$$R_{SRH} = c_p N_T (p - p_0) = \frac{p - p_0}{\tau_{pSHR}} \quad (2.11)$$

$$R_{SRH} = c_n N_T (n - n_0) = \frac{n - n_0}{\tau_{nSHR}} \quad (2.12)$$

where R_{SRH} – recombination rate, $\frac{1}{cm^3 \cdot s}$; N_T – trap density, cm^{-3}; n, p – concentration of electrons, holes, cm^{-3}; n_0, p_0 – equilibrium concentration of electrons, holes, cm^{-3}; $\tau_{n,pSHR}$ – electron, hole lifetime, s. $C_{n,p}$ – proportionality factor, $\frac{cm^3}{s}$;

Eq. 2.11 corresponds to the n-type semiconductor, while eq. 2.12 is derived for the p-type one. The illustration of Shockley-Read-Hall recombination is presented in the fig. 2.6.

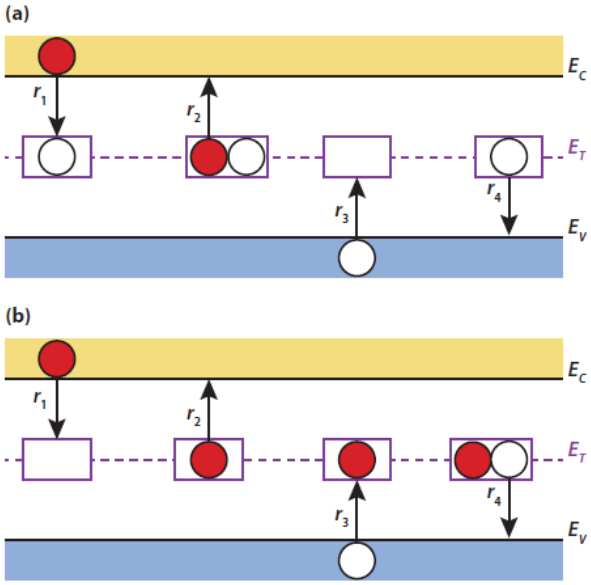

Figure 2.6 – Processes, that occurs during the SRH recombination for a) n-type semiconductor; b) p-type semiconductor [4]

SRH recombination consists of 4 processes, which probabilities define the recombination rate. These are: r_1 – capture of the electron; r_2 – emission of the electron; r_3 – capture of the hole; r_4 – emission of the hole.

3. Auger recombination is a three-particle recombination process. It involves the energy transfer from the particles, which recombine to the third particle. This results in the excitation of the third particle to the higher energy level.

Auger recombination strongly depends on the concentration of the electrons and the holes.

In case of electron-electron-hole process, one gets the expression:

$$R_{eeh} = C_n n^2 p \tag{2.13}$$

For the electron-hole-hole recombination:

$$R_{eeh} = C_p n p^2 \tag{2.14}$$

Then the resulting Auger recombination is the sum of both processes:

$$R_{Aug} = R_{eeh} + R_{eeh} = C_n n^2 p + C_p n p^2 \tag{2.15}$$

where R – recombination rate, $\frac{1}{cm^3 \cdot s}$; n, p – concentration of electrons, holes, cm^{-3}; $C_{n,p}$ – proportionality factor, $\frac{cm^3}{s}$;

Schematically this is illustrated in fig. 2.7.

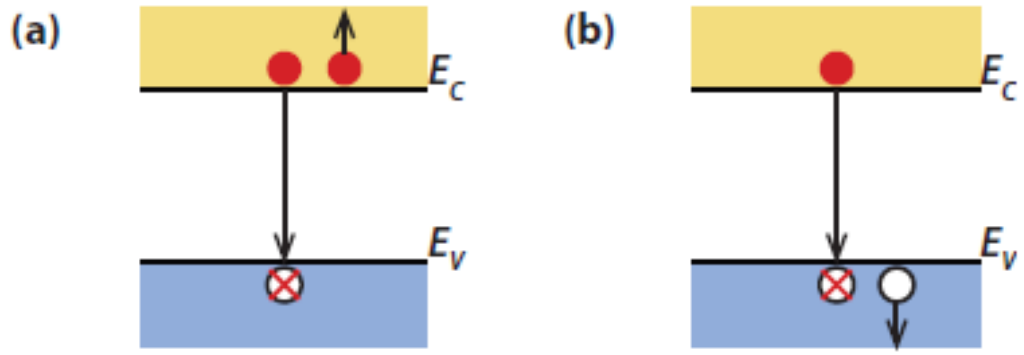

Figure 2.7 – Auger recombination for: a) electron-electron-hole process; b) electron-hole-hole process [4]

The recombination processes, which one can observe in Silicon solar cells, are Shockley-Read-Hall recombination and Auger recombination. As Silicon is indirect bandgap material, bandgap-to-bandgap processes, as direct recombination, are unusual for this type of material. As Auger recombination rate has a square dependency on the carrier concentration and doesn't require the appearance of the trap states, one should consider this type of recombination as most probable to occur. However, total recombination is defined as the sum of all the types of recombination.

2.4 Limits of solar cell's performance

There are several aspects that limit the performance of solar cells. One is them is the thermodynamical limit, which consists of the thermal losses of the cell. This means that part of the solar power, incident to the surface of the solar cell, is not converted into electrical energy, but to thermal one, thus is used to heat up the cell. These losses can be reduced by using solar concentrators.

Another limit is the optical one. Optical losses are occurred due to the reflection of the sunlight from the cell's surface. Because the incident light is crossing the surface between two mediums(air-absorber layer), there's a change of refractive index present. That means that certain wavelengths will be reflected from the surface. Another optical loss is the *shading effect*, which is due to the reflection from the metal electrodes, which cover the part of the surface. Metal electrodes effectively reflect or absorb the sunlight, so almost nothing goes through; thus, they create a kind of shade on the cell's surface. The optical losses can be minimized by making electrodes as narrow, as possible, and also by patterning the surface of the cell to achieve multiple reflections from one part of the surface to another, and thus to increase the absorption (fig. 2.8).

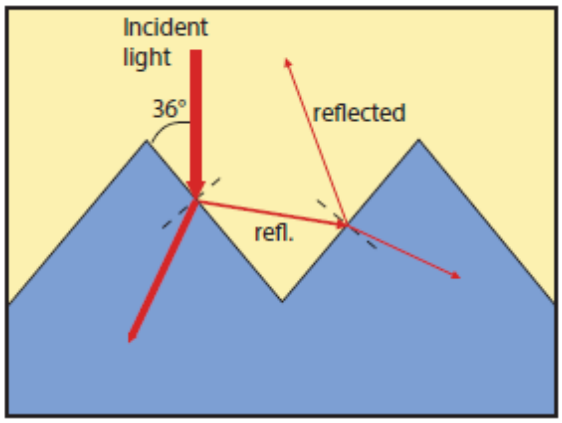

Figure 2.8 – The effect of patterning [4]

Recombination losses is another limiting factor. Not all the generated charges reach the electrodes and are collected. Some of them recombine on the way due to the trapping, insufficient lifetime and interactions with the lattice.

All the losses, described above, can be considered in the parameter, called EQE – external quantum efficiency. Physically, this is the measure of how many of incident photons are converted into the charge carriers that contribute to the electrical power generated. Analytically, EQE is derived as:

$$EQE(\lambda) = (1 - R^*)IQE_{op}(\lambda)\eta_g(\lambda)IQE_{el}(\lambda) \qquad (2.16)$$

Finally, the most important limiting factor is the utilization of the optical spectrum of the sun by the solar cell. This factor is often called the Shockley-Quiesser limit.

This one takes into account the fact that only the photons with energies, larger than the bandgap value, are absorbed by the active layer of the solar cell, as photons with lower energies cannot excite the electron to transfer it from the valence to the conduction band. The utilization of the solar spectrum by the crystalline silicon cell is shown in fig. 2.9.

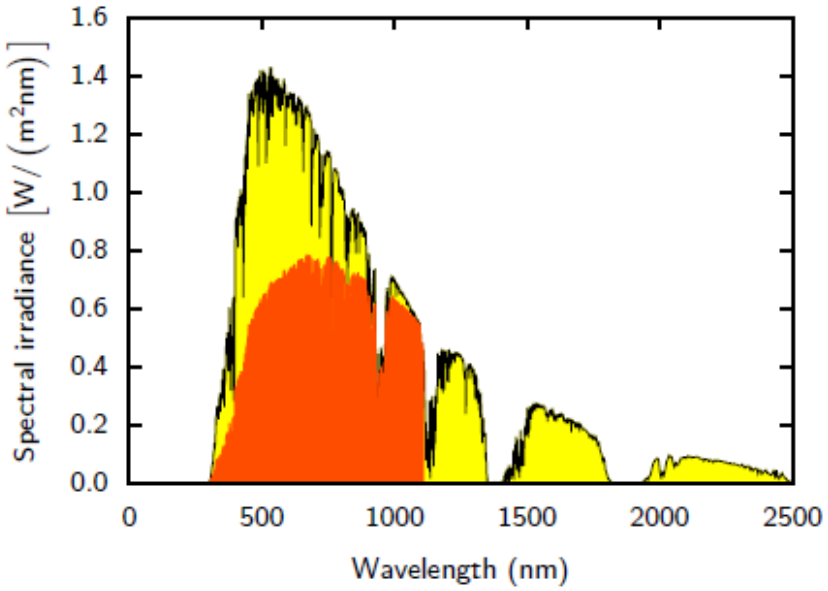

Figure 2.9 – The fraction of the AM1.5 spectrum by the crystalline silicon solar cell [4]

Another factor taken into account while calculating the SQ-limit is the heat emission by the solar cell. This is due to the relaxations of hot charge carriers generated by the photons with energies larger than the bandgap value. Electrons, excited in that

way, emit the excess energy during the relaxation to the lowest energy level of the conduction band, and this energy is transferred to the lattice atoms, which oscillate, emitting it in the form of heat. Thus, only the part of the incident energy is actually converted into electrical power.

The quantitative expression of the SQ-limit is the dependence of the power conversion efficiency on the energy of the incident light:

$$PCE = \frac{E_g \int_0^{\lambda_g} \Phi_{ph,\lambda} d\lambda}{\int_0^{\lambda_g} \frac{hc}{\lambda} \Phi_{ph,\lambda} d\lambda} \tag{2.17}$$

The value of PCE for the crystalline silicon, predicted by the Shockley-Quiesser limit, is around 30%.

To summarize: there are several sources of losses in the solar cells. These are thermal losses, optical losses, and spectral mismatch. The last one is the hardest to overcome, as this requires the development of new materials with lower bandgaps and utilization of several connected cells to minimize thermal losses. The summary of losses is shown in fig. 2.10.

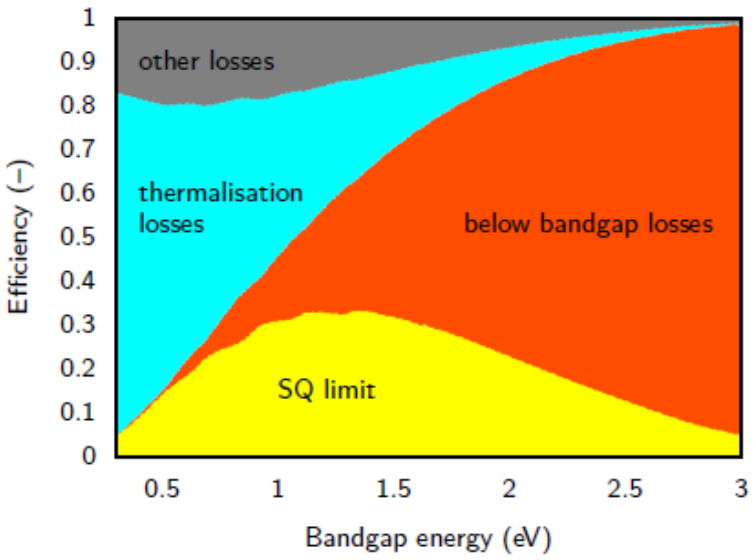

Figure 2.10 – Summary of losses in the solar cell [4]

2.5 The equivalent model of the solar cell

When photons are absorbed by the cell, their energy is converted to the electrical power drawn from the device's output terminals. Then, if one considers a lossless solar cell, the valid equivalent model for this will be a current source, which is the model of the photocurrent, connected in parallel with the ideal diode, which represents the cell (fig. 2.11).

Then the output current of the cell:

$$I = I_{PV} - I_D = I_{PV} - I_0[\exp\left(\frac{qV}{akT}\right) - 1] \quad (2.18)$$

where I – output current, A; I_{PV} – photogenerated current, A; I_D – dark current, A; I_0 – saturation current, A; q – electric charge, C; T – temperature, K; k – Boltzmann constant, $\frac{J}{K}$; a – ideality factor.

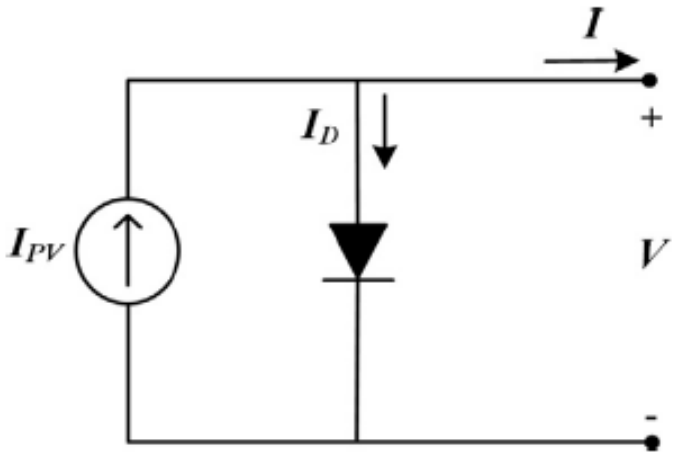

Figure 2.11 – The lossless model of the solar cell [6]

However, this cannot be the working model. One should take into account the effects of contact resistance, current flow resistance and the resistance of the electrodes. All these factors can be embedded in a series resistance R_S, which is included in the modified model. Other factors, that contribute into cell's losses, are temperature dependence and the leakage current of the p-n junction. This is modeled by the parallel resistance R_P. Together with the ideal model, they compose the real single-diode model of the solar cell (fig. 2.12).

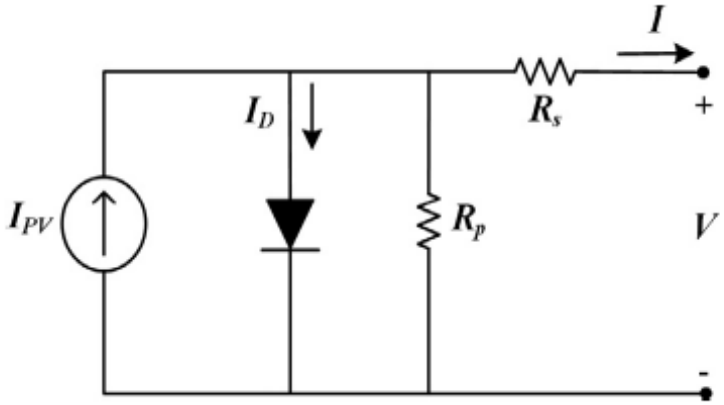

Figure 2.12 – The real single-diode model of the solar cell [6]

Then the expression for the output current is given by:

$$I = I_{PV} - I_D = I_{PV} - I_0 \left[\exp\left(\frac{q(V + IR_S)}{akT}\right) - 1\right] - \frac{V + IR_S}{R_P} \qquad (2.19)$$

where R_S – series resistance, Ohm; R_P – shunt resistance, Ohm;

Although this model is sufficient for most cases, the superior accuracy [6] of the equivalent model is achieved by including the recombination losses. Being the most precise among existing, it has only the one small modification comparing to one described above (fig. 2.13).

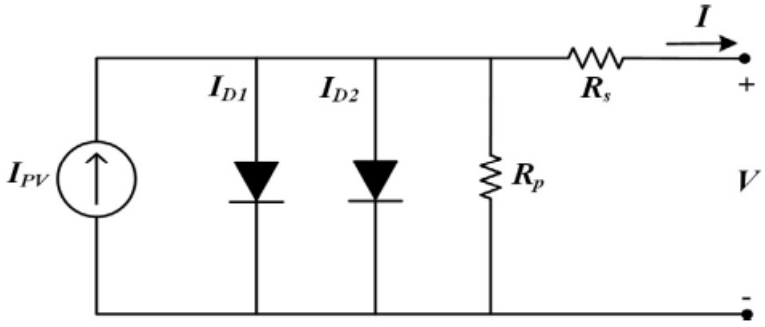

Figure 2.13 – The two-diode model of the solar cell

In this model, the second diode represents the recombination current within the depletion region of the cell's p-n junction.

The output current in this case is:

$$I = I_{PV} - I_D = I_{PV} - I_{01} \left[\exp\left(\frac{q(V + IR_S)}{a_1 kT}\right) - 1\right] -$$

$$-I_{02}\left[\exp\left(\frac{q(V+IR_S)}{a_2kT}\right)-1\right]-\frac{V+IR_S}{R_P} \qquad (2.20)$$

Although this model has two exponential dependencies and seven parameters to consider, it remains attractive due to the ultimate accuracy, comparing to other existing models [6].

2.6 The scheme of the solar cell

As it was said before, the solar cell is, in fact, a diode structure sandwiched between two metallic electrodes. However, the structure like that is not going to perform good, as it's not optimized in terms of minimizing the losses. Another drawback is that a structure like that, without proper incapsulation, is exposed to the environment, thus has low stability. The main factors that influence stability are humidity, oxidation processes, temperature and radiation.

That's why the practical realization of solar cells has a slightly different structure (fig. 2.14). The main factors that influence solar cell's stability are humidity, oxidation processes, temperature and radiation.

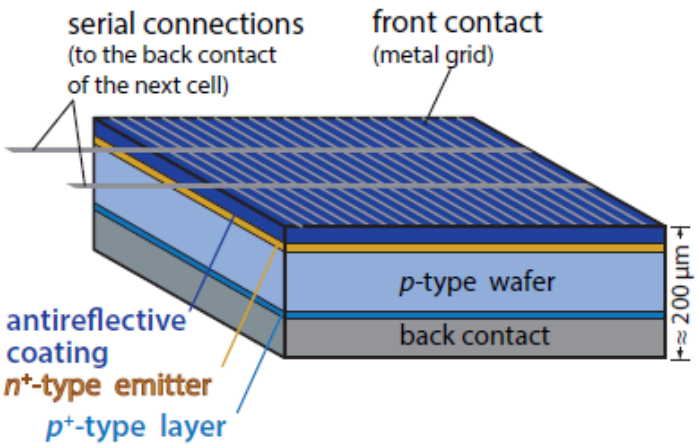

Figure 2.14 – The scheme of the practically realized solar cell [4]

So, the practical solar cells consists of the n^+-p diode structure with an additional p^+ layer, which has a proper value of the work function, so generated charges could be

transported to the electrodes. Another essential detail is antireflective coating, which increases light transmission into the active layer. Finally, the whole structure is sandwiched between two metallic electrodes. The top electrode has a grid structure in order to minimize the shading effect.

One essential detail about solar cells is that the thickness of the absorber layer, which is normally one of the active layers, should be thin enough. This is because the absorbance decreases dramatically with the depth in silicon (fig. 2.15). So, by making the absorber layer thin, one ensures the maximum of the generation of charge carriers within the diffusion length of the carriers. This means that recombination is low, and thus, the maximum charge is collected.

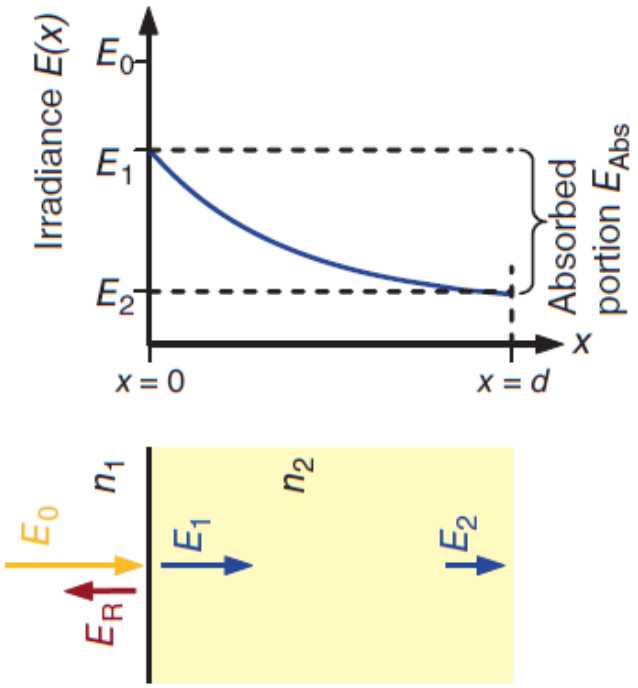

Figure 2.15 – The absorption process in the solar cell [7]

So, that's why in this structure, the n-type layer is made very thin – to ensure, then the maximum of charges is generated within the diffusion length, and thus the larger fraction of it will be transported to the electrodes and collected.

However, even this structure is not optimized enough and needs to be slightly changed in order to minimize optical losses, as the reflectance.

One way to decrease the reflection is to use a patterned surface, such as a pyramidal pattern. As it was described before, multiple reflections from the pyramid's surfaces lead to several absorption events, which results in lower optical losses. The typical device's structure with the patterned surface is shown in fig. 2.16.

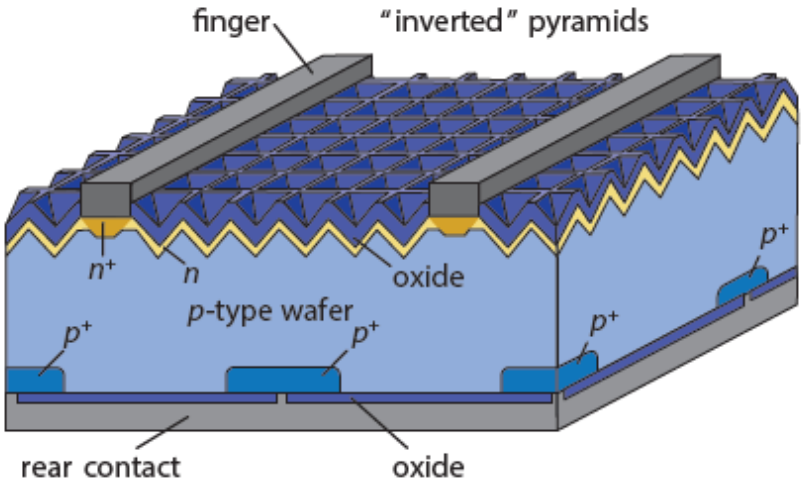

Figure 2.16 – The solar cell with the patterned surface

So, as one can see, the solar cell structure is quite simple; however, it still requires the utilization of sophisticated concepts to optimize it.

In the last section, the fabrication process will be discussed.

2.7 Fabrication of silicon solar cells

The fabrication of silicon solar cells includes several steps. The technology itself is quite simple and doesn't require any submicron techniques utilization. However, the expensive equipment and sophisticated processes are still used. A good example of that is high-temperature diffusion. This technique requires a high vacuum, high temperatures, as well as utilization of the expensive and hazardous technological gases, as phosphine and silane. This process also makes recycling of the broken cells impossible, because it is very costly – to purify the wafer from one type of the dopants. So one should consider the ways to simplify the process and to substitute hazardous materials with safe and sustainable analogs. Simplifying the fabrication process flow

allows enabling reverse processing of the devices, which results in cost-effective manufacturing and reusable materials usage. This will be discussed in detail in the upcoming chapters.

Talking about the fabrication of solar cells, one should consider the process flow diagram, which represents a chain of technological operations, which modify the device's structure. Fig. 2.17 depicts the process flow, and each step is discussed further in detail.

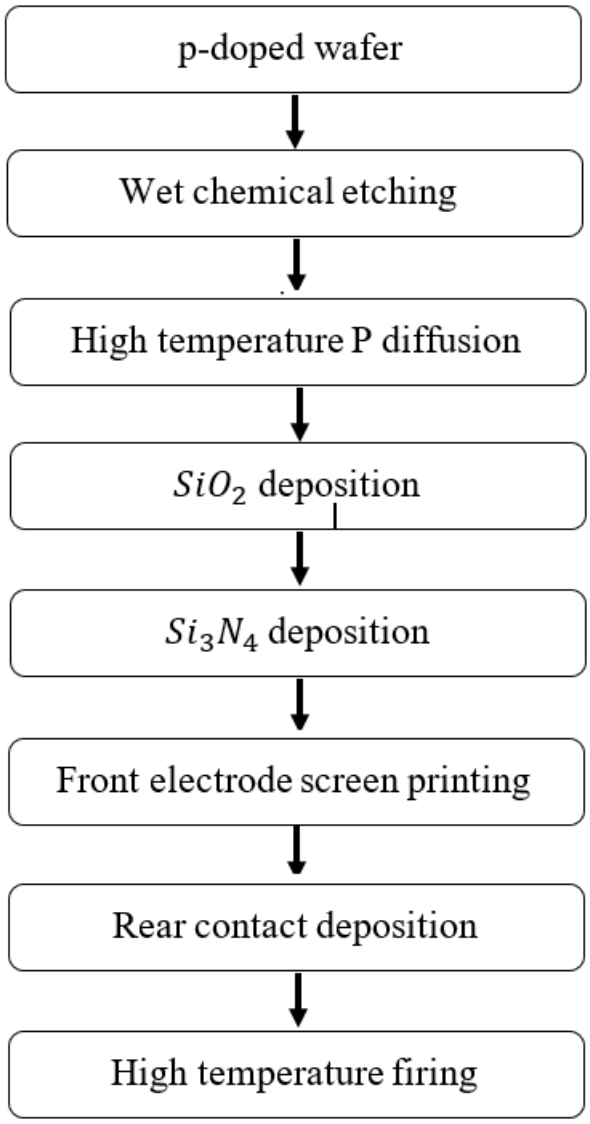

Figure 2.17 – Solar cell fabrication process flow

Fig. 2.18-2.19 depict the modifications, made to the wafer.

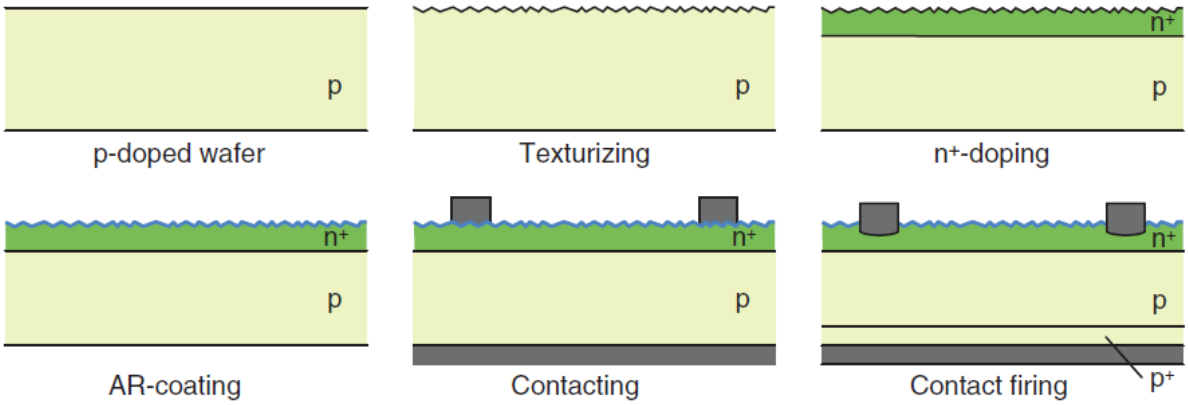

Figure 2.18 – The layer-by-layer modification of the wafer [7]

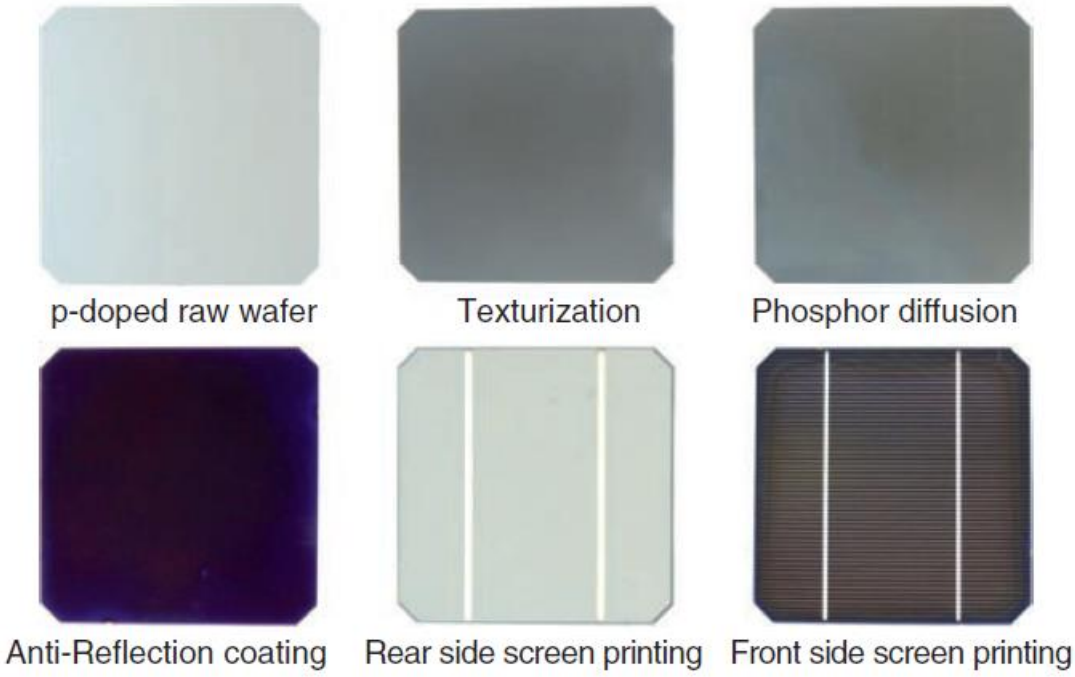

Figure 2.19 – The front view of the wafer after every fabrication step [7]

Let's have a closer look at every process present in the fabrication itinerary. So, the initial material is the p-type silicon wafer, normally with the crystal surface of (100). To obtain the solar cell from the raw wafer, a series of steps is performed:

Texturizing: this step is used to form the pattern on the wafer's surface. For these purposes, different etching compositions are used, like hydrofluoric acid, nitric acid, potassium hydroxide, etc. To perform anisotropic etching, which is needed to create the pattern, normally KOH:H2O solution is used with weight proportion 1:3 at 80 °C. This

solution etches <110> a hundred times faster than <111>. For <100> wafers etching, this solution is normally modified by the addition of propanol[8].

High-temperature diffusion: this is used for inserting dopants into the wafer. Those create the additional charge carriers, which sign depends on the type of dopant. Diffusion is normally performed in the vacuum with the temperatures around 1000-1300 °C. If the temperature is lower than 1000 °C, the diffusion coefficients decrease dramatically. Thus it's impossible to insert the dopants into the wafer [9]. Temperatures higher than 1300°C may damage the surface of the wafer, thus going higher than these values is kindly discouraged [9]. Diffusion is performed in two steps. During the first step, the dopant is inserted into the thin layer of the wafer. After that, the wafer is heated up, and dopant atoms diffuse to a certain depth under the temperature gradient. The concentration profiles after each step are defined by Fick's laws, which describe the statistical distribution of the dopant with respect to temperature and time of the process [9].

Anti-reflective coating(ARC) deposition: this layer decreases the reflection of light dramatically, minimizing optical losses. As anti-reflective materials, silicon dioxide and titanium dioxide are used because of chemical stability and suitable refraction constants. The processes of deposition of this layer include spin-coating [10], sputtering [11], chemical vapor deposition(CVD) [12], screen printing [13], etc. All these processes, except for the spin-coating, can be implemented in large scale manufacturing.

Contact deposition: contacts of the solar cell are normally created by sputtering or chemical vapor deposition. To create the pattern for the front contact, one uses a photolithography procedure, after which etching is performed to remove the unused part of the metallic layer. The lithography process is illustrated in fig. 2.20. However, modern industrial technology uses additive manufacturing instead of old inefficient processes. Thus, screen or ink-jet printing is normally used to create front contact[4]. Back contact is normally doped with Boron, which is used to create the ohmic contact to the p-type layer of the cell.

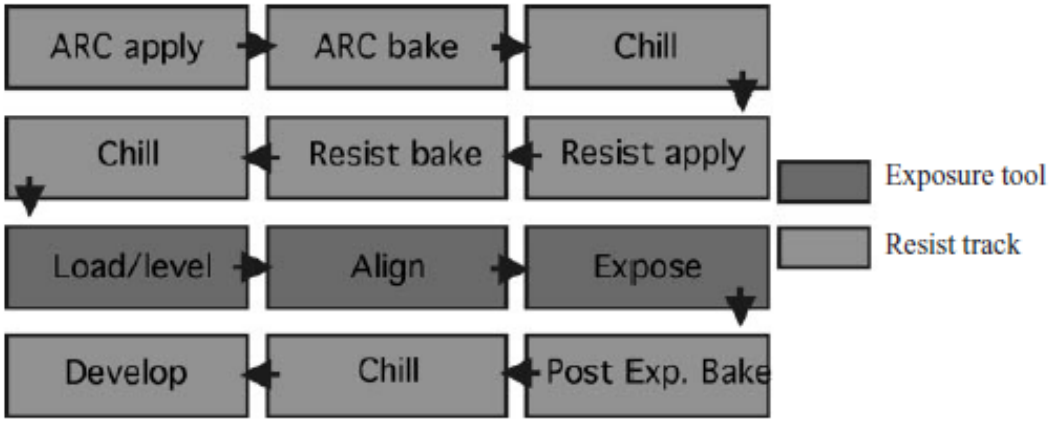

Figure 2.20 – Lithography process flow

Firing: this is the very last step before encapsulation of the wafer into the solar panel module. This process removes all the mechanical tensions along the wafer and additionally forces the dopant from the rear contact to diffuse into the wafer to create the additional contact layer to create the appropriate energetic alignment of the layers, thus to obtain ohmic contact instead of Shottky barrier [4]. The temperature of the firing process is around 500 °C [14].

To summarize, in this chapter, the physical processes and manufacturing technology, as well as the structure of silicon solar cells, were discussed. The main processes, which occur in the cell, are photogeneration, separation and collection of charge carriers. The main recombination processes observed in silicon are Shockey-Read-Hall and Auger recombination, with the last one dominating. The main structural elements of the silicon solar cell are the p-n junction, the p^+ - type ohmic contact, the electrodes and the anti-reflecting coating layer.

3. SEMICONDUCTOR PROPERTIES OF ORGANIC MATERIALS

In this section, the overview of the semiconductor properties of organics is given. Although the processes that occur in organic materials, such as organic crystals, molecules and polymers, are slightly different from the ones for inorganic semiconductors, with a certain degree of validity, the same physics can be applied to describe these systems.

In this chapter, only the most relevant details concerning organics will be highlighted, as the complete overview of physics behind the processes within these materials exceeds the main topic of this work.

3.1 Types of organic semiconductor materials

Like inorganic, organic semiconductor materials can be crystalline or amorphous. The first ones are characterized by the lattice structure, but, instead of atoms, they have molecules as a basis. Another difference stands from the type of interaction, that holds the basis' elements together. Instead of covalent bonds, which, for example, keeps together the atoms of silicon crystal structure, the molecules in the organic crystal are coupled with weak van-der-Waals interactions [15]. These forces are based on interactions between fluctuating dipoles [15] of two neighbor molecules. This results in two consequences:

1. Organic crystals are generally formed by flat molecules with large outer π-orbitals [15].
2. The molecules are tightly packed because of the strong distance dependence of the van-der-Waals forces [15]. However, sometimes, the basis of the crystal is made of two weakly interacting molecules [16].

A typical structure of organic molecular crystals is shown in the fig. 3.1.

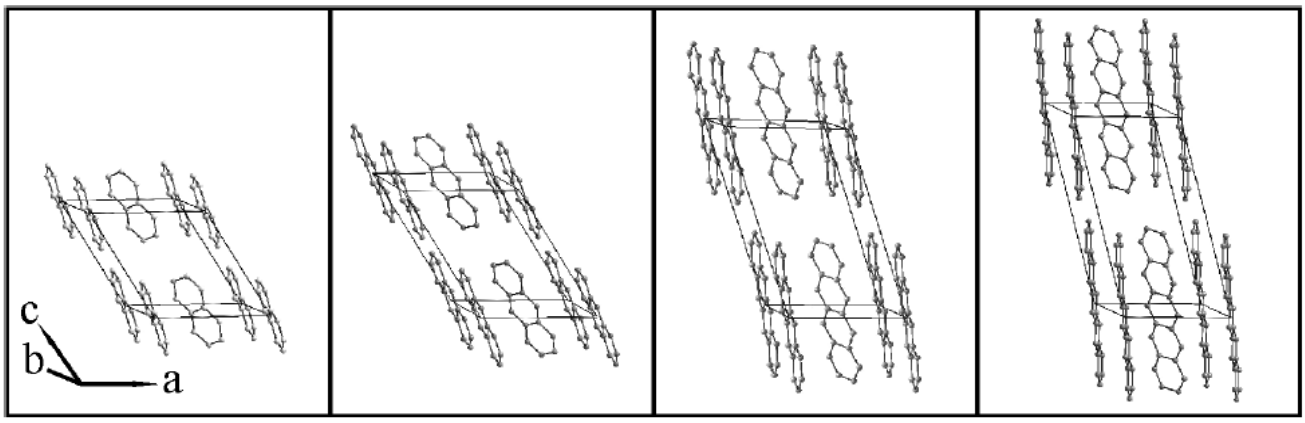

Figure 3.1 – The crystal structure of different single crystals [16]

Another type of organic semiconductor is molecules, made of amphiphilic structures [16], one part of which is hydrophobic when another is hydrophilic. They often form so-called Langmuir-Blodgett films. Being only partially soluble in water, those molecules form tightly packed thin films, when deposited on the surface and the solvent, containing molecules, evaporates.

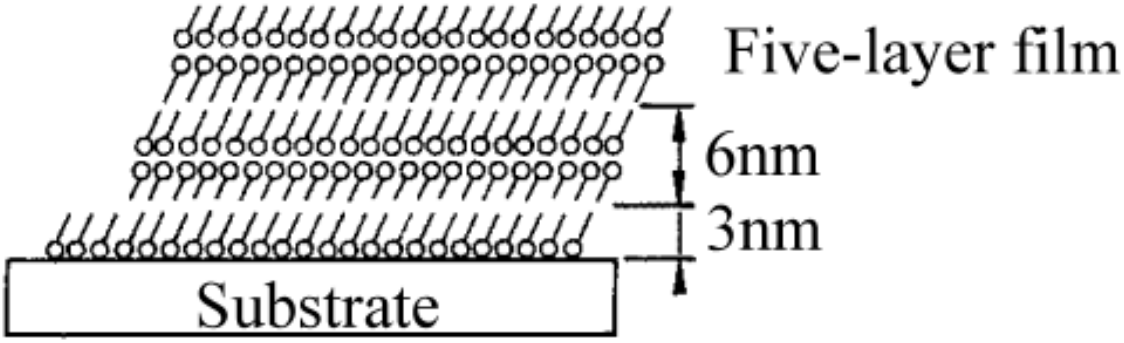

Figure 3.2 – Langmuir-Blodgett film on a substrate [16]

Finally, conjugated polymers are actively used as organic semiconductor materials due to their processability. The last term means that one can engineer the properties of such molecules by adding, removing and changing radicals connected to the molecule's backbone. The most illustrative example is solubility in water, which for unsoluble molecules can be achieved by adding –H or –OH groups to the outer of the backbone. The type of the polymer molecule differs according to its structure: "if all repeat units are identical, they form a homopolymer, while copolymers are formed when different repeat units are joint" [15]. Depending on the electronically active(thus non-inert) part of the molecule, it could either be named a main chain or side chain polymer.

The different types of polymer semiconductor materials are shown in the fig. 3.3.

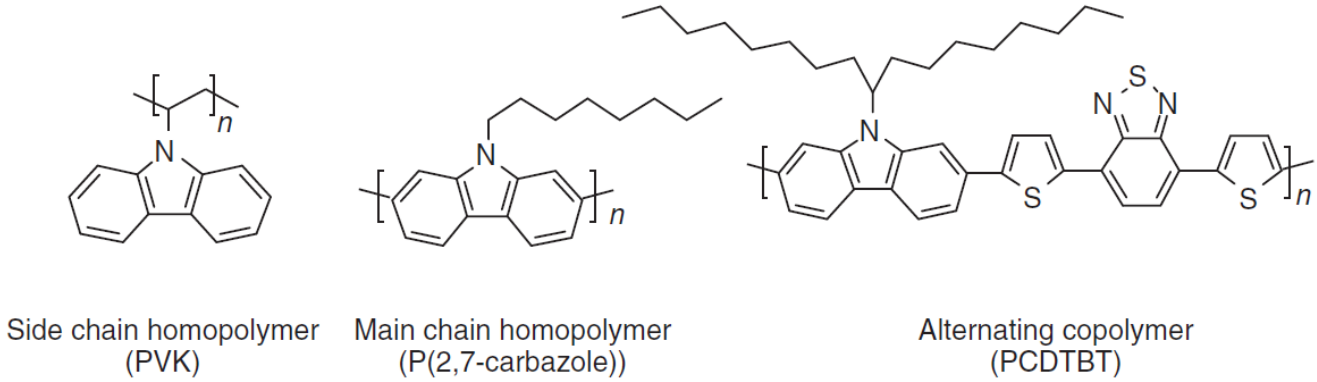

Figure 3.3 – Different types of polymer molecules [15]

Thus, organic semiconductor materials are represented by molecular crystals, small molecules, which form amorphous thin films, or by polymer structures (so-called conjugated polymers).

3.2 Electronic structure of organic semiconductors

To get the insight into electronic structure of the organic materials, one should start by considering the atomic orbitals of Carbon. As it is the main building block of the organic molecules, Carbon's properties somehow derive the electron distribution within molecular orbitals.

The electronic structure of Carbon consists of two types of atomic orbitals. Depending on the position of the spatial probability density of electrons with respect to the lines, connecting two atoms, these are called either s- or p-orbitals (fig. 3.4) [15].

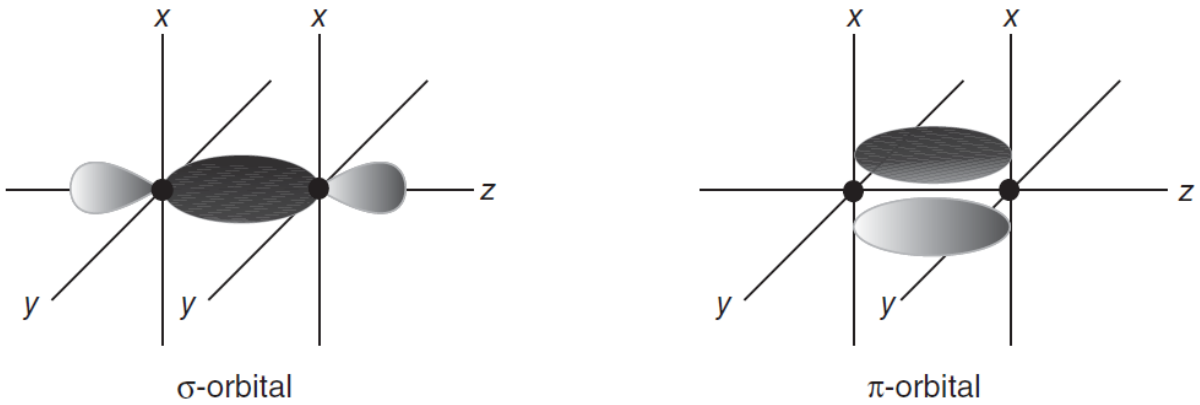

Figure 3.4 – S- and p-orbitals of the organic molecules [15]

When connected together, atoms share their orbitals with each other, forming so-called hybrid orbitals (fig. 3.5).

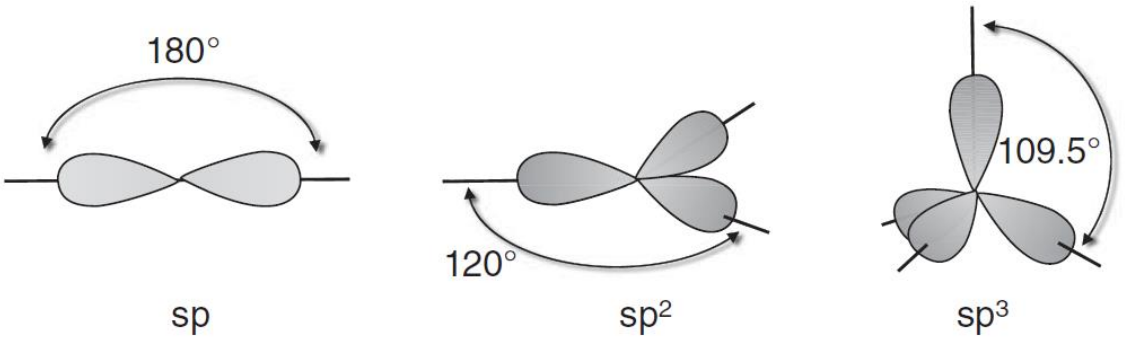

Figure 3.5 – The hybrid orbitals [15]

The number of such orbitals defines how many bonds can be formed by the molecule. For example, those with sp^3 orbitals can form 4 bonds. Two atoms with such configuration will form 4 s-bonds. Another situation is observed when connecting those with sp^2 orbitals. Then a $2p_z$ orbital of one atom will be connected with that of another one, forming the molecular p-bond, as $2p_z$ is parallel to the line, which connects two atoms.

Let's define the energies of the molecular bonds. When two atomic orbitals overlap, this can be considered as either constructive or destructive interference of the corresponding electron's wavefunctions. Then splitting of energy levels takes place. The picture of the resulting levels will be different depending on the difference between the initial energies of molecular orbitals (fig. 3.6).

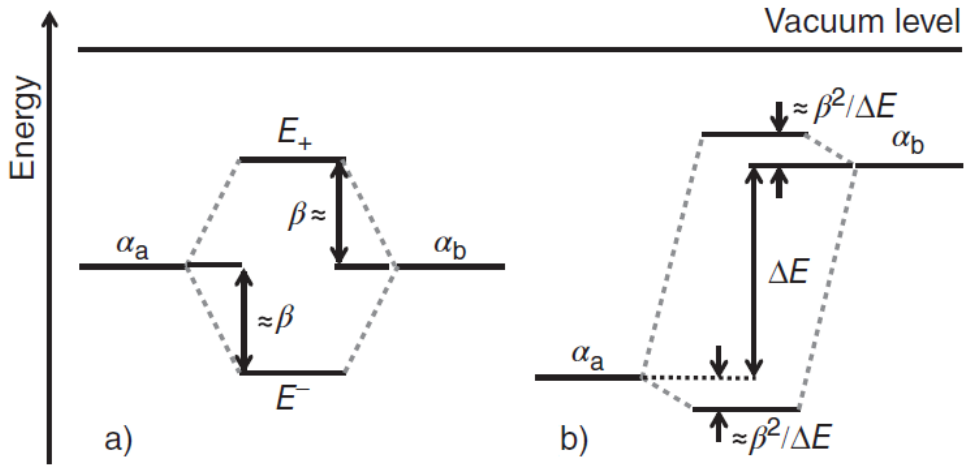

Figure 3.6 – Energy splitting due to resonance of two electrons of molecular orbitals with a) two equal or close energies; b) different energies [15]

Let's assume, those only orbitals with the close energy values interact, as the contributions from the interactions of ones with different energy are negligible. A good example is the ethene molecule. Its 1s orbitals form bonding σ- and antibonding σ^*-orbitals with small energy splitting [15]. In a similar way, the two orbitals are formed by sp^2 hybrid ones. However, $2p_z$ form π- and π^*-orbitals. Now, as its electron probability density distribution is located further from nuclei, compared to the other orbitals, the splitting between π- and π^*- energy levels will be smaller. Then, if the electrons will fill the resulting orbitals instead of parent ones, it appears that the highest occupied molecular orbital(HOMO) is the π- one when the lowest unoccupied(LUMO) is the π^*- (fig. 3.7).

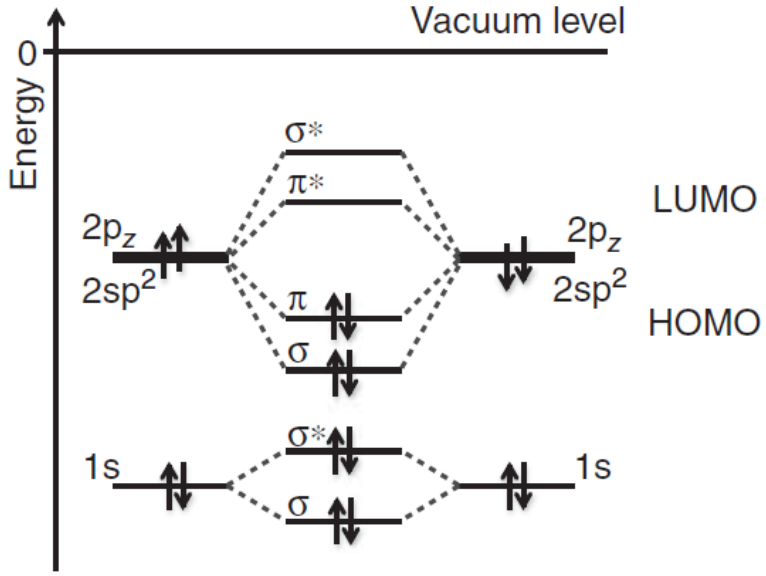

Figure 3.7 – The resulting molecular orbitals [15]

These HOMO and LUMO energy levels are thus responsible for the optical and electrical processes within the molecule [15]. When the electron or the hole are injected, they will occupy the LUMO or the HOMO level, respectively, if the work functions alignment with the electrodes is right.

The very last concept to discuss in this section is the *excited state***.** This concept refers to any configuration of the molecule, where not only the lowest orbitals possible are filled, but at least one electron is present at the higher state. The situation, when all

the electrons occupy the levels with minimal energy, corresponds to the *ground state* of the molecule.

3.3 A comparison of organic materials with inorganic semiconductors

As it was stated before, the physical processes that occur in the organic materials can be described by those for inorganic semiconductors, with only several modifications made regarding the specialties of the organics.

Two main factors define the difference between these two types of materials. The first one is the electron screening, or the dielectric constant ε_r, which determines how strong are the interactions between charges. The lower it is, the stronger will be the bonding. For example, for inorganic semiconductors, this value lays around 12-13, which results in quite good electronic screening, while for organic semiconductors $\varepsilon_r \approx 3$, which means that the interactions between the electrons cannot be neglected. A good concept to observe this effect is the capture radius, or the Coulomb bonding radius, which is given by:

$$r_c = \frac{q^2}{4\pi\varepsilon_0\varepsilon_r kT}, \qquad (3.1)$$

where r_c – is the Coulomb radius, m; ε_r – dielectric permittivity; ε_0 – dielectric constant, $\frac{F}{cm}$; q – electric charge, C; T – temperature, K; k – Boltzmann constant, $\frac{J}{K}$;

As one can see, the interaction length in organics is approximately four times longer than in classical semiconductors.

The high dielectric constant also results in a good electron delocalizing. Thus its scattering length is much bigger than the lattice constant value. This means excitations create free charge carriers, which propagate freely through the conduction band. This is often called the *coherent transport*. On the other hand, the low value of ε_r for organics results in the electrons having short scattering length(the order of a lattice parameter), the large Coulomb radius, which together makes the coherent transport impossible and results in the *incoherent transport*, or so-called *hopping.*

Another important point is the type of coupling which holds the crystal structure together. The strong covalent bonding in inorganic semiconductors results in a solid alignment of energy levels, which results in valence-to-conduction band transitions as in major process. On the other hand, the weak van-der-Waals forces, which couple the organic molecules, lead to the formation of the narrow bands, which vanishes completely at room temperature [15]. They are then decomposed into many delocalized states, and charge carriers can travel from one state to another. This means no way for the electron to propagate through the structure. Thus it is mainly scattered on the phonons or vibrons on almost every molecular site [15]. So in the organic systems, there are almost no free charges created. In contrast, absorption results in the excited state of the molecule, thus in the promotion of the electron to the higher molecular orbital. Moreover, this event can also result in a transition of the electron to the neighbor molecule, thus creating the charge-transfer state.

So, the absorption creates the excited state of the molecule in the organic semiconductor. This state is also called the exciton. Due to the translational invariance of the crystal, it can reside on any neighboring molecule [15]. This migrating state is then called *the Frenkel exciton*.

3.4 The traveling exciton

As it was previously said, the excited state of the molecule can travel along the molecular chain. An analogy can describe it with the mechanical system of pendulums, coupled by springs [15]. When one of those gains mechanical energy, it starts to oscillate, and this excitation propagates along the chain of coupled pendulums.

The Frenkel exciton describes the delocalization of the excited state over the crystalline array [15]. Approximately, it can be visualized by an additional electron in the LUMO and a hole in the HOMO, traveling together through the system of molecules. However, the electron-electron correlation effects should be considered in the real systems.

The described above concept takes the assumption that there is no energetic variation between different sites. But it never happens in reality, so the transport properties of the exciton depend on the energy misalignment as well, as on the coupling between different molecules. One should consider two cases:

1. The coupling is strong comparing to the site energetic variation [15]. This results in a well-defined exciton band, through which exciton can travel coherently.
2. The variation in energy of different molecules exceeds the coupling energy. In this case, the exciton band is destroyed, and the excited state of the system is described by the localized exciton, which may be transferred to another localized state by incoherent transport, so-called hopping.

The second case most probably occurs in the real molecular systems, which means that the actual charge transfer mechanism in the organic semiconductors is moving from one localized molecular state to another by the fast transitions, called hopping.

3.5 Generation and dissociation of excitations

Consider a system of two organic materials mixed together, so they form a blend. This is a typical structure of an organic BHJ-cell(Bulk Heterojunction). As the diffusion length of the charge carries in organics is low comparing to one in inorganic systems, the formation of the blend is favorable compared to the bilayer structure, as carriers need to travel less to the interface.

Now let’s have a closer look at the processes that occur in such systems when the incident beam of light falls on the surface of the solar cell (fig. 3.8):

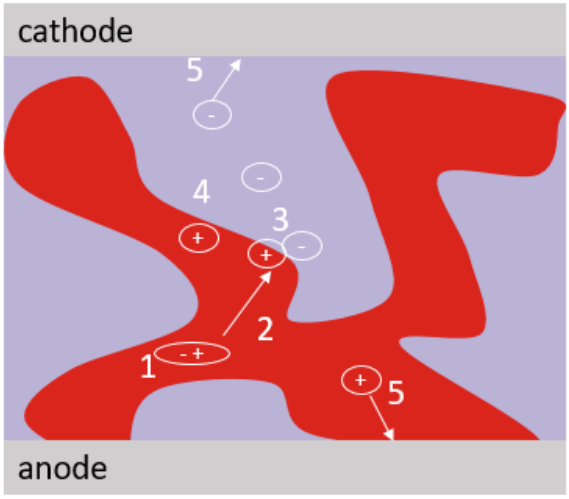

Figure 3.8 – The processes in the BHJ solar cell under illumination

So, there are several steps between the light absorption and the current generation in the external circuit:

1. When light is absorbed, it excites the molecule, which can be described as a promotion of the electron to the higher orbital.
2. The created exciton travels to the interface of two mediums.
3. At the interface, the exciton creates a geminate pair of two charge carriers.
4. The geminate pair is further separated by the internal electrical field into two independent charge carriers.
5. The carriers travel through the medium towards the electrodes, where they are collected.

So, the process of charge generation in organics is quite similar to the one of inorganic semiconductor, with the difference that before the free charges, the exciton is created.

3.6 Recombination in organic semiconductors

In organic semiconductors, recombination may occur either *geminately* or *non-geminate* [15]. *Geminate* recombination refers to the annihilation of two charge carriers, which were produced during the same excitation, thus the two particles of the same exciton. This can be illustrated by the electron from the LUMO “falling back into the

hole" of HOMO. In contrast, the recombination of charges from different geminate pairs or even injected ones is called *non-geminate*.

One distinguishes two types of recombination in organic semiconductors:

1. Langevin-type recombination. In this case, the charge carriers recombine with each other directly, no transfer through trap states is included. The rate of recombination is determined by the interaction velocity and by the concentrations of the electrons and the holes:

$$k_L = \gamma np \tag{3.2}$$

where γ is given by:

$$\gamma = \frac{q}{\varepsilon_r \varepsilon_0}(\mu_n + \mu_p) \tag{3.3}$$

where ε_r – dielectric permittivity; ε_0 – dielectric constant, $\frac{F}{cm}$; q – electric charge, C; n, p – concentration of electrons, holes, cm^{-3}; $\mu_{n,p}$ – electron, hole mobility, $\frac{cm^2}{V \cdot s}$

Thus, Langevin recombination is similar to the bimolecular one of inorganic systems.

2. Trap-assisted recombination(SRH-like). Similar to the Shockley-Read-Hall process, trap-assisted recombination can occur when there is an available trap state with energy value in the middle between HOMO's and LUMO's ones. The recombination rate for this type is:

$$k_t = 4\pi R_{Te} D_e N_T \tag{3.4}$$

The two types of recombination are illustrated in fig. 3.9:

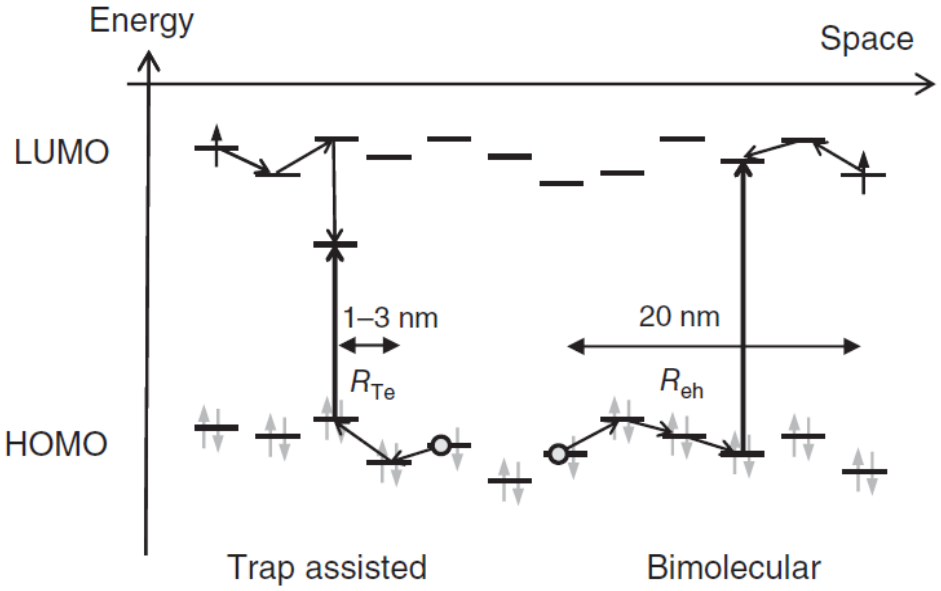

Figure 3.9 – Trap-assisted(SRH-like) and bimolecular(Langevin) recombination processes [15]

So, let's summarize. The two main differences between the inorganic semiconductors and the organic ones are the bonding type(strong covalent for inorganic, weak van-der-Waals for organics) and the electron screening. Thus, one cannot neglect electron-electron interactions in organic semiconductors. As the analog of the valence and the conduction band, in organics, one considers HOMO and LUMO levels. When the electron is promoted from the HOMO to the LUMO, the excited state of the molecule is created, so-called the exciton. The processes of generation and recombination of charge carriers are similar for both types of materials, with the difference that, in organics, prior to free charge creation, the exciton appears and needs to be dissociated.

4. SILICON-POLYMER SOLAR CELLS

In this section, the concepts of hybrid solar cell structures and working principles will be discussed. The advantages of the organic-inorganic cells will be highlighted.

4.1 The concept of hybrid solar cell

A hybrid solar cell is similar to the classical one, with only one essential difference. In this type of device, one of the active layers, which form a p-n junction, is changed from silicon to organic. This means that instead of doping the silicon wafer, one uses a deposition to put the organic layer on the top of the wafer. There are three main concepts in building hybrid solar cells. One is to create a bilayer structure (fig. 4.1, a), another is to create a heterojunction by blending the organic layer with the inorganic one, often made of quantum dots, dispersed in the medium [17] (fig. 4.1, b), and the last one – to use ordered nanostructures on the top of the inorganic material and coat it with the organic layer (fig. 4.1, c). The schematic structures of the described above hybrid solar cells are shown in fig. 4.1.

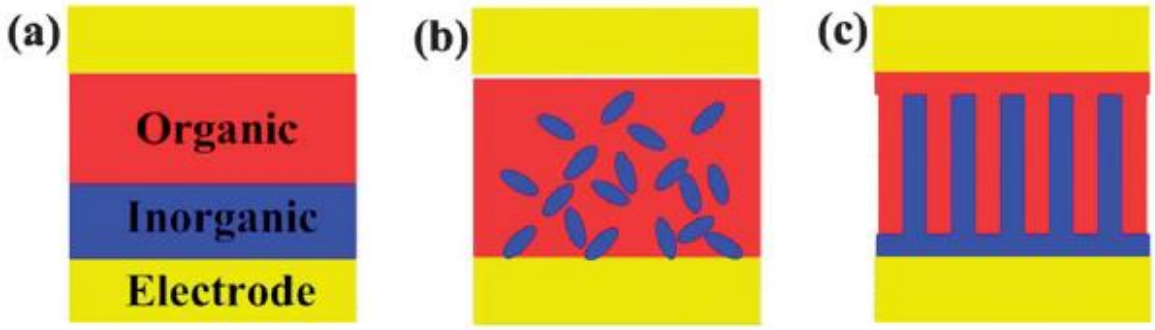

Figure 4.1 – The typical structures of the a) bilayer; b) bulk heterojunction; c) nanostructured hybrid solar cells [17]

Every concept has its advantages and drawbacks, which will be discussed in detail later. However, the main principle remains the same: one uses the interplay of organic and inorganic layers in order to create a kind of diode structure. Thus, the

organic material should be either p- or n-type, with respect to the conductivity type of the inorganic part.

4.2 Types of the hybrid solar cell

Three types of HSC (Hybrid Solar Cells) have been introduced above. Let's have a closer look and describe the specialties of each of mentioned:

1. The bilayer cell: is the closest to the classical p-n silicon junction structure. The fabrication process is the simplest comparing to two other types. One drawback is that the efficiency of these cells is highly influenced by the recombination processes in the organic layer, as the recombination lengths in this type of semiconductors are generally lower than the layer's thickness, so only few excitons can reach the interface, where they can be dissociated.
2. The BHJ cell: the active layer is formed by blending both organic and inorganic parts. The main advantages of this configuration are the enhanced light trapping effects [18] and the large junction area [18]. As the interface between two types of material is distributed within the volume of the active layer, the path in which the exciton needs to travel to be dissociated is much lower than in the bilayer cell. This results in higher values of photocurrent. However, dead-ends and short-circuiting of charges are also present [17], which limits the performance of these devices.
3. Nanostructured cells: because of a well-structured interface and also because of the large surface area, this type of device is characterized by very low recombination. Charges can be collected at the same rate as the photons are absorbed [19], which is evidence of the well-optimized charge transport. The observed effects can be enhanced even more by using different nanostructured surfaces.

As the bilayer cells are the easiest to be fabricated, this structure will be used in this study, as its focus lays on the other aspects which influence HSC's performance.

4.3 The fabrication process flow of the hybrid solar cell

One of the main advantages of the HSC is that instead of doping by high-temperature diffusion, one uses a deposition technique to create one of the active layers. Deposition of organic materials is usually done at room temperature and doesn't require a high vacuum; thus, one doesn't need any expensive equipment to manufacture this type of solar cell. This, besides others, allows reducing the cost of fabrication dramatically.

So, the main difference of the manufacturing process of HSC is that the diffusion step is changed to the low-temperature deposition. Sometimes, the additional step of deposition of the electron or hole transport layer (ETL or HTL, respectfully) is performed. Besides that, the manufacturing steps are very similar. A simplified diagram of the HSC fabrication process flow is illustrated in fig. 4.2.

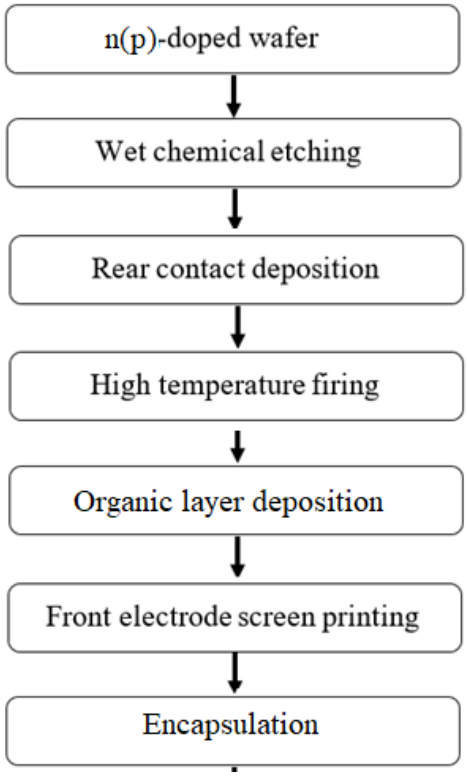

Figure 4.2 – The manufacturing process chain of the HSC

There are several methods of organic layer deposition. We will discuss in detail only those which are going to be used in this work:

1. Deposition from the aquatic solution: the organic material is dissolved in the liquid solvent, then the substrate is put into the vial with the prepared solution. Because it is energetically favorable for material's molecules to connect to the substrate's surface, the organic film is grown.
2. Spin-coating: the first step is again the solution preparation. Then the substrate is put on the spin-coater, and when the right amount of the solution is put on the wafer's surface, the whole system starts to rotate with the high velocity. Because of the mechanical tensions, the deposited solution is equally(in the ideal case) distributed along the surface, forming an organic film. The drawback of this process is that it is almost impossible to scale it to the industrial manufacturing size.

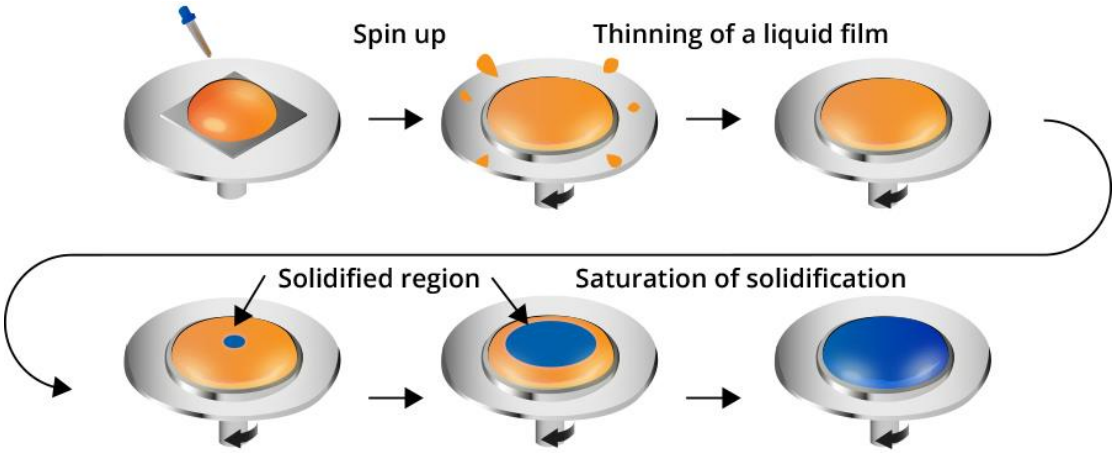

Figure 4.3 – The steps of the spin-coating process [20]

3. Blade coating: a process, similar to the spin-coating, but instead of a centrifuge, the organic material is distributed along the wafer by the blade. This is very similar to putting some butter on the bread. Between the surface and the blade itself, there's a tiny gap, so the wafer remains unharmed.

Among the described types of deposition, only blade coating is easily scalable to the industrial process. However, for lab purposes, the first two methods are preferable due to simplicity.

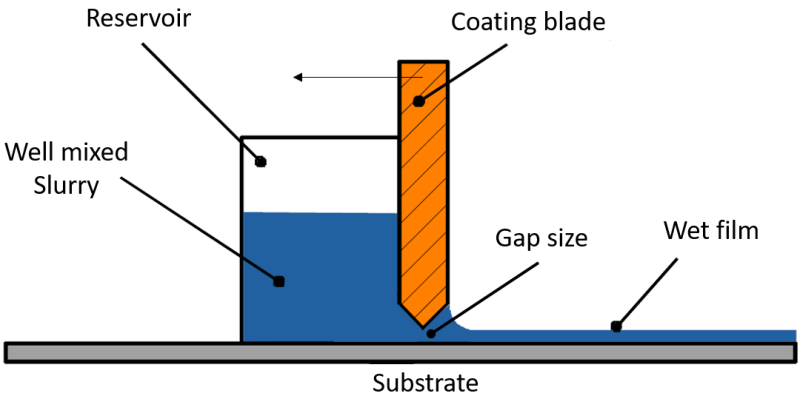

Figure 4.4 – Blade coating process [21]

4.4 The true “green” solar energy

It is common nowadays to treat solar cells as the “green” energy source. However, it is not like that. Although solar cells don’t produce any waste during their life cycle, they appear to be wasted once they’re out of working capacity. As there are 2 different types of dopants in the silicon solar cell, it is impossible to reuse the wafer in the fabrication processes, like crystalline silicon growth. In order to do that, the wasted module needs to be purified from one of the types of dopant. This can mainly be achieved by chemical etching. The common solvents for that include mixtures of hydrofluoric [22], as well as nitric and acetic acids [22]. However, the process requires high temperatures and a special atmosphere(pure nitrogen or in mixture with oxygen) [22]. This makes the reuse of the wasted silicon cells not economically rentable, so it’s way easier just to keep the old modules as the junk.

Another aspect to consider is the technological gases used for silicon cell fabrication. The main are diborane, phosphine and silane. All those are extremely toxic and highly flammable [23], and require the special security and transport systems to be implemented.

The opposite situation can be observed with the HSC. As the wafer is doped only by one type of chemical, it can be reused afterward as raw material for crystalline silicon growth with the particular type of conductivity obtained in the new crystal. In

order to be able to recycle the module, all other layers need to be removed. The easiest way is just to use the old-fashioned chemical etching. For organic films, this can be done with the utilization of affordable solvents under the room temperature(for most cases). It also doesn't require any special atmosphere.

Besides the active layer treatment, the electrodes need to be removed as well. This can be achieved by using the selective solvent, which will react only with the electrodes' material. But one might need two different types of the solvent, as the front and the rear electrodes are normally made from different metals or even conductive oxides (like ITO – Indium Tin Oxide).

The possibility to reuse the wasted solar modules enables the very new vision of the cell's life cycle, but also might reduce the price of the devices dramatically.

Let's briefly describe the process of the solar cell's recycling. The structure of the device we're trying to reuse is shown in fig. 4.5.

Figure 4.5 – The structure of the device to be recycled

As the metal layer is on the very top and the bottom of the cell, this one is the first to remove. This can be done using the common inorganic bases and acids. For example, Al can be removed by using the NaOH or KOH bases, as they're reacting with the oxide on the surface of Al. After this is done, the organic layer needs to be removed. The best way of doing that is to put the wafer into the proper solvent and then sonicate it for a while. The suitable solvent needs to be chosen according to the organic layer used. Some organics are even water-soluble, which makes the process even more simple and low-cost. The very last step is to remove all the leftovers from the wafer's surface. This is achieved by using the HF or HNO_3 acid. After this, one obtains the clean substrate,

ready to be used for the device fabrication or, at least, for the reuse while growing new silicon crystals.

So, the way of making the solar cell to be truly “eco” has been shown. Recycling these devices also has an extra economical advantage, which will be shown in chapter 7.

4.5 The energy band diagram of the hybrid solar cell

Although the hybrid cells contain much more crystalline material, their properties are very similar to the organic ones. Once again, one observes the exciton formation, dissociation on the built-in potential barrier, and only then, collection of the charge carriers. This process is the result of inserting the organic layer into the solar cell’s structure. However, the main principle of the formation of the p-n junction and obtaining the diode-like behavior still holds: one needs to align the bands of the device properly. This means that the offset between HOMO of the organic and the valence band of silicon, as well as between LUMO and the conduction band, needs to be made in order to minimize recombination and define the paths for photocurrent to flow [24]. Moreover, the electrode materials should be chosen carefully in order to get a proper work function values. The energy band alignment is shown in fig. 4.6.

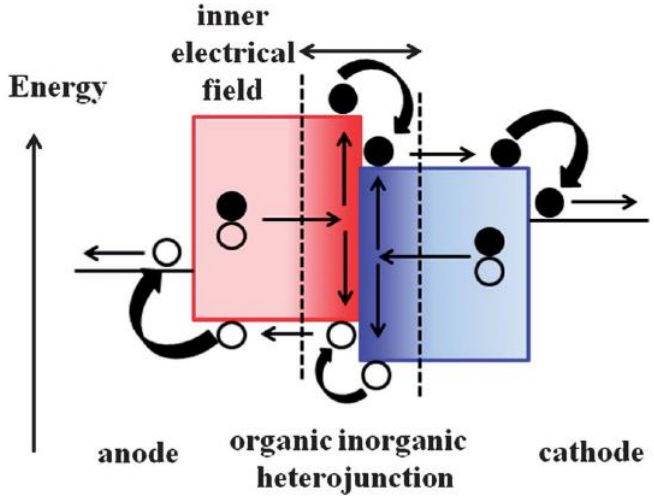

Figure 4.6 – Band alignment in the HSC [17]

It can be shown that proper band engineering can ameliorate the performance of the hybrid solar cell dramatically. It is well known that the p-n junction serves as the

barrier to separate the carriers, thus to enhance the photocurrent, as well, as to prevent electrons from contributing to the saturation current, thus to reduce the recombination [24].

In order to maximize the performance of the cell, one should improve its electrical parameters, in particular, the open-circuit voltage and the short-circuit current. This is possible to achieve by doing wise band engineering.

In the hybrid cells, the V_{OC} is defined by the offset between the LUMO of the organic layer and the conduction band of silicon. Thus one should look for the organic semiconductors with the positions of the LUMO in the energy band [24]. On the other hand, one should not obstruct the holes traveling to the anode. Thus the offset between silicon and the HOMO of the organic layer should be minimized. Fig. 4.7 illustrates this principle. Thus, separate control over both V_{OC} and J_{SC} is achieved, opening wide possibilities to tune the solar cell's properties.

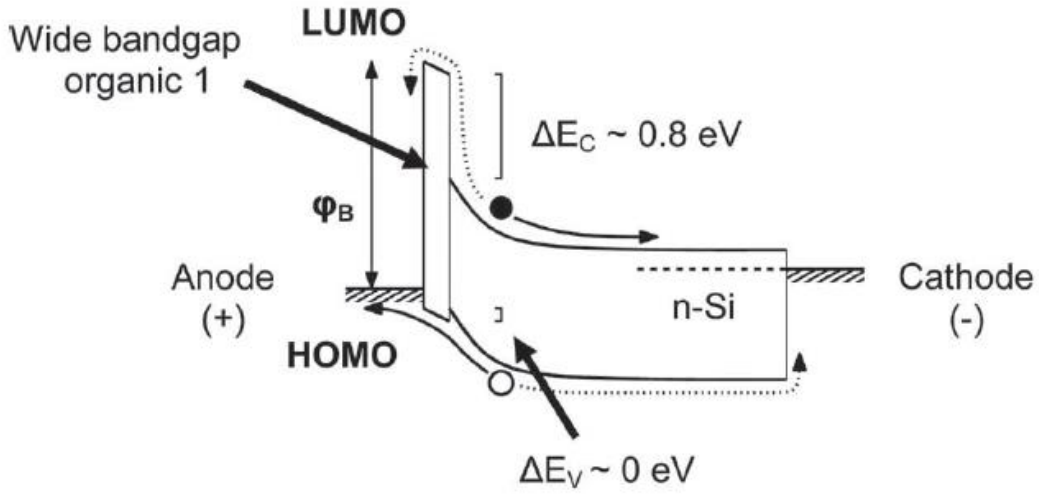

Figure 4. 6 – The right energy offset between organic and inorganic layer enhances the performance of the HSC [24]

The very last thing to mention is that the holes also contribute to saturation current, thus after optimizing the LUMO-conduction band offset, one should look for the ways to prevent holes injection [24], thus to reduce recombination, included by this type of charge carriers.

4.6 The advantages of utilizing hybrid solar cells

As it has been already mentioned, the most important advantages of the hybrid solar cells in comparison with the silicon ones are the simplicity of fabrication and the possibility to recycle the wasted modules. The best way to highlight these advantages is to compare two types of cells.

Table 4.1 – The comparison of the hybrid solar cell with the silicon one

Parameter	Silicon technology	Hybrid technology
Efficiency	23%	15%
Device lifetime	20-30 years	Defined by the lifetime of the silicon module
Technology complicity	Requires high-temperature processing under the vacuum	Can be deposited from under the room temperature
Scalability	Easily scalable	Needs investigation
Recyclability	Economically not affordable, requires special conditions	Can be recycled with materials reused afterward
Cost	Affordable	Extremely low-cost

So, let’s discuss every aspect more in detail:

1. *Efficiency:* as silicon turns to be a crystalline material, which means that it has a regular space alignment of the unit cells, it is extremely efficient material with minimal recombination losses. In turn, hybrid solar cells have an organic film as one of the active layers. As these types of semiconductor materials are known to be not well-structured, there’s now long-range delocalization paths for charges to travel across the active layer towards the electrodes. This means the higher recombination and thus results in lower efficiency. However, with careful energy band engineering and utilization of different materials, it is possible to minimize this difference in efficiencies [25-27].

2. *Stability*: in both cases, the device's lifetime is defined by silicon. However, it can be that the additional organic layer protects silicon from the radiation, which can result in an improved lifetime.
3. *Technology complicity:* silicon is one of the most processable semiconductor materials, as its manufacturing technology is almost perfectly studied nowadays. However, when comparing with the hybrid solar cells, it turns that silicon technology is way more complicated. To create a p-n junction device, the high-temperature diffusion step needs to be implemented. This means utilization of the complicated equipment in order to ensure vacuum, but also expensive and dangerous gases, like phosphine, silane, etc. On the other hand, when fabricating hybrid cell, pretty much all the steps are performed at room temperature or higher, but not more than required for contact material evaporation. Thus, creating hybrid devices is way easier, comparing to the classical wafer processing methods.
4. *Scalability:* It is obvious that nowadays, silicon technology is easily scalable. The more complicated situation is observed, when it comes to hybrids, as one needs to precisely control the deposition parameters when creating large-area devices, as it turns to be problematic to ensure the uniformity of the deposited films. However, several techniques can be adopted at the industrial scale, with the most promising among those – the blade coating.
5. *Recyclability:* as it was sown above, it is possible to recycle silicon solar cells by implementing chemical etching techniques. However, this still requires high temperatures(around 950 °C) and special ambient conditions(like nitrogen atmosphere). This is due to the different types of dopant available at the different depth of the wafer. This also means that the part of the wafer will be removed anyways and cannot be reused. It turns that the cost of such a process is quite high, which makes the recycling unaffordable. The opposite situation is observed with hybrid devices. The organic layer can be removed with the appropriate solvent under room temperature conditions and doesn't have any limitations concerning the ambient atmosphere, which makes the

process extremely cheap. After the recycling, the obtained silicon wafers contain only one type of the dopant, thus they can be used as raw material when growing the new crystal of the same conductivity type.

To conclude, hybrid solar cells are the photovoltaic devices, consisting of the silicon wafer as one active layer and the organic film – as another. The low-temperature simple deposition techniques, together with the nature of the film, enable certain advantages in the utilization of this technology. The main are simplified processability, lower cost comparing to the fully silicon cells, and recyclability.

5. PHOTOVOLTAIC APPLICATIONS OF CLONIDINE, SULFACETAMIDE AND ITS MIXTURES

This research was inspired by the idea of utilizing affordable materials in photovoltaic devices. The advantages of this approach were widely described in the previous chapter. However, the most efficient organic materials for hybrid solar cells are still hard to produce and, thus, the cost of the device, containing these layers, is comparable to the price of the classical silicon cell.

In contrast, the materials, which properties will be investigated in this work, are easy to get, affordable and low-cost in processing. Although not the pure materials are used to investigate the properties of the devices, but rather the medical drugs containing these materials as an active ingredient, the general properties, which are in the scope of this work, are still observable.

5.1 The working horses of the hybrid cells: Clonidine and Sulfacetamide

Two materials were used in this study. Both of them are polymer structures, commercially available in the form of medical drugs, either solution or pills. The chemical structure of the polymers is shown in the fig. 5.1.

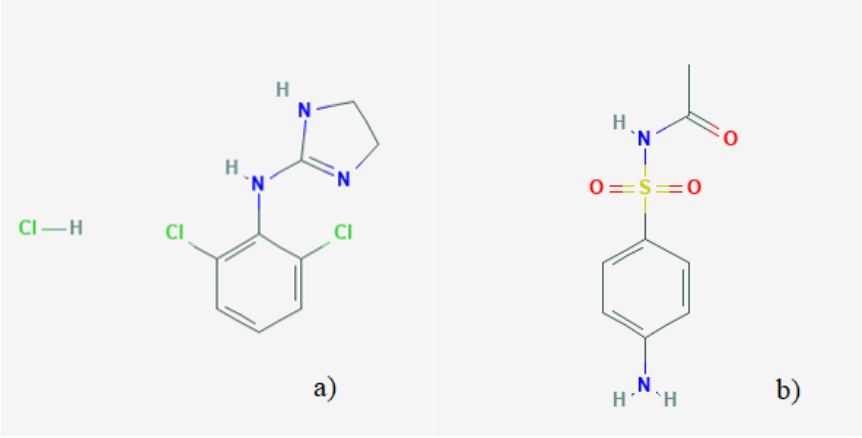

Figure 5.1 – The structural formulas of a) clonidine; b) sulfacetamide

One great advantage of these materials is their water solubility. So, in order to prepare the solution of medical drugs, one just needs to dissolve the solid phase in the distilled water and filter the additives, the presence of which could influence the

devices' performance. Another important thing is that the medical drugs, containing these materials, are extremely low-cost, although it's impossible to get the pure structure out of it. However, even with non-pristine materials, we were still able to observe the relative change in the device's parameters with the variation of the morphology and/or the composition. This will be further described in detail.

5.2 The first steps

The first part of this study was performed in the Lashkaryov Institute of Semiconductor Physics. Doing scientific research in Ukraine, one should be extremely brave and creative in order to get the most of information from the very limited resources available and to face the obtained results without losing faith.

But besides all the challenges one could face, this is also the perfect environment for people to discover their ingenuity and to connect with the colleagues, who shows the same passion about discovering the secrets of nature at any price.

During this period of study, two important features of the hybrid solar cells were studied. First – the influence of the composition and the deposition time on the structure of the organic films were observed, and second – the dependence of the performance of the cells on the structure was researched.

5.2.1 Devices preparation. A typical structure of the hybrid solar cell is shown in fig. 4.5. The similar structure was used for the devices prepared: the substrate was chosen to be n-type crystalline silicon with the orientation of <100>; the surface of the wafer is patterned in order to form the pyramid structures to decrease the reflectance and enhance the film growth; the back of the substrate has a thin n+ layer, which is fully covered by Al, which forms the back contact; Al, together with n+ form the ohmic contact, which prevents charge injection; on the front side the organic films is deposited in order to create the specific energy level alignment(the diode structure); the front contact was formed by printings the frame with silver conductive paint. The uncovered

area defines the area of the cell (this will be used for the J-V measurements). Devices cross-section is shown in fig. 5.2.

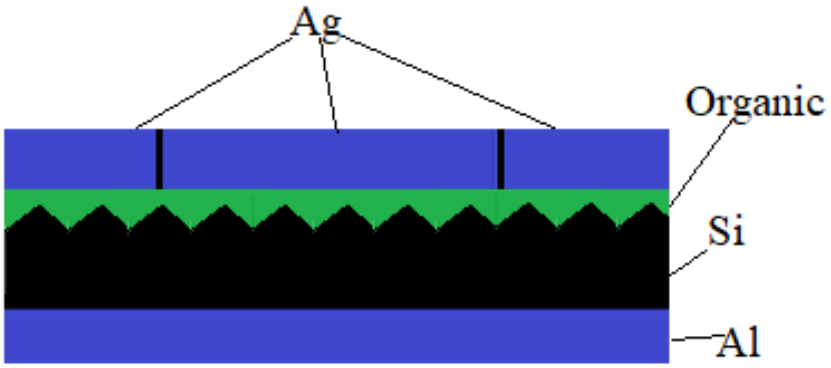

Figure 5.2 – Devices' structure

Four different solutions were prepared: both pristine clonidine and sulfacetamide, and two mixtures with different volume ratios: 1:3 and 3:1, clonidine:sulfacetamide, respectively. The substrates were dipped into the solution and deposition was taking place because of the unbonded chemical connections on the silicon surface. The process was taking place under normal ambient conditions. Process parameters are grouped into table 5.1.

Table 5.1 – Parameters of the organic films deposition process

Parameter	Value			
Ambient temperature	25 °C			
Ambient pressure	101 kPa			
Deposition time	90 min		100min	110min
Volume ratios, CLO:SULF	1:0	0:1	1:3	3:1

Solutions for the deposition were prepared using the pristine materials, dissolved in water. For sulfacetamide, the medical drug itself is a solution; thus, it was used without any modifications. Clonidine hydrochloride is commercially available in the

form of the tablet, so it was first dissolved in double-distilled water, and then filtered using filter paper to remove the large solid particles. The resulting solutions were either used directly for deposition or were mixed together.

After deposition, the cells have been taken out, they dried, and the front contact was manually deposited on top of the structure. The conductive silver paint was used as the contact's material. The top view of the resulting devices is shown in fig. 5.3.

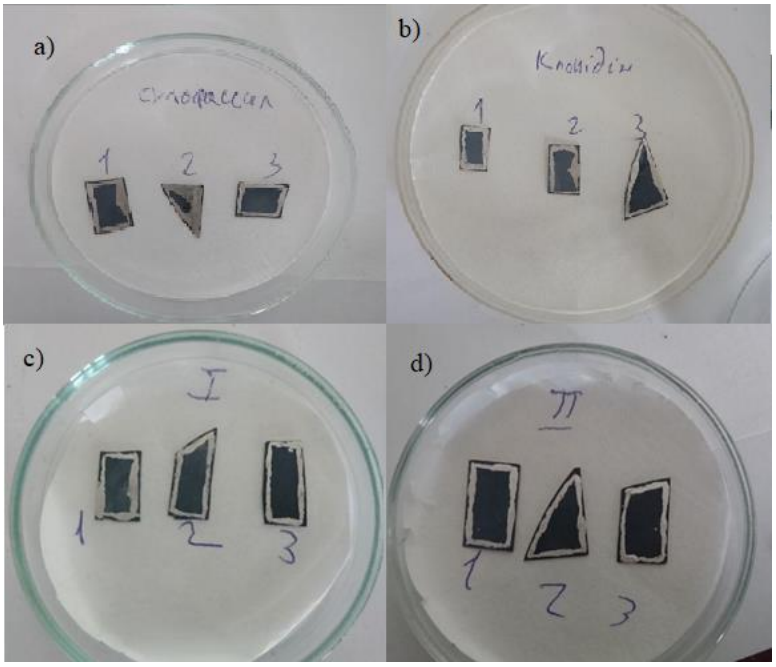

Figure 5.3 – The top view of resulting devices with a) sulfacetamide; b) clonidine; c) 3:1 CLO:SULF; d) 1:3 CLO:SULF

One thing to mention about the samples is that the shapes of the substrates and, thus, the areas of the devices are different. This was made on purpose, in order to maximize the number of samples obtained from one wafer and, thus, to minimize waste of material. However, in order to avoid taking into account the shape and area factors, the experimental results were normalized to the areas of the devices, respectively(the measured J-V characteristics are not area dependent).

To facilitate the morphology observations, the optical microscopy of each sample was performed primarily to the front contact deposition.

5.2.2 Morphology study using optical microscopy. The samples were placed on the microscope slide, and the optical imaging has been done using the semi-professional camera. The full evolution of the film, depending on the composition and deposition time, can be seen in Appendix A, here we will focus on slices, which correspond to the same composition, and analyze the deposition time dependence.

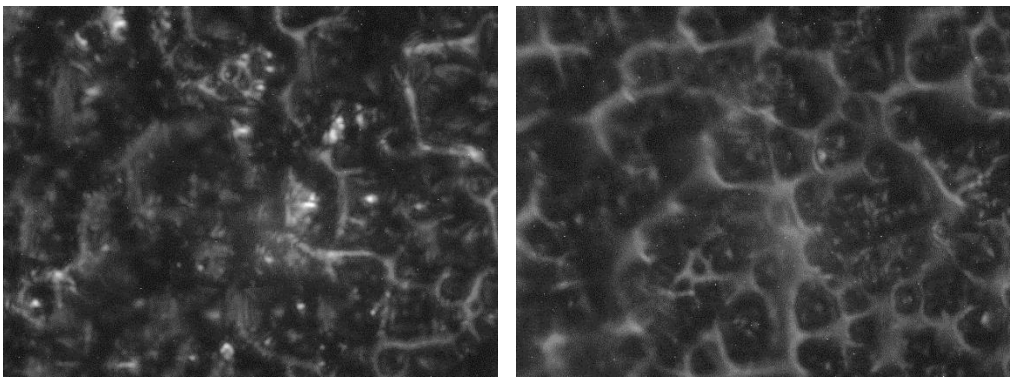

a) b)

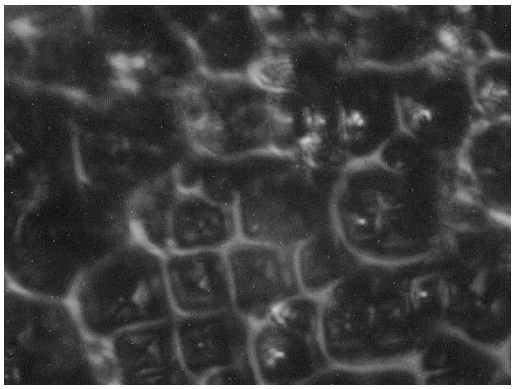

c)

Figure 5.4 – The sulfacetamide film morphology with the deposition time of a) 40 min; b) 60 min; c) 100 min

With any value of time, one still can see the uncovered areas of silicon. This means the weak interaction of the organic molecules with the substrate's surface. However, the matter of interest here is the pattern, formed by sulfacetamide. Even after 40 min of deposition, it is already seen that the net structure starts to be formed. Although this could be a sign of the self-organization process taking place, the valleys between the pyramids seem to be uncovered by the organic material, resulting in the

short circuits between silicon and the top electrode, which can be seen from the J-V characteristics.

Even with the addition of clonidine, the organized figures, formed by the film, remain. This is an indication that sulfacetamide is responsible for the self-organization process within the film. Fig. 5.5 shows that in every film, even with the minimal deposition time, the net structure is formed.

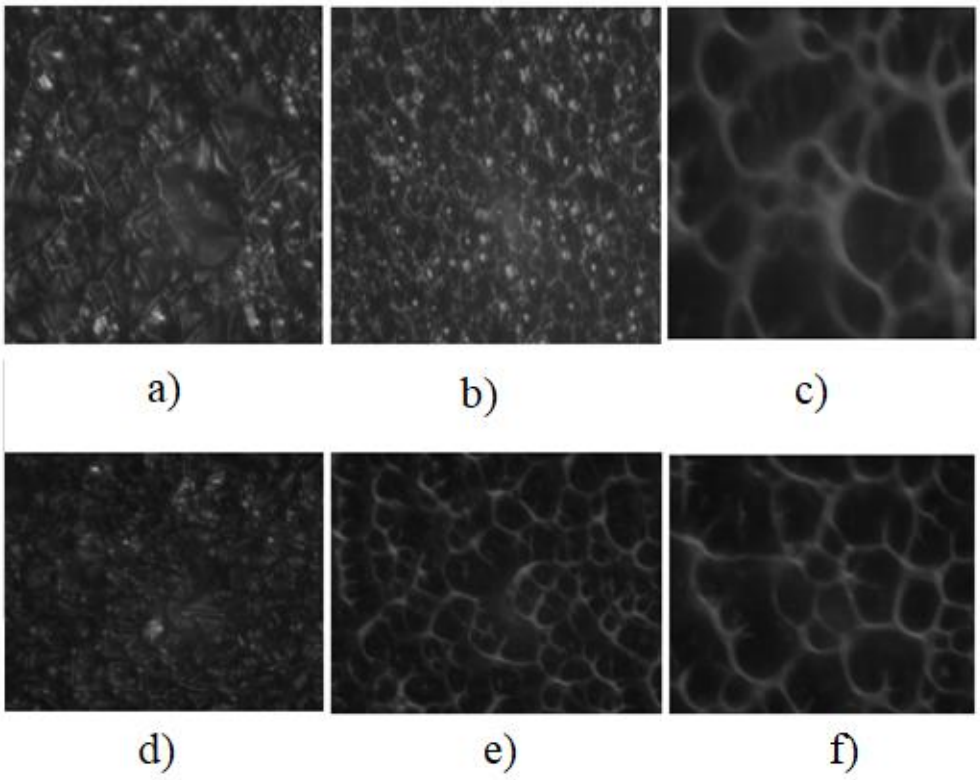

Figure 5.5 – The deposited films of CLO:SULF with the ratios of 3:1 (a-c) and 1:3 (d-f), with deposition times of 40 min (a, d), 60 min (b,e) and 100 min (c,f)

Another thing that proves the properties of sulfacetamide is that no organized structure is formed with the pure clonidine (fig. 5.6). Although the growth time of the film is much higher, probably because its molecules are more active to Si than the SULF ones, and the wafer's surface is covered already after 60 min of deposition time.

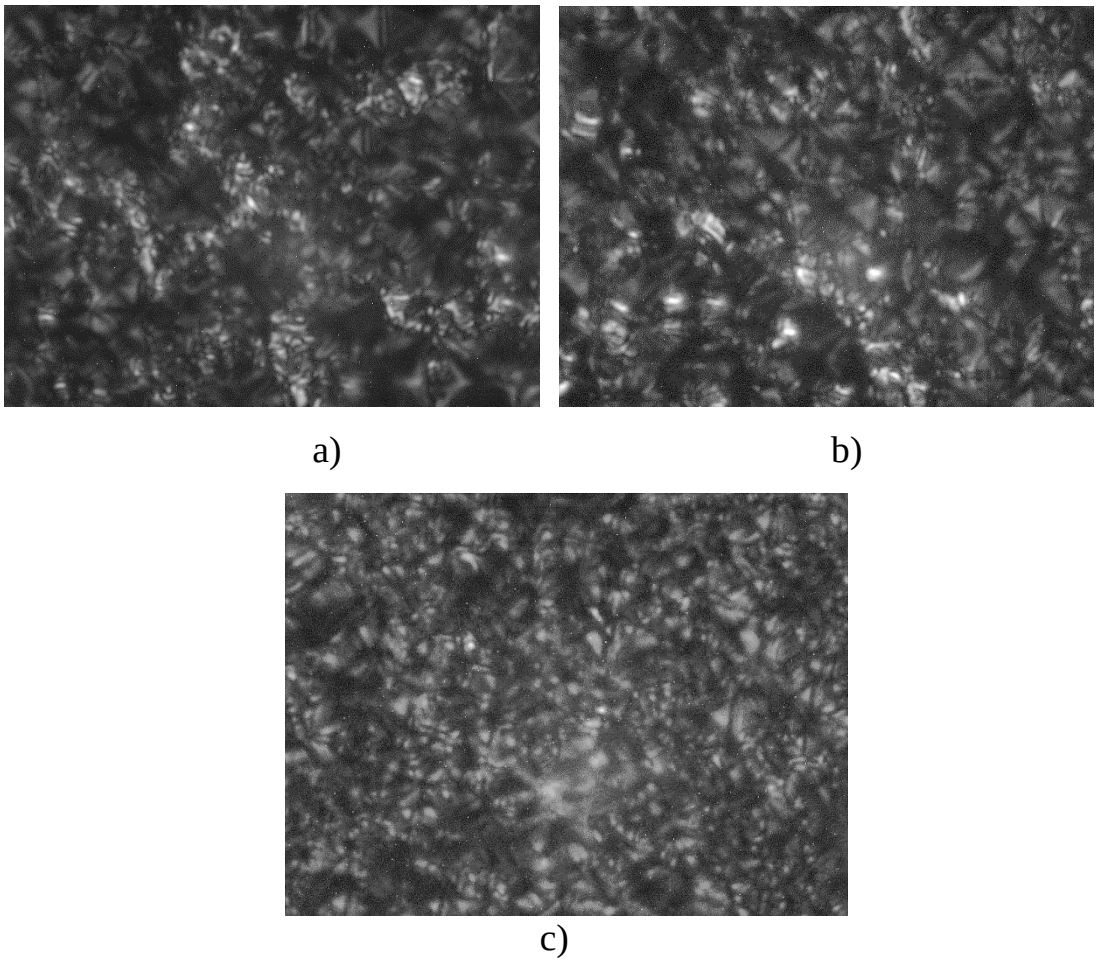

a) b)

c)

Figure 5.6 – Clonidine films on Si after a) 40 min; b) 60 min; c) 100 min of deposition

Another thing to be noticed is that clonidine distributes more uniformly along the surface, which results in more carefully covered pyramids and smoother surfaces.

Finally, the very last moment to state is that all the films were grown during the same fabrication cycle; thus, the ambient conditions were the same and the solutions were made of the same precursors.

5.2.3 Devices characterization by J-V curves measurement. In this subsection, the correlation analysis of the electrical performance of the devices on the composition and morphology of organic films will be performed.

5.2.3.1 The experimental setup. The experimental setup is dedicated to dark I-V curves measurements of the devices. With the small additions that one was turned into solar simulator, thus the option of the I-V measurements under illumination has been added. The building blocks of the setup are the measurement chamber, the light

source, the control and measurement block, and the analog-to-digital converter (ADC), which samples the measured points and outputs it into the computer. The structural scheme of the setup is shown in the fig. 5.7.

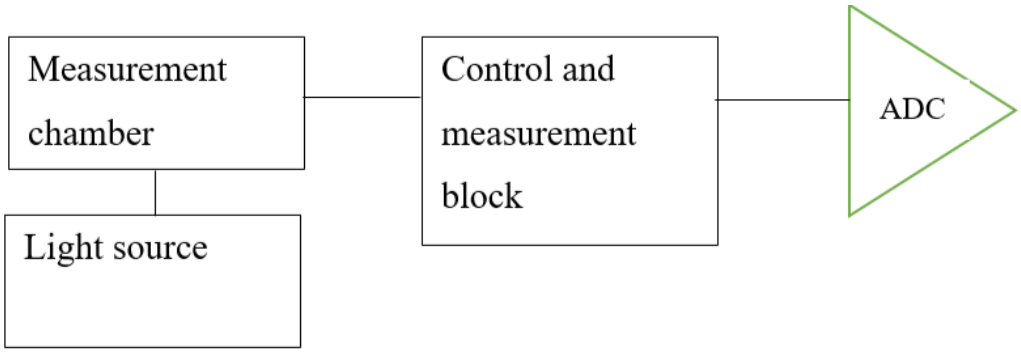

Figure 5.7 – The structural scheme of the I-V measurement experimental setup

Let's have a closer look at every part of the setup:

1. The light source: the xenon or mercury lamp is used to create a light spectrum, which is stated in the Standard Test Conditions (AM1.5G), or the sun spectrum.
2. Measurement chamber: the dark chamber, not transparent at all for the outer light, in order to ensure the proper measurements in the dark. The chamber has a sample holder, two-point electrodes to contact the sample's electrodes and a slit for the light source.
3. Control and measurement block: is dedicated to switch the applied signal polarity and to measure the data points, while creating the bias for the sample. Normally one changes the voltage across the sample while measuring the output current. Then these pairs of data values are transferred to the ADC.
4. ADC: the electronic circuit which converts the analog values of current and voltage to the binary numbers, readable by the computer logic.

As the control and measurement block, the «TKC-006» machine was utilized, as it's designed for the I-V measurements and can sense currents down to nanoamperes. The machine is shown in fig. 5.8, a) and ADC are visualized in fig. 5.8, b).

Figure 5.8 – The a) control and measurement block; b) ADC

The measurement procedure consists of the next steps:

1. Loading the sample into the measurement chamber.
2. Positioning of the point contacts, in order to establish the electrical connection with the sample.
3. Closing the chamber.
4. Input the range of measurements.
5. Measure the dark curve in the 1st quadrant (forward bias).
6. Switch the polarity of the applied voltage.
7. Measure the dark curve in the 3rd quadrant (reverse bias).
8. Turn on and insert the light source.
9. Repeat steps 5-7.

Measured data points are then transferred into the computer and saved as a binary text file.

5.2.3.2 Measured J-V characteristics. To clarify the origin of the I-V curves shape, the correlation analysis with the OM(optical microscopy) images will be performed. By this, one should understand that the surface images and the I-V curves for the particular devices will be compared.

The advantage of this method is that one can actually determine, which artifacts on the surface cause the particular behavior of the I-V characteristics, and then connect

these artifacts with the deposition process in order to see, if it's possible to improve the procedure, in order to get better performance.

Let's start with pure sulfacetamide. Fig. 5.9 show the evolution of the film and the I-V curves for different deposition times:

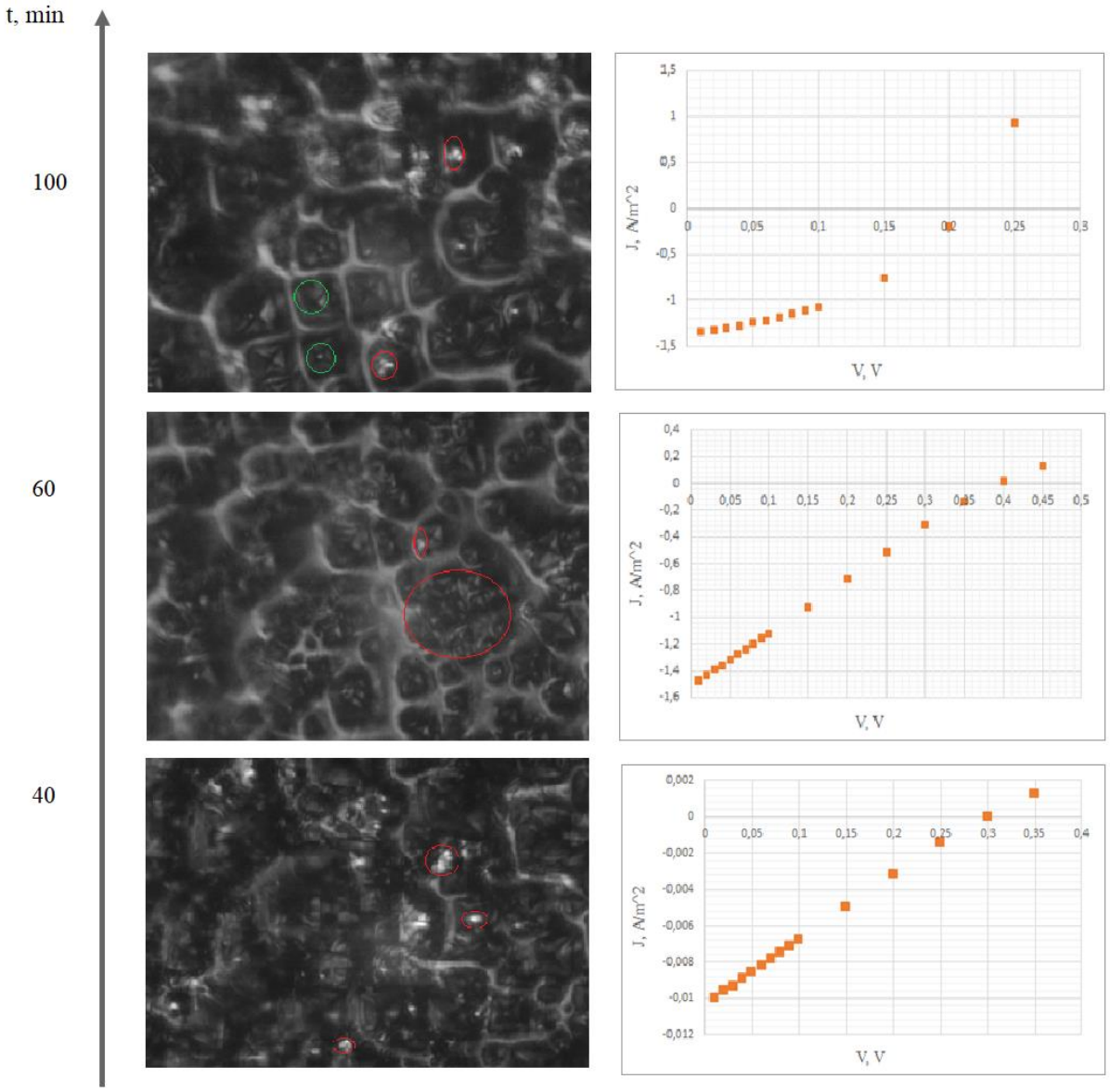

Figure 5. 9 – Film morphologies and corresponding J-V curves for sulfacetamide

As can be seen, for both 40 and 60 min of deposition, there are still uncovered areas of silicon, this can be seen from the shining of the pyramid tips(marked with red circles). This results in short circuits across the p-n junction; thus, no internal electric field is created for charge separation, and thus there's no diode-like behavior observed

on the J-V curves. Recalling the equivalent model for solar cell, the short circuits result in a large value of R_{sh}, and thus the J-V curve resembles the shifted resistor curve.

The performance of the cell is enhanced, when deposition time is increased up to 100 min. Then one sees the S-shaped diode-like curve. However, on the surface, there's still uncovered zones, and, probably, the valleys between the pyramids remain free of the organic film as well(marked with green circles). Also, the influence of the shunt resistance is, however, still considerable, which can be seen from the almost straight region of the J-V(0…0,1 V).

Better performance was achieved with the pristine clonidine films:

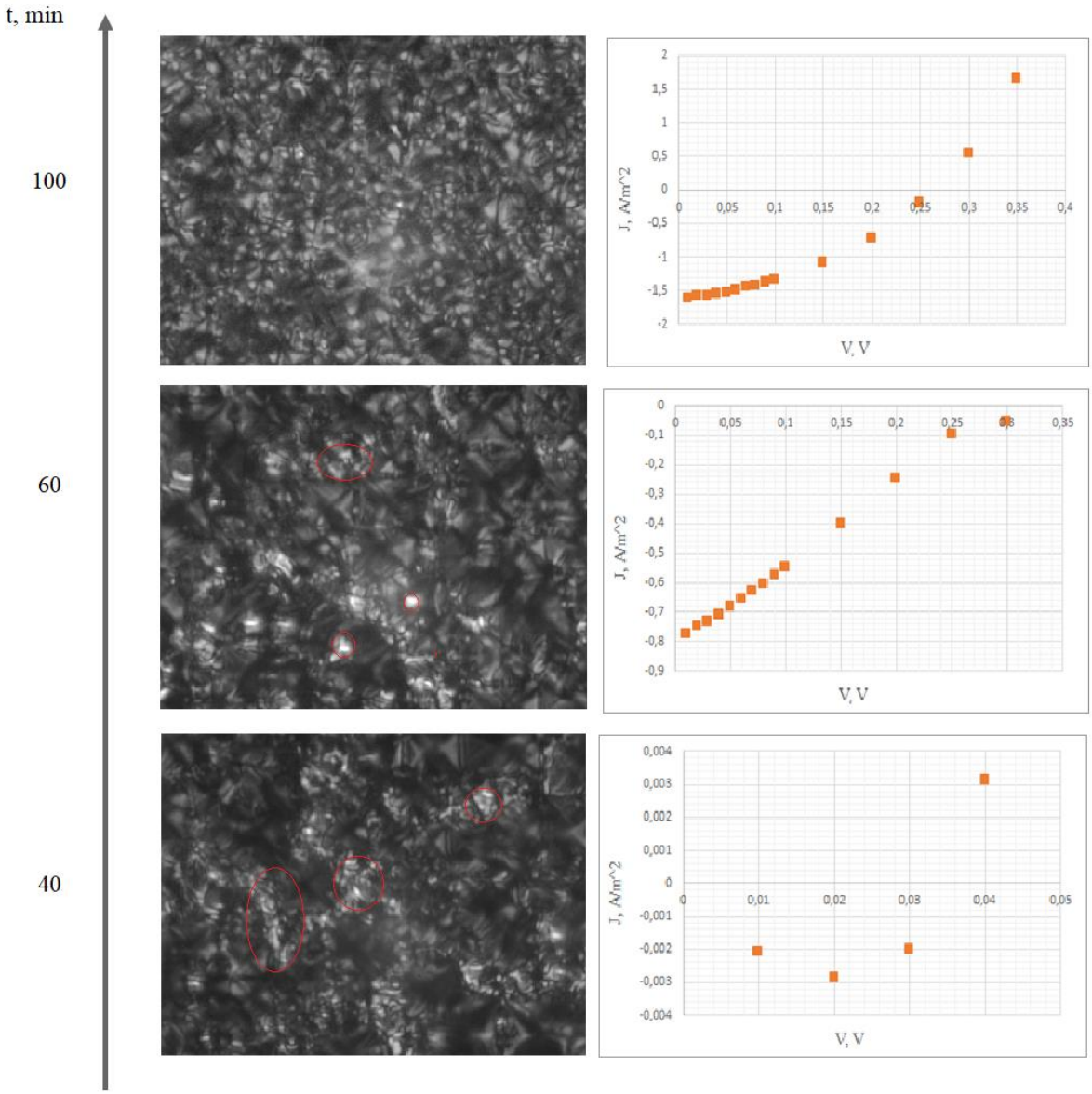

Figure 5.10 – Film morphologies and corresponding J-V curves for clonidine

Although the first sample(40 min) seems to be measured in a wrong way, having the J-V curve's shape, which cannot be fit with any of models, it's included in the graph just to visualize the reasons, why it's not taken into account when calculating the device's parameters.

The problem with 60 min sample is the same, as for sulfacetamide: not all the pyramids are completely covered, and, thus, there're short circuits, resulting in the noticeable shunt resistance.

When deposition time is increased to 100 min, the device behaves like a proper solar cell, which can be seen from the J-V plot. Another evidence for that is the absence of the artifacts on the wafer's surface. All the pyramids seem to be covered by the organic film of clonidine.

Other situation can be observed with the blends:

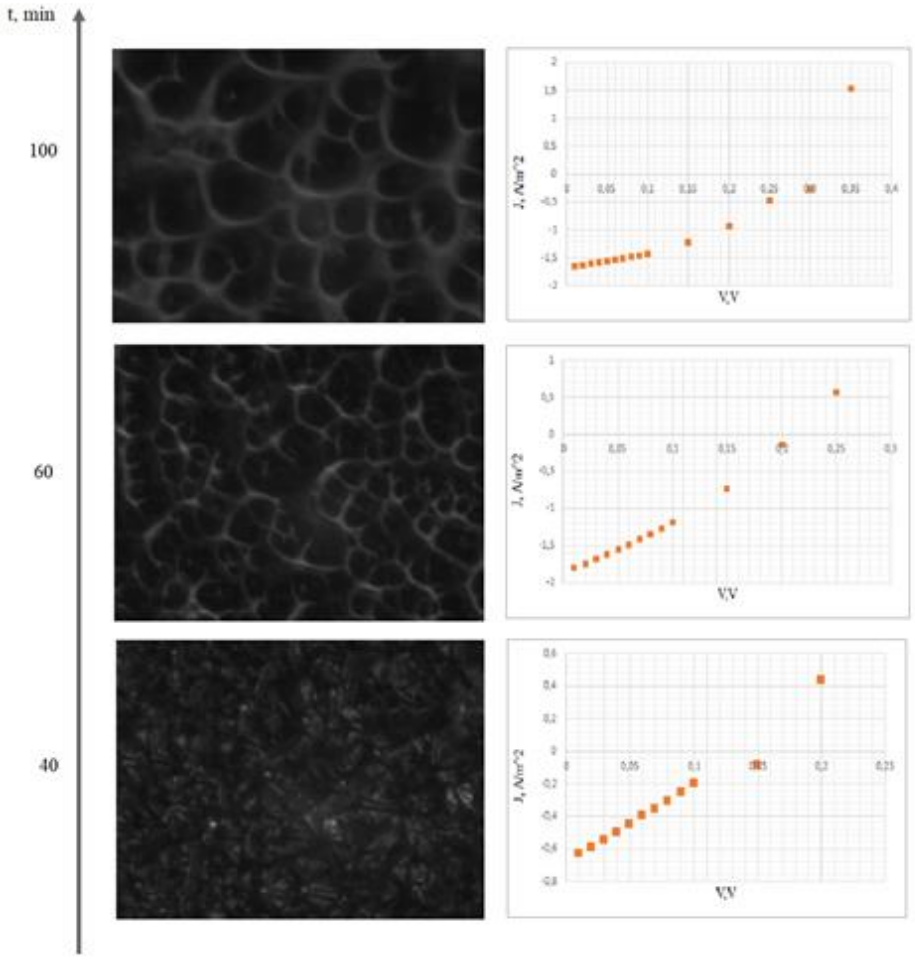

Figure 5.11 - Film morphologies and corresponding J-V curves for 1:3 - CLO:SULF

Here we can see that 40 min is still not sufficient for the film to cover the surface completely. However, already with 60 min, one can observe the diode-like behavior of

the J-V characteristics. Another thing is the enhanced electrical parameters, as compared to pristine films, especially the short-circuit current value. The V_{OC} is also larger than in pristine SULF films, which is probably the result of the clonidine addition. As can be seen from the previous graph, devices with pristine clonidine films have V_{OC} values around 0,25…0,3 V. The I_{SC} is, supposedly, enhanced by the sulfacetamide, as pristine clonidine films have this value lower than the blend. The net structure within the film can also be a feature; however, this requires further investigation.

Finally, the graphs for the second blend are shown in fig. 5.12:

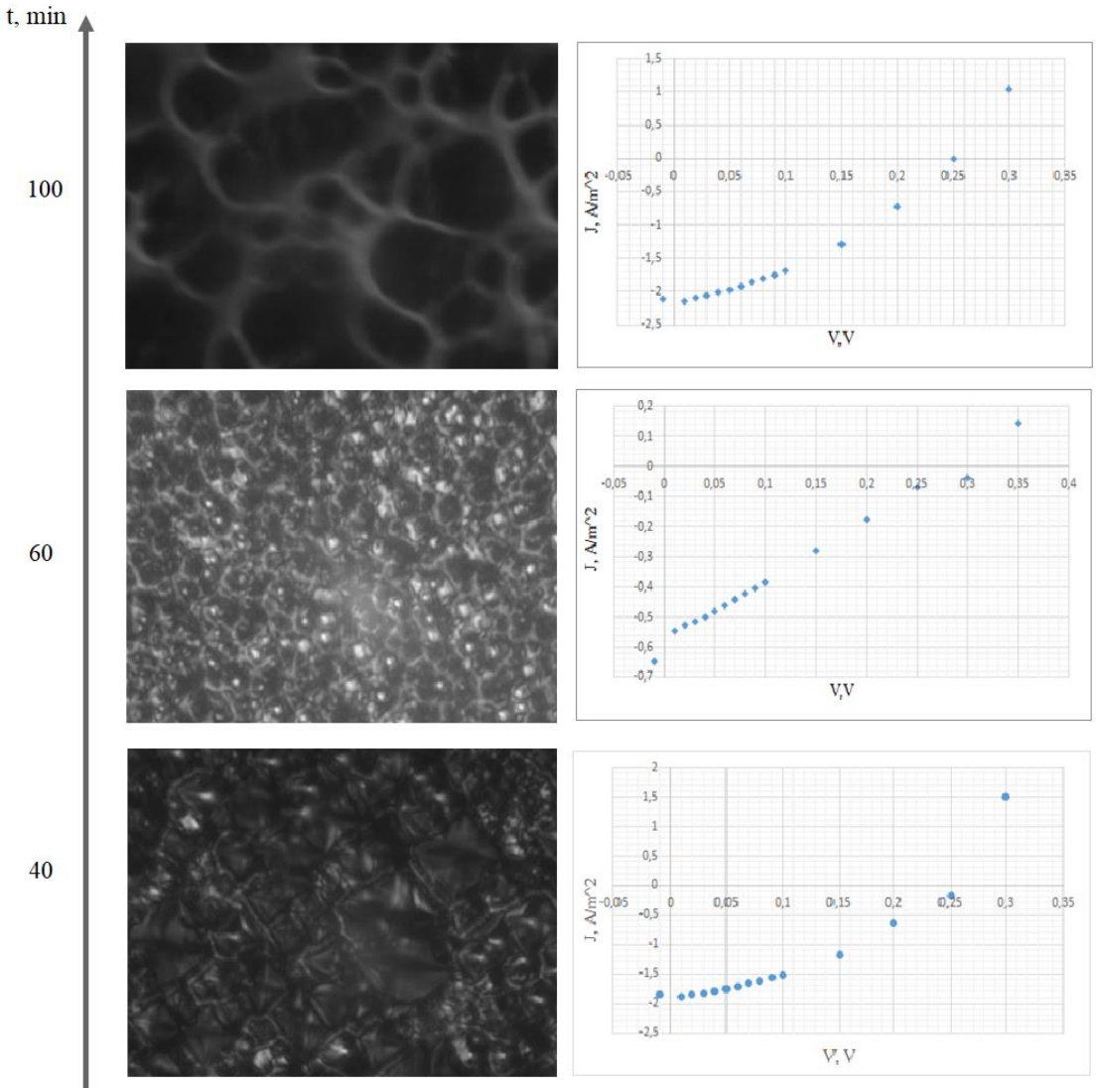

Figure 5.11 - Film morphologies and corresponding J-V curves for 1:3 - CLO:SULF

Here all the devices behave like diodes; however, the one with deposition time of 60 min has a drop-in I_{SC}, which means the increased recombination within the device.

The problem could be the structure of the film because, in this moment of time, the net structure hasn't been formed yet, but the wafer's surface is already covered. This "edge" structure of the film could result in higher recombination; however, to prove this, the role of the net structure of the organic layer needs to be figured out. Another fact to state is that the organized film(deposition time of 100 min), expresses enhanced I_{SC} value, which again returns us to the question of the structure's contribution to the device's performance.

The evolution of the J-V curves depending on the composition and morphology of the films, is shown in Appendix B.

5.2.3.3 Devices' parameters calculation. Basing on the obtained data and using equations 2.1-2.5, the electrical parameters of the devices were calculated. The input power, or the power of the light source, incident to the device's surface, was $P_{IN} = 30\ \frac{W}{m^2}$. The maximum output power P_{max} was determined from the J-V graphs by calculating the values of power for every data point, fitting the obtained curve and finding the maximum value. The example of such plotting is shown in fig. 5.12:

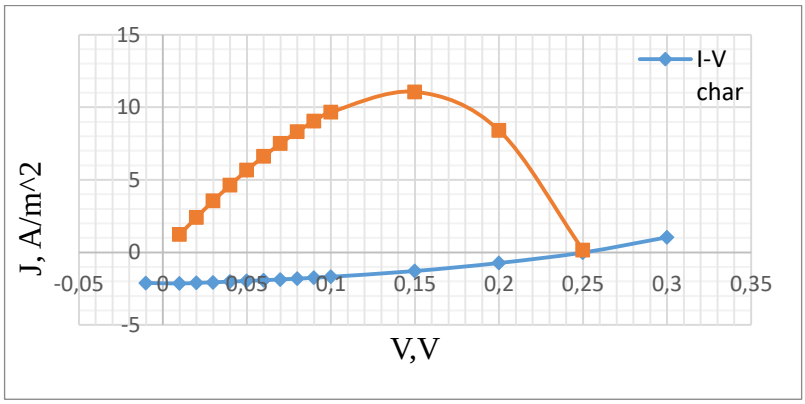

Figure 5.12 – Determining the maximum value of power

It can be clearly seen that the maximum power is produced by the device when the voltage across the sample is 0,15 V. In the same manner, the values for the rest of the samples were determined. This data is grouped into table 5.2.

Table 5.2 – Maximum output power

Sample name	Deposition time, min	P_{max}, uW
CLO	40	-
	60	2,17
	100	13,89
SULF	40	0,07
	60	1,63
	100	7,5
1 CLO:3 SULF	40	6,7
	60	2,17
	100	11,07
3 CLO:1 SULF	40	1,79
	60	5,22
	100	12,2

After determining maximum output power, the electrical parameters of the cells were calculated. To make calculations insensitive to the device's area, it was also measured and the results were normalized to the obtained values. Using the formulas mentioned above, the values of the fill factor (FF) and power conversion efficiency(PCE) were calculated. The values of V_{OC} and I_{SC} were determined from the measured J-V characteristics.

Here, the example of the calculations for one sample will be presented. The same has been done for the rest, and values are grouped into table 5.3.

Consider the 3 CLO:1 SULF sample, deposition time of 100 min. The measured J-V characteristic is shown in the fig. 5.13:

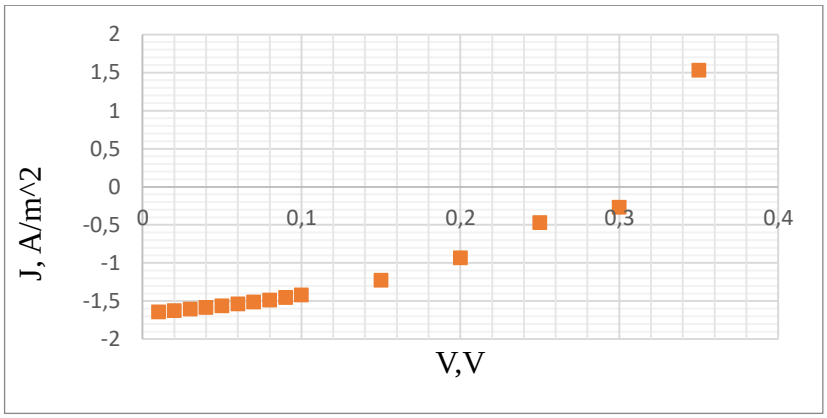

Figure 5.13 – The J-V curve for 3 CLO:1 SULF sample, deposition time of 100 min

Measured $V_{OC} = 0{,}31\ V$, $I_{SC} = 1{,}64 \frac{A}{m^2}$. From table 5.2 $P_{max} = 12{,}2\ uW$. The active area of the device was measured manually, S=64,5 mm^2.

Calculating the fill factor:

$$FF = \frac{12{,}2 \cdot 10^{-6}}{1{,}64 \cdot 64{,}5 \cdot 10^{-6} \cdot 0{,}31} = 0{,}383 \cdot 100\% = 38{,}3\ \%$$

Calculating PCE:

$$PCE = \frac{1{,}64 \cdot 0{,}31 \cdot 0{,}383}{30} \cdot 100\% = 0{,}65\ \%$$

The values for all the samples are listed in Appendix C.

5.2.4 First steps: results and discussion. As the result of the first part of the research, 4 sets of samples were prepared in order to observe the influence of the composition of the organic films and its morphologies on devices' performances. It was shown that the best performances one can get with the deposition times of around 100 min. However, this isn't the valid parameter to control the process, as this value will be changing with the change in ambient conditions and with the substrate's surface parameters, as it will be shown later on. Thus, the valid criteria are that the film should be thick enough to cover the whole pyramids on the wafer's surface but thin enough to prevent the dramatic increase in recombination. The indicator for this is the formation of the net structure on the film's surface, which takes place when sulfacetamide is present in the chemical composition. As it was shown in [28], the net structure is forming after

the film has covered the tip of the pyramid. Thinner films result in non-uniformly covered surface, which leads to the short circuits between the top electrode and silicon.

Among the samples with different compositions, the ones with a slight addition of clonidine have demonstrated the best performance, resulting in the highest value of the open-circuit voltage and the fill factor. However, the highest values of current were obtained for the 3 CLO:1 SULF film, which may indicate several statements:

1. The film acts as an anti-reflective coating, resulting in lower losses of the incident light.
2. The blend reduces recombination, ensuring better charge transport.

The addition of clonidine also enhances the open-circuit voltage, as can be seen for the 1 CLO:3 SULF film. This may be the result of either additional absorption peak in the spectra or of the photon-down conversion, which means that the film absorbs light and then re-emits it with different wavelengths, which is absorbed by silicon. The prove of this requires photoluminescence measurements to be done.

5.3 The shape of sulfacetamide

In this section, the properties of sulfacetamide will be discussed. As clonidine is a controlled medical drug in many countries, it's sometimes tricky to get it even for scientific purposes; thus, the second component was studied. Sulfacetamide is legally distributed as the medical drug in the form of eye drops. Although one cannot get the pristine material out of the solution, it still makes sense to study its properties, as all the devices discussed before, were made using medical drug solution; thus all the dependencies one has seen, are coming from the SULF drug properties.

5.3.1 Devices preparation: the native oxide aspect. Three sets of devices were prepared: one - by deposition from aquatic solution, another – by spin coating, and the last one also by spin coating, but with the glass substrate. First two were used for the characterization of the devices, while the last set was made to research the properties of the pristine sulfacetamide. The detailed description of the process will be given in the corresponding sections. Here, only one aspect will be highlighted.

First two sets were prepared using textured silicon substrates. By texturing, one should understand the wafer's surface, covered with pyramids. One key As sulfacetamide is present in the form of the aquatic solution; silicon surface should be hydrophilic for the organic molecule to connect to it by H^+ and/or OH^- groups. The easiest way to ensure this is to induce a thin layer of native silicon oxide to grow at the wafer's surface. For this purpose, thermal annealing of substrates was performed prior to deposition.

As this step hasn't had a place in the devices fabrication process, performed during the first part of the research, this is the key indicator, giving the idea of how to optimize the deposition process for sulfacetamide by enhancing dramatically the speed of film growth. Devices, which substrates were previously annealed, had extremely high film thicknesses, which is completely different for the devices discussed above when even after 100 min of deposition, the surface wasn't completely covered. Thus, thermal annealing enhances the speed of organic film growth, in case deposition is taking place from the aquatic solution. The evidences that will be presented in the upcoming sections.

5.3.2 Silicon-polymer interface and organic film thickness characterization. SEM of silicon-polymer cells. In order to determine film thickness and to observe the interface between silicon and the organic film, the cross-section SEM(Scanning Electron Microscopy) imaging has been done.

5.3.2.1 SEM basics. Scanning electron microscopy(SEM) is a powerful tool to analyze the samples. The principle of the measurement is that one scans the surface of the sample with the electron beam; thus, a raster image of the surface is formed, when the detectors collect either scattered from the surface or secondary electrons. The contrast in the image is formed because different materials at the surface have different conductivity, so they will reflect electrons in a different way. The same can be applied to the inhomogeneities at the surface of the sample. The structure of the SEM setup is shown in fig. 5.14, and the collection of electrons is illustrated in fig. 5.15.

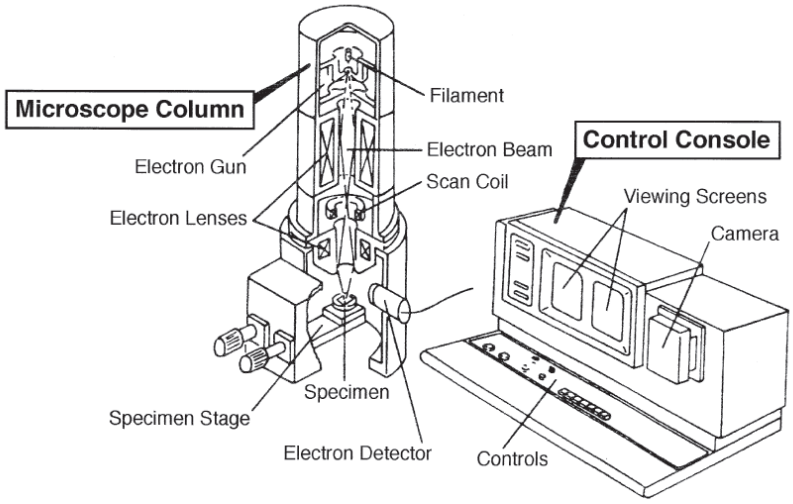

Figure 5.14 – the SEM measurement setup [30]

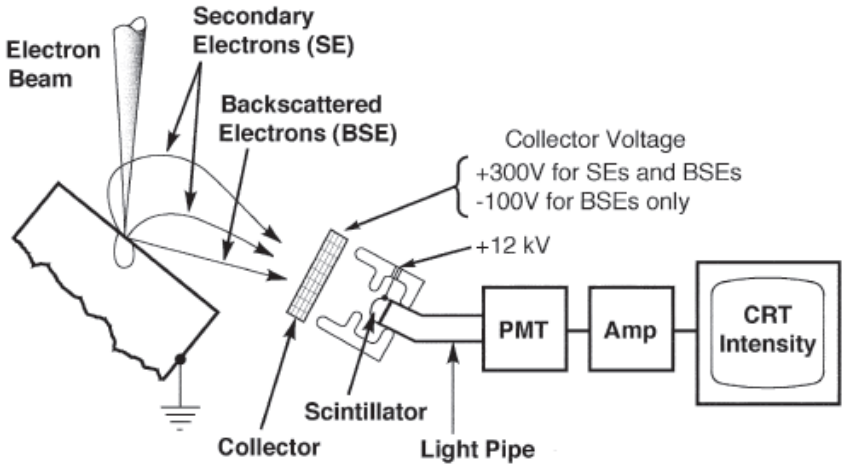

Figure 5.15 – Collection of electrons [30]

The advantage of SEM is also the ability to view the cross-section of the samples with good contrast; thus, it's possible to study the interface between different layers in the sample.

5.3.2.2 Samples preparation. Samples were prepared by dipping the silicon substrates into the aquatic solution of sulfacetamide for 40, 60, 90, 100 and 110 min. Silicon substrates were primarily thermally annealed on the hot plate, temperature 300°C, annealing time was 10 min. An example of the prepared sample is shown in fig. 5.15. As can be seen, the film on the substrates is very inhomogeneous, this is because of the big value of thickness, at some point the film starts to grow on the previous layer of itself, resulting in the weird figures formed from the organic material's molecules.

Figure 5.16 – Substrates with deposited films

5.3.2.3 Imaging: results and discussion. The surface and cross-section imaging was performed using SEM tool. Observing the surface, we were able to notice, that, although the deposition process was performed in the same way, as it has been done in the previous section, no net structure is formed at the surface (fig. 5.17, 5.18). This is the consequence of the fact, which can be seen from the cross-section SEM (fig. 5.19). Also, the height of the pyramids on the silicon surface has been determined from the cross-section imaging (fig. 5.20).

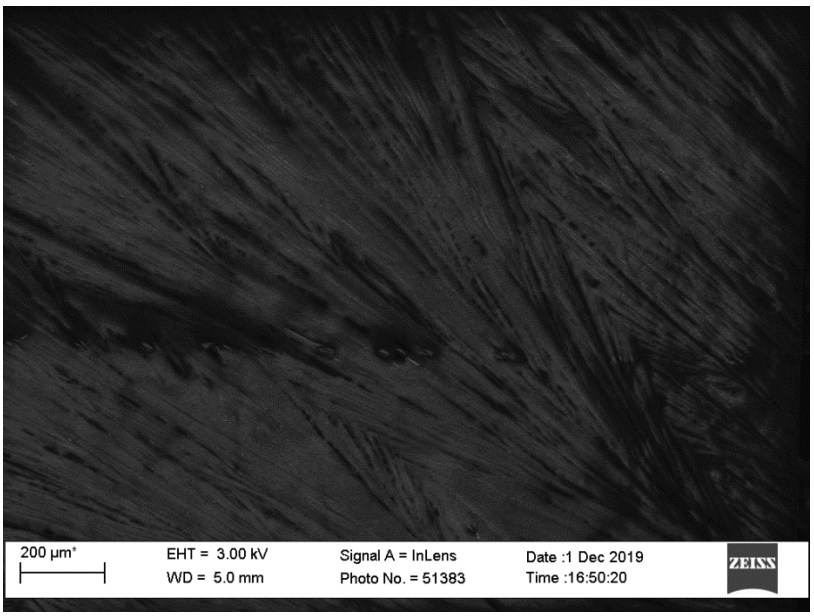

Figure 5.17 – SULF surface’s SEM image, deposition time 90 min

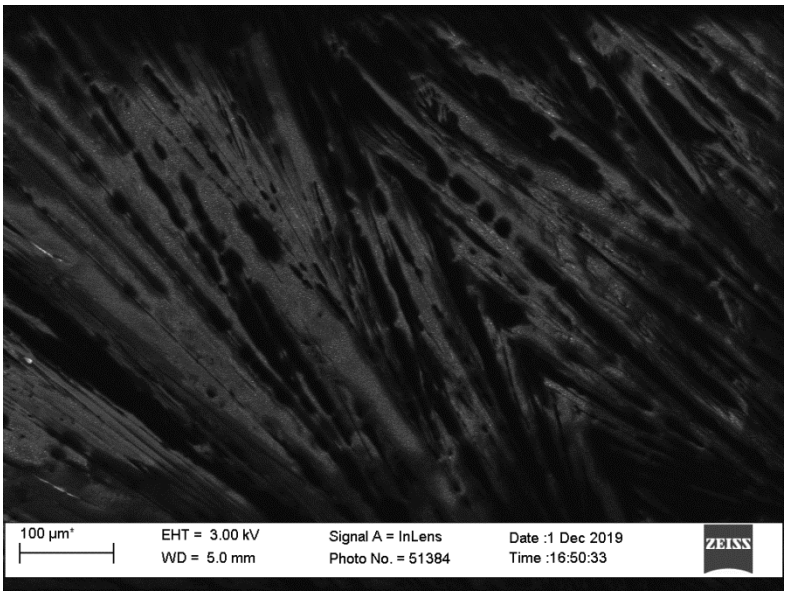

Figure 5.18 – Zoom in to image 5.17

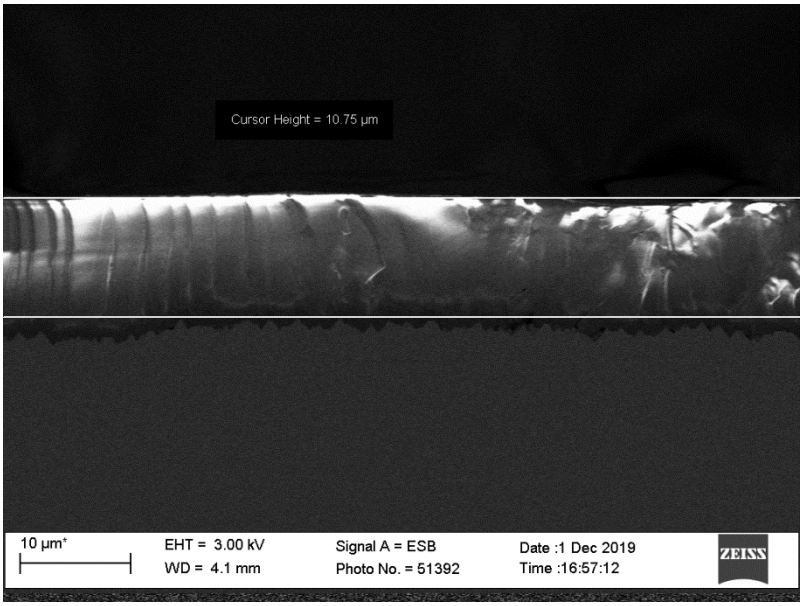

Figure 5.19 – Cross-section SEM, film thickness is determined

Surprisingly, the film thickness for 90 min sample exceeds 10 µm! It was even hard to distinguish the pyramids because of such a big difference in the sizes of the objects. This has happened, because the additional step – the annealing of the substrate, has been done, creating a hydrophilic surface, which is favorable for the film to grow. This step has basically enhanced the speed of the film growth. However, in such thick film, the net structure cannot be formed anymore, as there's no access to the pyramids' tips, which play a role of the nodes, connected by the net, made of organic material. So,

in order to form the regular structure, film thickness should be around the same value as the pyramid's height, in this case – around 2 μm.

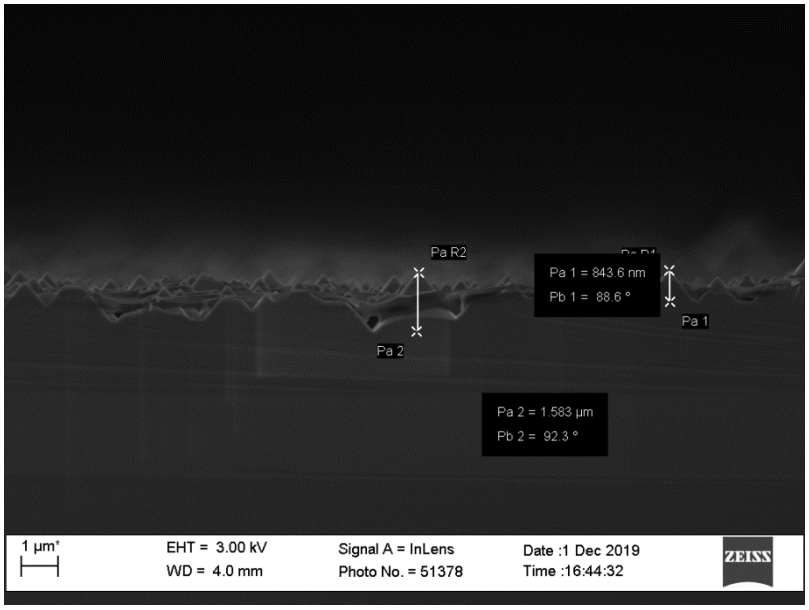

Figure 5.20 – The height of the pyramids is determined from cross-section SEM

Another small detail to highlight is that for deposition time of 60 min, there are cavities present in a cross-section image, which means that the valleys between the pyramids are not covered with the organic film, but only masked by it. However, this is not seen at another image, for the 90 min sample.

Thus, this experiment has proven that thermal annealing of the substrates (or, in fact, oxidation of the silicon surface) increases the speed of film's growth.

5.3.3 Characterization of films' morphology of spin-coated samples

5.3.3.1 Devices preparation. Five samples were prepared for the optical microscopy study. Substrate size was selected to be 1x1 inch, as this size is suitable for most of the equipment we had access to. Primarily to spin coating, substrates were thermally annealed, in order to grow the native oxide layer on the top and, thus, make wafer's surface hydrophilic.

The spin coater used in the fabrication process is shown in fig. 5.14. It consists of the rotating plate, the control panel and the vacuum pump. The last one is needed to keep the sample on the plate while rotating. Using the control panel, one selects the pre-saved recipe or defines the new one. The degrees of freedom are the rotation

speed(rounds per minute, or rpm), the coating time, number of steps, ramp, etc. The tricky part about using it is that the sample's area should be big enough to cover the holes on the plate, which creates the vacuum. Otherwise, the sample won't be fixed and can fly away in the worst case, or in the best – the machine just detects it and stops. The solution for the spin-coating was put on the substrate, using a micropipette.

Figure 5.21 – The spin-coater

Four structures were made for the morphology study. The coating speeds were 500, 1000, 1200, 1400, rpm. This was made to try to observe a trend in the morphology change with changing film thickness. Also, the increase of rotation speed led to the more uniform distribution of the film along the substrate, as after 500 rpm, it was extremely inhomogeneous. After the spin-coating thermal annealing on the hot plate was made in order to speed up the process of drying of the organic layer. The annealing temperature was 150 °C and the time was around 5 min.

5.3.3.2 Morphology characterization. The morphology control was performed using Zeiss SteREO Discovery v12 microscope. This one has a camera onboard, which can take pictures of the sample and send it directly to the software for further processing. The main advantage of this microscope is the maximum magnification of x150 [29]. The microscope is shown in fig. 5.15:

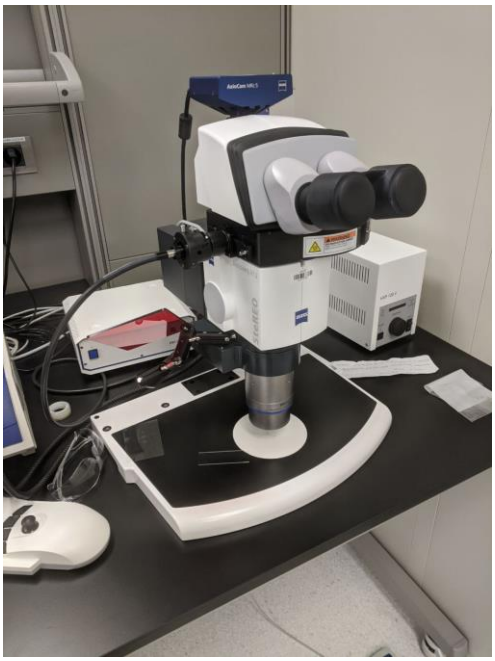

Figure 5.22 – Zeiss SteREO Discovery v12

Several images of each sample were taken; however, only the best will be highlighted here:

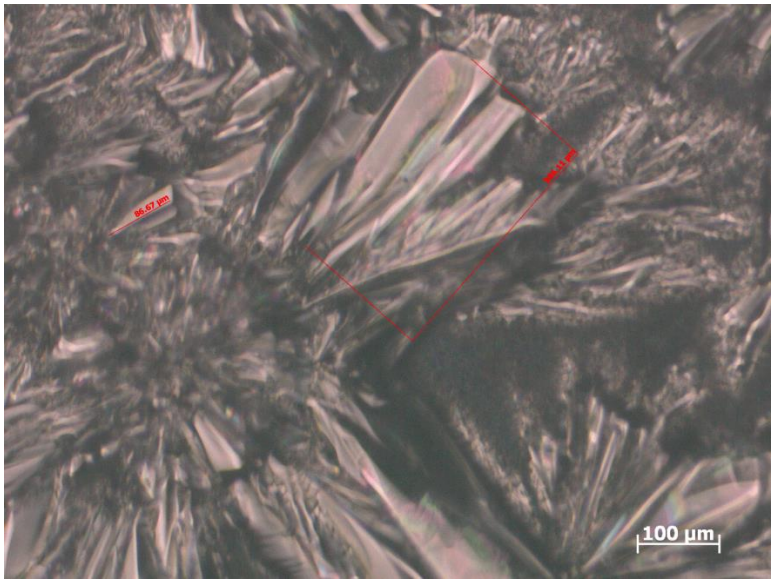

Figure 5.23, a – SULF surface, 500 rpm

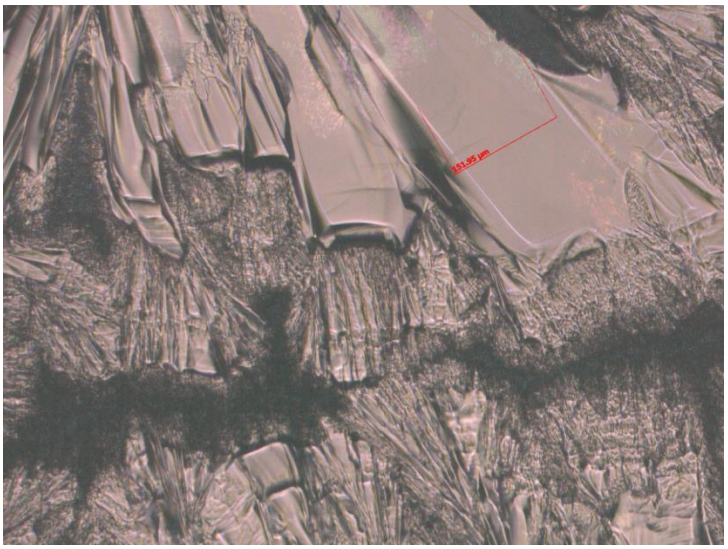

Figure 5.24, b - SULF surface, 500 rpm

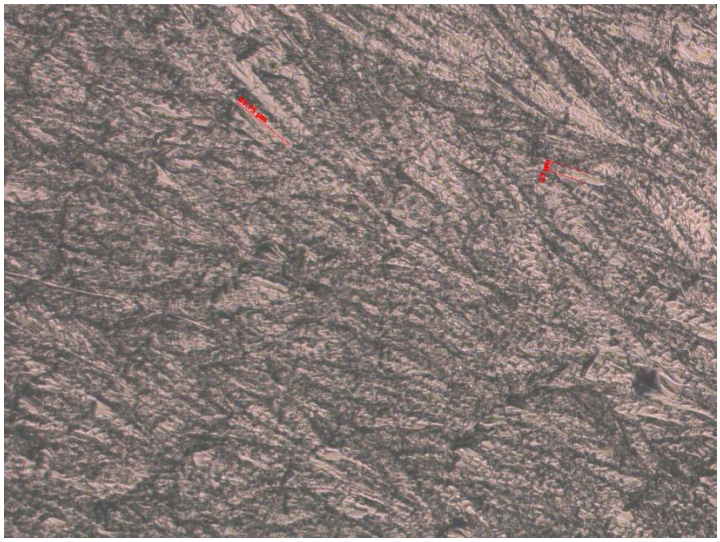

Figure 5.25 – SULF surface, 1000 rpm

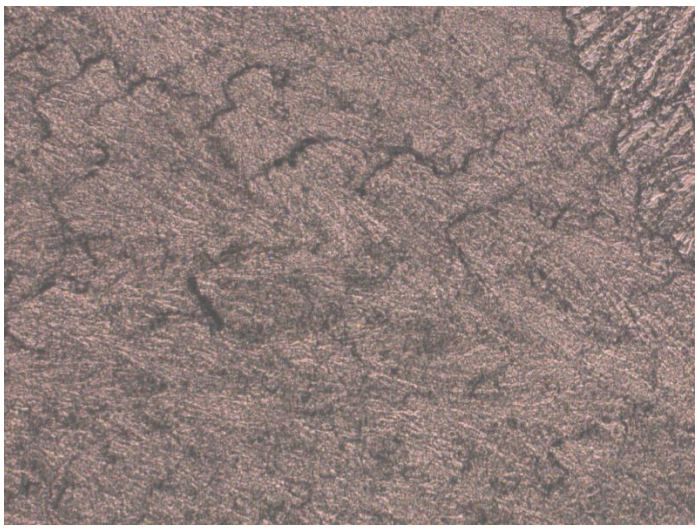

Figure 5.26 – SULF surface, 1200 rpm

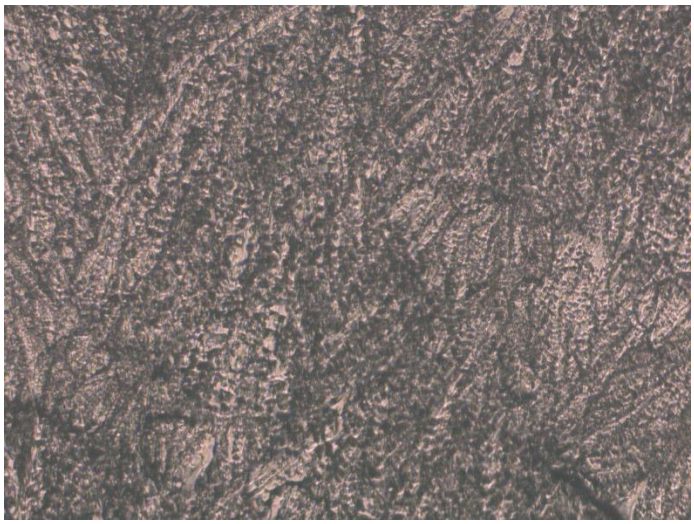

Figure 5.27 – SULF surface, 1400 rpm

Analyzing surface, one can notice, that with an increase or rpm, the uniformity of the film is improving. The first sample (500 rpm) shows us very inhomogeneous surface, with the big clusters of material and some parts of the substrate, which are not covered. Another takeaway message is that in none of the cases, the organized structures are formed within the film, there's no net structure observed, as it was for the samples, prepared by deposition. The only one slight trace of self-organization is observed for 500 rpm, as the huge clusters with sharp and regular edges are formed. It worth to be noticed that the homogeneity of the film is improved, comparing to deposited samples. Another advantage of this method is that the thickness of the film can be controlled by the rpm, which can be broadly changed and goes under automatic control, excluding the human factor from this step of device fabrication. However, there is a drawback as well, in particular, that the spin coating of the samples is not scalable; thus, only small substrates can be covered well by this method.

So, the take-away messages from this experiment are that the homogeneity of the films is improved by spin-coating the material and that the regular self-organized structure of the film can be formed only with the stable, non-turbulent conditions, like when depositing the film from aquatic solution.

5.3.4 The optical properties of sulfacetamide. In the last section of this chapter, the optical properties of sulfacetamide, such as absorption, reflectance and

transmittance, will be calculated. Also, the absorption coefficient will be determined; by this, one can make the obtained values independent of the sample, but only on the material. Two types of samples were measured: the solution and the film on a glass substrate. As both the sample and the glass absorb light in the UV, blank glass substrates were also measured and the obtained data was subtracted from the measurements of the sample to make measured values substrate-independent.

5.3.4.1 Samples preparation. Liquid samples were put into a 1mm thick cuvette made of quartz. Assuming that quartz and solution have very close values of refractive index, the reflectance in this measurement was neglected.

Films were prepared by spin-coating the glass substrate with the solution. Some of the samples were thermally annealed afterward, some not. Before spin-coating, glass was purified in the 3-step process: distilled water+soap, acetone and, finally, isopropyl alcohol. After that, UV-Ozone treatment has been also done. The substrates were spin-coated with 1200 and 1400 rpm, and within the first value, the volume of the solution put on the substrate was also changing from 300 μl to 600 μl.

The resulting films are shown in fig. 5.28.

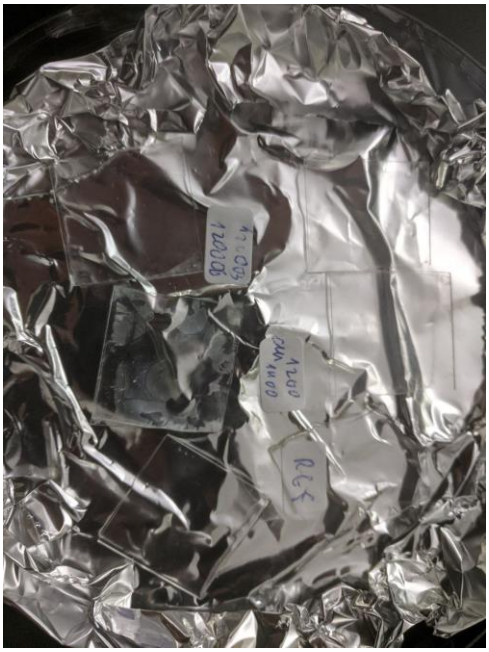

Figure 5.28 – Film-on-glass samples

For characterization, profilometry (thickness measurement) and UV-Vis spectroscopy (optical parameters) were used.

5.3.4.2 Thickness measurement. Profilometry. In order to determine absorption coefficients and to be able to compare different samples, their thicknesses have been measured. For this purpose, a profilometer was used. The measurement principle is essentially simple: the substrate level is taken, as 0 height, and the thickness of the film is calculated from this level. To measure it, a needle, connected to a spring, is moving towards the step-in height (Fig.5.29). When it reaches the step, the vertical position of the needle changes(height of the film is larger than 0 position), which loads the spring. The created tension is then recalculated into the thickness.

In this experiment, KLA-TENCOR P-6 was used for measurements (Fig. 5.30). This is a digital profilometer with a vertical resolution of 0,1 nm and an additional feature of the vacuum holding for the sample. This ensures that during the measurements, the sample will remain immobilized.

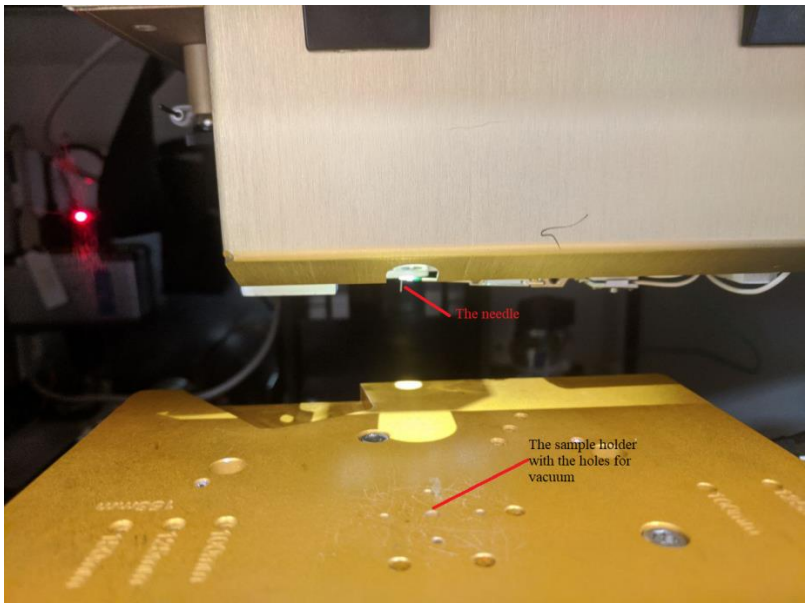

Figure 5.29 – The needle of the profilometer

The output of the device is a plot of the surface topography, from which the zero level and the film thickness are determined. In fact, the plot looks like a step function, where the height of the step is the film thickness (fig. 5.31).

Figure 5.30 – KLA-TENCOR P-6 profilometer

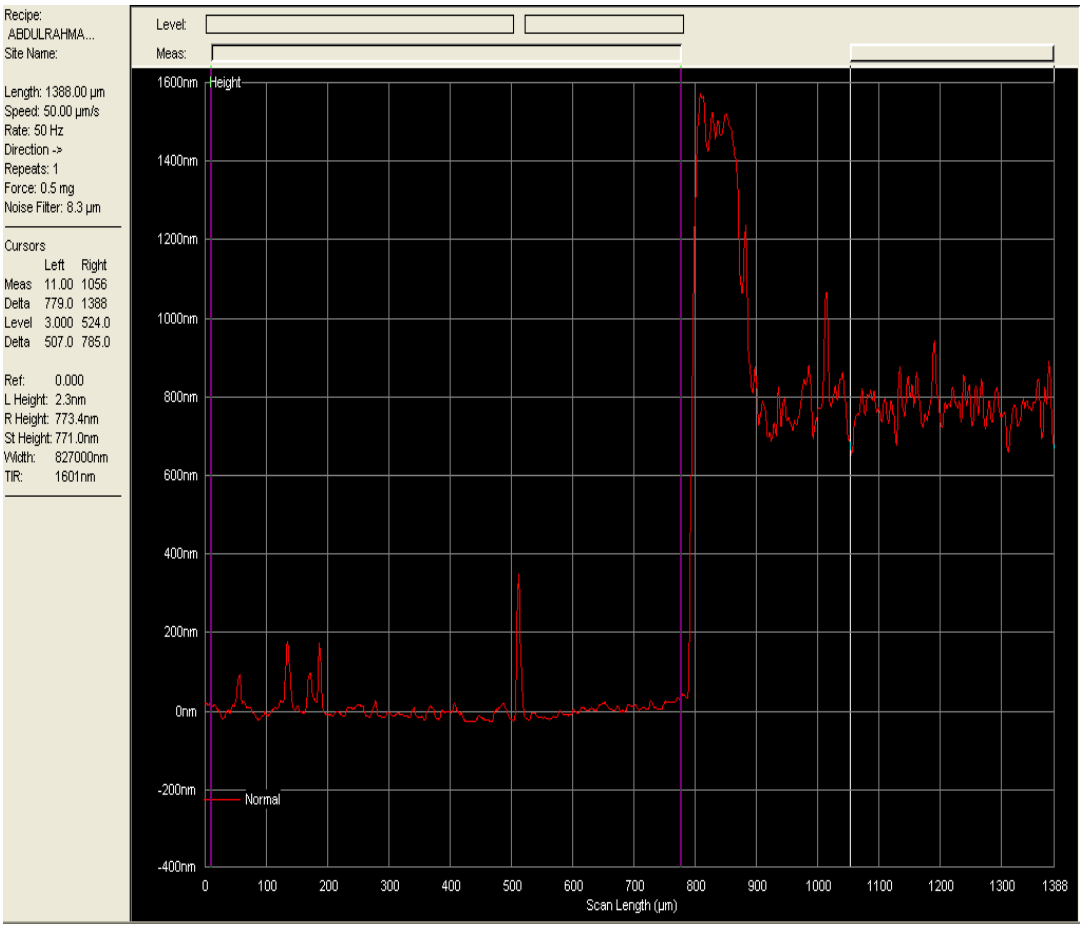

Figure 5.31 – The output data from the profilometer

On the graph above, one can easily distinguish two levels. The peak between it is an artifact, which is very common to observe when measuring the organic films. This peak means that the needle is scribing a piece of the film while moving towards the

step. The build-up of the film material causes the increased thickness of the film in this short region.

So, for each sample, the film thicknesses were measured in different regions of the substrate, and the data were then averaged within one sample. The obtained thicknesses are grouped into table 5.3.

Table 5.3 – The measured thicknesses of the samples

Sample name	d, nm
1200_03	670,2
1200_06	794,8
1200_03A	800,8
1400_03A	803,3

Thus, is it seen from the table that for spin-coated samples, the thicknesses are around 650-800 nm.

5.3.4.3 The UV-Vis. The principle of the UV-Vis spectroscopy is to measure light intensity, either transmitted through or reflected from the sample. This is done for each wavelength of the selected range. That's how one obtains the spectrum. Then, knowing these two values, it is trivial to calculate the absorption. The measurement principle is illustrated in fig. 5.32.

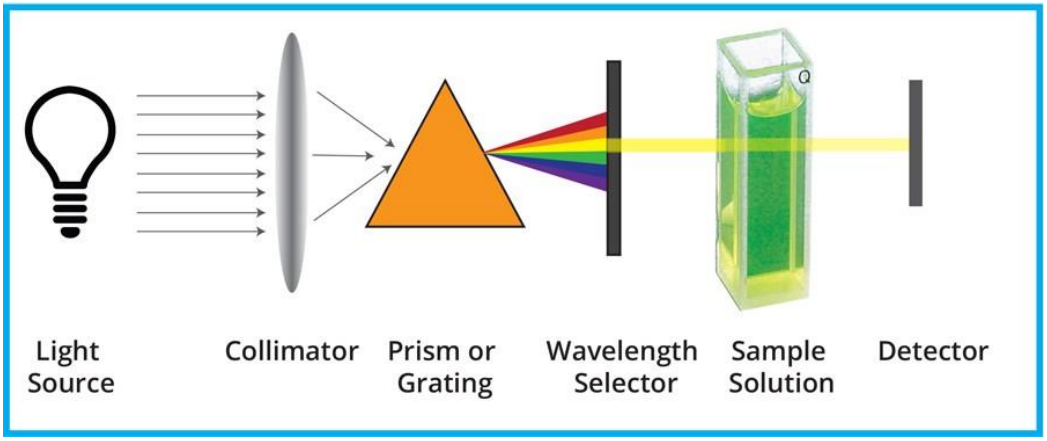

Figure 5.32 – The principle of the UV-Vis measurement setup

For the sulfacetamide solutions, Agilent Cary UV-Vis-NIR Spectrophotometer was used (fig. 5.33). It's measurement principle is exactly the same, as described and illustrated in fig. 5.32.

Figure 5.33 – Cary spectrophotometer

For the films, Lambda 950 was utilized. This device gives higher sensitivity because of the integrating sphere, installed in the measurement chamber. The principle of the integrating sphere is that all the light, transmitted or reflected, experiences multiple reflections within the sphere, and in the end, all the light is collected by the detector. Thus, there's no losses in the intensity.

Once the transmittance and reflectance are measured, the absorption can be determined from the conservation of energy[31]:

$$A + T + R = 1 \qquad (5,1)$$

where A – absorption; T – transmittance; R – reflectance.

In order, the absorption coefficient can be determined, as [32]:

$$k_a = \frac{1}{d}\ln[\frac{(1-R)^2}{T}] \qquad (5,2)$$

where k_a – absorption coefficient, nm^{-1}; d – film thickness, nm.

Normalized values of the transmittance for pristine sulfacetamide solutions are shown in fig. 5.34:

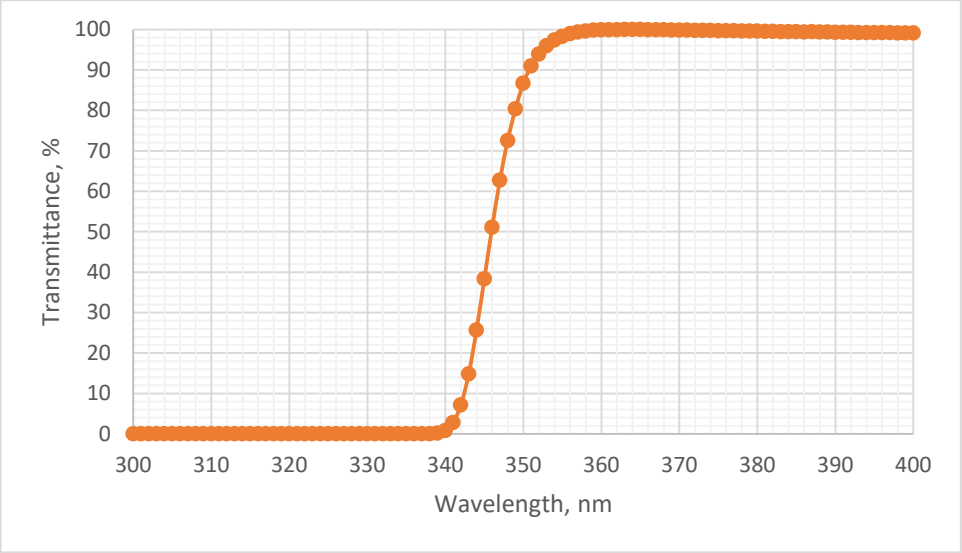

Figure 5.34 – Transmittance of sulfacetamide solution

In case one wants to know the absorption, this graph for it would be just inverted, as we neglected the reflectance for this measurement.

As one can see, sulfacetamide has its absorption in the UV range, below 340 nm.

A bit more tricky is the situation with films on glass substrates. As both the film and the substrate absorb nearly in the same wavelength range, the measured data needs to be corrected by subtraction the data obtained from measuring the blank substrates.

Thus next formulas were used to obtain the optical parameters of the pristine film:

$$T_f = 1 - |T_S - T_G| \quad (5,3)$$

$$R_f = R_S - R_G \quad (5,4)$$

where $T(R)_f$ – film's transmittance(reflectance); $T(R)_S$ – sample transmittance(reflectance); $T(R)_G$ – glass transmittance(reflectance).

Here, only the normalized plots will be shown.

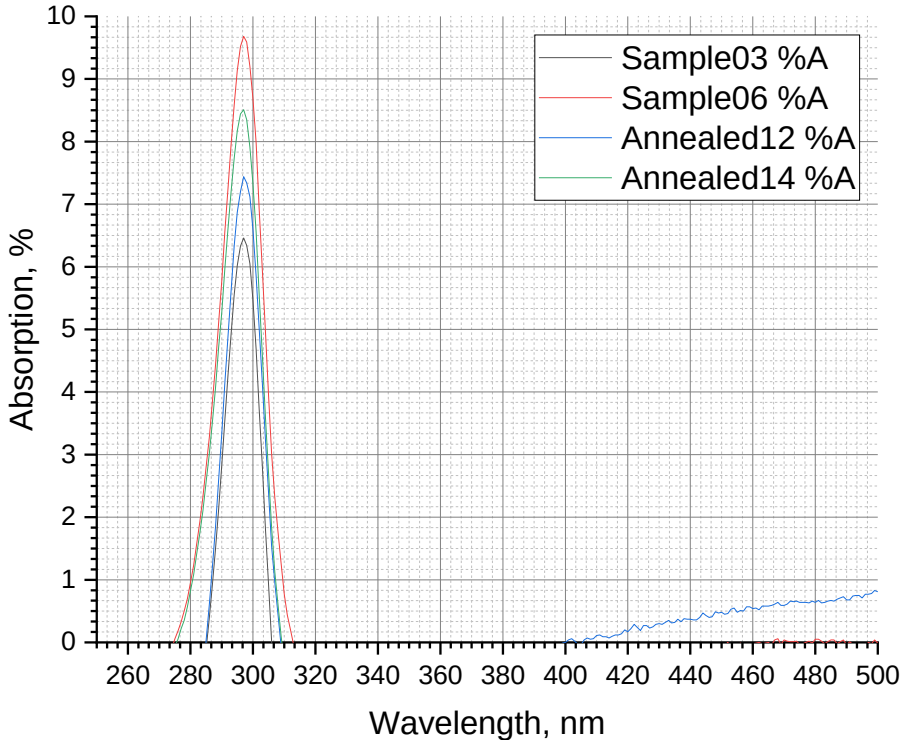

Figure 5.35 – Absorption of sulfacetamide films

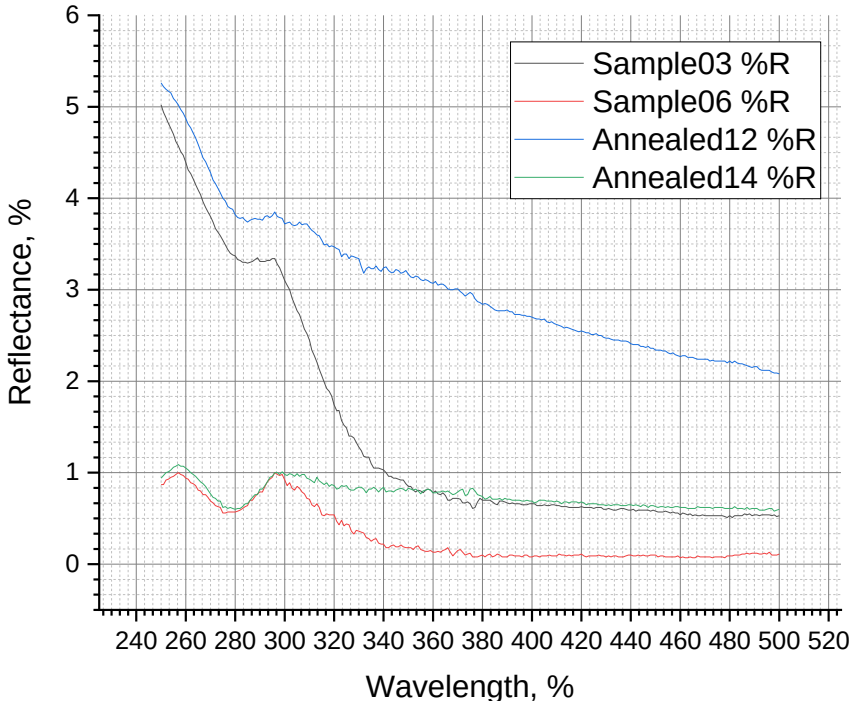

Figure 5.36 – Reflectance of sulfacetamide films

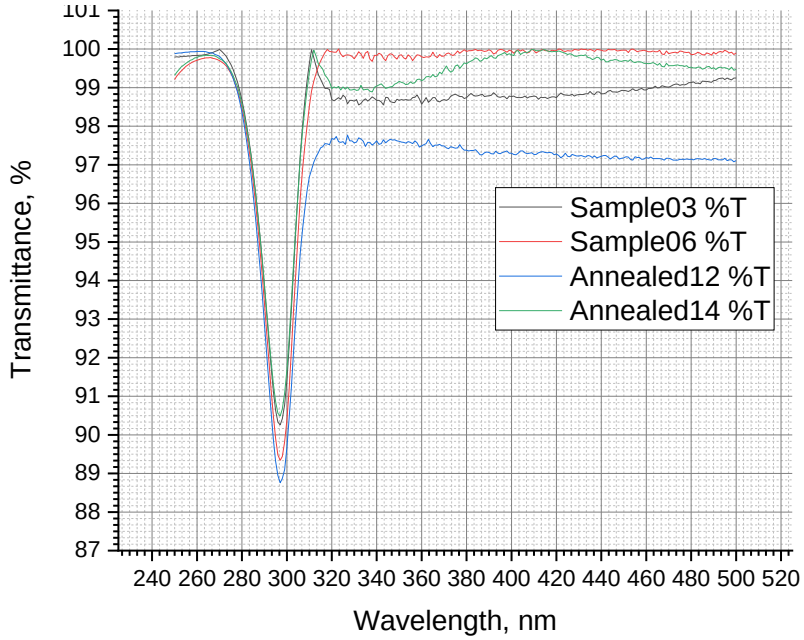

Figure 5.37 – Transmittance of sulfacetamide films

As one could notice, there is a difference in the behavior of 4 films. Slightly different parameters, however, they still make a difference. But the very first assumption, which should be made, is that the difference stands from the different thicknesses. So, to eliminate this dependence, we've plotted the absorption coefficient, which is a value, normalized to film thickness.

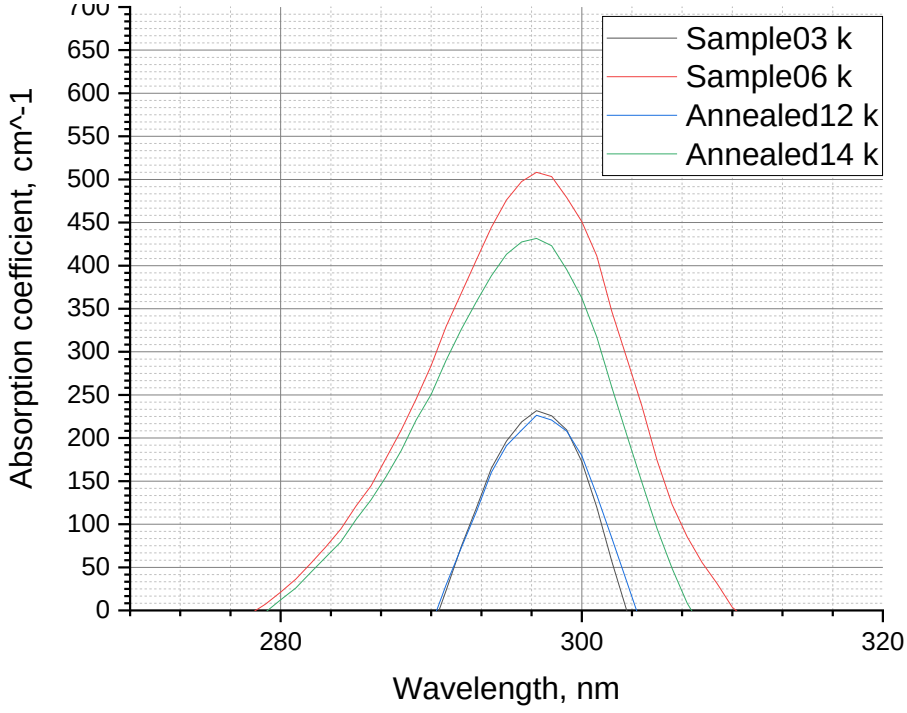

Figure 5.38 – Absorption coefficient of sulfacetamide films

As can be seen, with the annihilation of the dependency on thickness, the difference between 1200_03 and 1200_03A also disappeared. It also means that annealing doesn't actually influence the properties of the film. However, there's still a big difference between the two other samples.

If we stick to the region of interest – the UV, particularly to the range of the film's absorption, we can see, that the only significant difference between them is in the absorption. The answer could be that one sample was annealed, but as this process doesn't play any role in other pair of devices, one should not take it into account. Then, recalling the film structure, one could notice that the 1200_06 film has a spot right in the center of the substrate when, for 1400_03A, this area is uniform. The fact is that during the measurement, the major light passes through the center of the sample; thus, the non-uniformity in the first sample could be a clue to the observed difference in values. Thus, we suppose that the pristine sulfacetamide film behaves in the same way in all four samples, and the difference in the absorption coefficients stands from the non-homogeneity of one of the films.

This inhomogeneity has a background; those sulfacetamide films are extremely reactive with water, thus when exposed to air outside the lab (where the humidity level is very low), it starts to absorb water particles from the air, thus changing its structure.

5.3.4.4 Summary of the characterization of sulfacetamide. So, the set of experiments, including microscopy, profilometry and spectrophotometry, was performed. It was shown that the organic component becomes highly reactive with water and oxides (native oxide of silicon). The absorption spectra was determined; it lays in the range of 270-315 nm. Finally, it was stated that the annealing of the film doesn't influence its properties.

5.4 Recycling of sulfacetamide-based hybrid solar cells

Recycling the solar cell means bringing it back to the wafer state, thus removing all the additional layers, like ARC, electrodes, incapsulating and organic layers. Many methods have been developed to remove all these layers, for example, metal electrodes

are easily treated by the KOH, HNO3 and HF, depending on metal, and Br to remove ARC [32]. Here we will focus on how to remove the organic layer, particularly sulfacetamide. And the answer is extremely simple. As sulfacetamide was deposited from water solution, it means that the molecule is soluble in water. So the easiest way to remove it from the wafer is to use distilled water as solvent. The price of this process is close to zero, and the wafer is completely cured of the sulfacetamide traces. Fig. 5.39 shows the photo and the microscopic surfaces of the pure wafer, which was never contaminated by anything, and the cleaned one, from which SULF was removed by applying some distilled water.

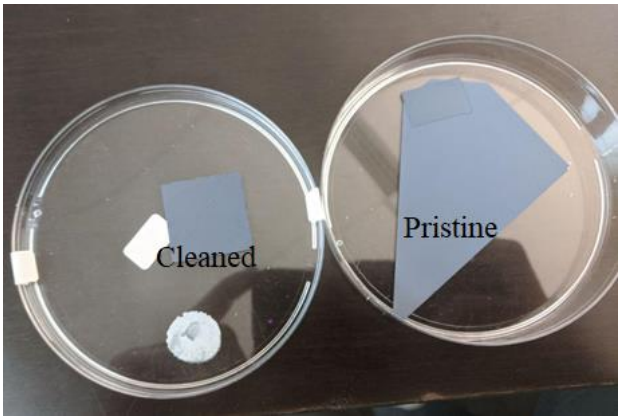

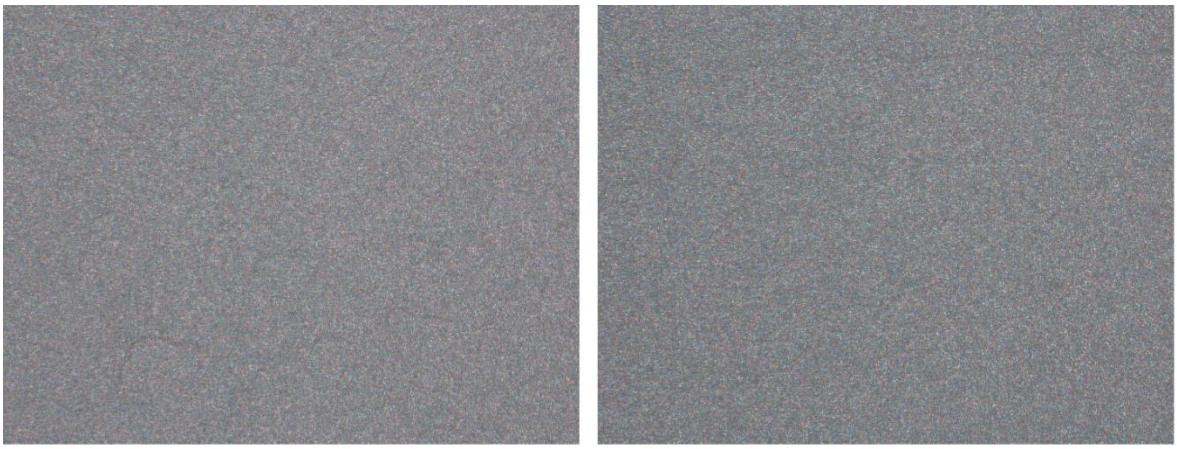

Clean Pristine

Figure 5.39 – Pristine wafer vs. cleaned

It is clearly hard to see the difference. But still, there’s a small chance that some molecules have stuck to the surface. Then one should sonicate wafers to ensure the complete removal of the organic layer. Thus, removing the organic layer of the HSC with sulfacetamide as organic layer is extremely simple and has zero cost comparing to any other process.

6. STARTUP

6.1 Idea description

Table 6.1 - Idea description of the startup project

Idea content	Applications	Benefits for user
Developing the technology of recycling the hybrid solar cell	1. Photovoltaics	Generation of energy by converting the power of the sunlight into electricity
	2. Electronics	Generation of energy for portable electronic devices
	3. Sustainable waste management	Recycling and reusing the building blocks of the device as raw materials

Table 6.2 - Determining the strong, weak and neutral characteristics of the project idea

№	Technical and economic characteristics of the idea	(potential) products/concepts of competitors				W (weak side)	N (neutral side)	S (strong side)
		My project	Competitor 1	Competitor 2	Competitor 3			
1.	Economic	100 y.o.	295 y.o.	175 y.o.	150 y.o.			+
2.	Applications	Recyclable hybrid organic-inorganic solar cell	Technology for recycling silicon solar modules	Technology for recycling silicon solar modules	Technology for recycling silicon solar cells(in			+

					cooperation with competitor 1)			
3.	Reliability	Warranty – 15 years	-	Warranty – 20 years	-		+	
4.	Technological	The active layer is removed using cheap organic solvents	Requires high temperature and part of the silicon wafer is lost due to chemical etching	Requires high temperature and part of the silicon wafer is lost due to chemical etching	Requires high temperature and part of the silicon wafer is lost due to chemical etching			+
5.	Ergonomical	-	-	-	-		+	
6.	Organoleptic	-	-	-	-		+	
7.	Esthetical	-	-	-	-		+	
8.	Transportability	Obtained raw materials are easily transportable	Obtained raw materials are easily transportable	Obtained raw materials are easily transportable	Obtained raw materials are easily transportable		+	
9.	Ecological	Ecological	Ecologica	Ecological	Ecological		+	
10	Safety	Safe	Safe	Safe	Safe		+	

Competitor 1: PV Cycle.

Competitor 2: 3R Recycling.

Competitor 3: Veolia.

6.2 Technological audit of project's idea

Table 6.3 - Technological realisability of the idea

№	Idea	Technological realization	Technology existence	Technology availability
1.	Developing the technology of recycling the hybrid solar cell	Metal electrodes are removed using chemical etching, active – by etching with organic solvents, encapsulation – by thermal evaporation	Exists	Available
		Everything is removed by thermal evaporation	Exists	Available, but not optimized for the separation of the components
		Everything is removed by etching in the strong acids	Exists	Available, but not optimized for the separation of the components
Chosen technology: to remove the components layer-by-layer using selective chemical etching				

6.3 Analysis of the possibilities of launching the startup-project at the market

Table 6.4 - Preliminary characteristics of the potential market for the startup-project

№	Market's characteristics	Value
1	Number of major players	3
2	Overall sells, UAH/unit	3000 units
3	Market dynamics	Growing up
4	Obstacles need to be overcome to enter the market	Settling large-scale manufacturing
5	Specific requirements for standardization and certification	None
6	Average norm of rentability in the domain(or at the market), %	175%

The market is attractive to enter.

Table 6.5 - Characteristics of the potential customers of the startup-project

№	Market needs	Key customers(market segments)	Difference in behavior of different customers	Customers' requirements
1	The fully recyclable and reusable product	Companies manufacturers of the solar cells and/or solid-state devices	-	The key components of the cell must be effectively separated, purified and processed into forms, suitable for the industrial manufacturing

Table 6.6 - Threats

№	Factors	Content of threat	The possible reaction of the company
1.	Qualified personnel availability	Quality control requires special skills	Hiring the personnel from the research institutions and/or organizations
2.	Resource needs	Manufacturing requires additional conditions to be fulfilled for creating the final product and its reliability and quality assurance	Dealing with the resource suppliers and rental of space for product testing and manufacturing

Table 6.7 - Opportunities

№	Factors	Content of opportunity	The possible reaction of the company
1.	Competition	Ameliorating product characteristics and reduction of the price	Ameliorating product characteristics
2.	Demand	Establishing the network of the selling points and cooperation with the dealers	Increase in the product’s demand. Establishment of the feedback from customers

Table 6.8 - Step-analysis of the competition at the market

Competition environment specialties	The key point of the characteristics	Influence on the company operation
1. Type of competition: - oligopoly	A large number of companies at the market	Product quality improvement by introducing new technologies into manufacturing. Marketing campaign.
2. Level of competition - international	Companies are territorially worldwide spread	Development of the multi-language website
3. Domain's trait - intradomain	Economic competition between the manufacturers of the product with similar characteristics. The existing differences are those of the quality, price, manufacturing costs, etc.	Competitors' market monitoring
4. Product type competition: - product form	Competition among two products of the same type	Product's quality improvement
5. Competitive advantages type - non-value	States that products quality prevails the price	The high-quality product is selling for the price, not lower, than the average at the market
6. Intensity - non-trademark	Trademark's role is negligible	Product advertising

Table 6.9 - M. Porter's competition analysis

	Direct competitors	Potential competitors	Suppliers	Customers	Substitutio-nal products
Components	«PV CYCLE». «Veolia». «3R Recycling».	Absent	Product is selling by the dealers and the manufacturers	Product's quality and lifetime	Absent
Conclusions:	The intensity is quite high; the competitors are settled at the market for a long time	Absent	Dealers set the additional requirements for the market	The product should fulfill the requirements	Absent

Qualified scientists and engineers need to be involved in product development for increasing product quality, improving its parameters and development of new goods. The involvement of qualified marketing specialists is also essential in order to improve the product's positions on the market and to substitute the competitors' ones.

Table 6.10 - Competitiveness factors justification

№ п/п	Competitiveness factor	Justification
1.	Level of amelioration of the process' characteristics	One of the competitors improves his product but doesn't ensure the additional protection to the product components
2.	Product quality in terms of purity(quality) and reliability(product lifetime)	The product should have a high quality when just manufactured and during its life cycle, comparing to the analogs
3.	Scientific research resources availability	Scientific resources are needed to improve the product

4.	Economic(price)	The price should be competitive and reasonable

Table 6.11 - The comparative analysis of strong and weak sides of the product

№	Competitiveness factor	Points 1-20	Rating of competitors' products according to "3M."						
			–3	–2	–1	0	+1	+2	+3
1.	Level of amelioration of the process' characteristics	19		+					
2.	Product quality in terms of purity(quality) and reliability(product lifetime)	16			+				
3.	Scientific research resources availability	14				+			
4.	Economic(price)	12							+

Table 6.12 - SWOT- analysis of the startup-project

Strong sides: low-cost, sustainable and efficient technology	Weak sides: Economic(product price)
Opportunities: development of the new technology enables the interest to the further investigation and improvement	Threats: Increasing price because of the change in resources' one

Table 6.13 - Alternative ways of pushing the product to the market

№	Alternative	The probability of obtaining the resources needed	Time frame
1.	Finding the dealer companies, the investors, the scientific resources,	75 %	1,5 years

	improving manufacturing		
2.	Cooperation with the solar cells manufacturers and creating the common strategy of conquering the market	60%	2 years

Alternative № 1 has been chosen.

6.4 Development of the project's market strategy

Table 6.14 - Selection of the target groups of customers

№	Description of the profile of the target group	Customers' readiness to accept the product	Estimated demand within the group	Competition intensity	The difficulty of entering the market
1.	Private companies	Ready	High	High	Medium
2.	Privates	Partially ready	Medium	Medium	Low
3.	Public(state) companies	Partially ready	Medium	High	High
The group №1 have been chosen as the target group.					

Table 6.15 - Decision on the basic development strategy

№	The chosen alternative of development	Strategy of conquering the market	The key competitive positions according to the chosen alternative	Basic development strategy

1.	Differentiated marketing	Innovativeness and wide-spread news of the technology because of the dealers' network allow to assure fast conquer of the market.	Innovativeness of the technology	Strategy of differentiation

The strategy of differentiation has been chosen.

Table 6.16 - Decision on the basic strategy of competition behavior

№	Is the project a pioneer in the market?	Is the company going to look for new customers, either taking over from the competitors?	Is the company going to copy some of the characteristics of the existing products?	Chosen strategy
1.	Yes	Yes	No	Competing against the leader

Table 6.17 - Decision on the positioning strategy

№	The requirements of the target group on product characteristics	Basic development strategy	The key competitive positions according to the chosen alternative	Associations to the project
1.	Higher quality and lifetime	Strategy of	Innovativeness of the technology	Optimal quality/price ratio, sustainability, simplicity

	compared to the competitors' products	differentiation		

6.5 Development of the marketing program of the startup-project

Table 6.18 - Determining key advantages of the potential product

№ п/п	Need	Profit	Key advantages compared to competitors' products
1.	Cheap and high-quality product	Sustainable and simple technology with minimal losses of the raw material	Competitors cannot ensure higher raw material gain, obtained from the process, as well as cannot decrease the price dramatically

Table 6.19 - Description of the three-level model of the product

Product levels	Content and components		
I. Idea	A low-cost, simple and sustainable recycling process		
II. Reality	Characteristics	М/Нм	Вр/Тх /Тл/Е/Ор
	1. Selective solvents utilization 2. Price 100 units per wafer 3. Highest materials yield	М М М М	
	Warranty: 15 years		
	Packaging: separate packages with different components		
	Mark: "ReCell"		
III. Product with supplies	Before vending: warranty		
	After vending: consulting, shipments		
Protection against copying: patent			

Table 6.20 - Determining the price limits

№	Prices of the substitutional products	Prices of the analogs	Income of the customers	Верхня та нижня межі встановлення ціни на товар/послугу
1	-	125 – 200 units/pcs.	>1000 units for privates >10000 units for companies	0 – 250 units/package

Table 6.21 - Sales system

№	Specifics of the customer purchasing behavior	Sales functions of the supplier	Sales channel depth	Optimal salse system
1	Ordering through the website or buying from the dealers' shop	Consulting, warranty cases handling, quality assurance	Zero-level channel	Sales through the dealers

Table 6.22 - Concept of marketing communications

№	Specifics of the customer behavior	Communication channels of the customers	Key positions of targeting	The task of the advertisement	The concept of the advertisement
1	The utilization of the product as raw	Direct channel	Cheaper technology with higher quality and yield	To inform prospective customers about the innovative product with the	The advertisement is based on the difference between the

	material for manufacturing			improved characteristics and to stress the positive sides of the product: lower price, higher yield, higher quality, sustainable technology	product and the competitors' analogs, but also on the influence that the product could have on the customers' feelings.

6.6 Conclusions

The probability of the commercialization of the product is quite high because of the innovativeness of the technology and the absence of direct competitors. Throwing out the product with the optimized ratio quality/price in the market allows conquering its part because of the rapidly growing solar cells segment. The possible obstacle could be increasing manufacturing costs.

CONCLUSIONS AND OUTLOOK

To summarize, in this work, an alternative approach to making the solar cells was discussed. In order to make the converter more affordable, environmentally friendly and easily processable, the new structure of the device was introduced, where one of the active layers is replaced by the organic film. The electrical properties of such devices were studied and one of the materials used to create the organic film was characterized. And now, let's discuss each aspect more in detail.

The manufacturing process of the HSC itself justifies several points already: first of all, these devices are low-temperature processable, the film is deposited from the aquatic solution and this can be done even at room temperature. Because one gets rid of the high-temperature processing, the cost of the device drops dramatically.

After the device has worked its resource out, the organic layer can be removed easily, as it's water-soluble. However, this could be also a drawback, as one needs this type of cell to be waterproof; otherwise, there's a risk to find the organic layer degraded or even dissolved.

Thus, the first task was achieved and profoundly studied: both silicon polymer structures and the devices based on it were manufactured and studied.

Then the fabricated samples were measured using different characterization techniques.

It was shown that the performance of the cell improves when one uses an organic blend instead of one pristine material. In this work, CLO:SULF blends were studied and it was shown that clonidine's probably playing a crucial role in the improvement of the electric parameters. Another important thing to highlight is that devices perform better when there's a net structure of the film present. This is achieved by the addition of a small portion of SULF into the blend.

However, the best results are obtained for 100 min in all 4 cases: the increase is 10-15% for short-circuit current, 40-96% for the fill factor and 15-27% for the open-circuit voltage depending on the organic layer's material used.

Thus, both components influence the performance of the devices, but one should stick to the blends with higher concentrations of CLO, as the addition of this component improves pretty much all the electrical parameters of the cell. However, a small fraction of SULF is still needed to form the net structure on the surface; thus, this organized pattern probably improves the photogenerated current behavior.

For the future work, second material will be properly studied and characterized, the fabrication technology of the devices will be improved (the addition of the annealing step is crucial), and charge transfer mechanisms will be modeled and studied profoundly, as well, as the processes at the silicon-polymer interface.

REFERENCES

1. О. В. Борисов. Основи твердотільної електроніки: навч. посіб. / О. В. Борисов; за ред. Ю. І. Якименка. – К.: Освіта України, 2011. – 462 с.
2. N. Bohr. On the constitution of atoms and molecules // Philosofical magazine – 1913 – Vol. 26, № 6. – P. 476-502.
3. S. M. Sze and K. K. Ng. Physics of Semiconductor Devices / S. M. Sze and K. K. Ng – M.: John Wiley & Sons, 2007. – 815 p.
4. Smets, Arno. Solar Energy - The physics and engineering of photovoltaic conversion, technologies and systems / Smets, Arno & Jäger, Klaus & Isabella, Olindo & Van Swaaij, R.A.C.M.M. & Zeman, Miro – M.: UIT Cambridge Ltd., 2016. – 462 p.
5. P. R. Gray. Analysis and Design of Analog Integrated Circuits / P. R. Gray, R. G. Meyer – M.: John Wiley & Sons, 2009. – 896 p.
6. Chin, Jack & Salam, Zainal & Ishaque, Kashif. Cell modeling and model parameters estimation techniques for photovoltaic simulator application: A review / Applied Energy – 2016 – Vol. 154. – P.150-159.
7. Dr.-Ing. Konrad Mertens. Photovoltaics: fundamentals, technology and practice / by prof. Dr.-Ing. Konrad Mertens – M.: John Wiley & Sons, 2014. – 280 p.
8. K. E. Bean. Anisotropic etching of silicon / IEEE Transactions on Electron Devices – 1978 - Vol. 25, № 10 – P. 1185-1193.
9. Технология производства полупроводниковых приборов и интегральных микросхем: Учеб. Пособие для вузов по спец. «Полупроводники и диэлектрики» и «Полупроводниковые приборы»/ Курносов. А. И., Юдин В. В.; 3-у изд., перераб. и доп. – М: Высш. шк., 1986 – 386 с.
10. Kumar, Vikas. Anti-Reflection coatings for highly efficient solar cells / National Conference on Photonics and Material science – 2015 – P. 360-364.

11. S. Schiller, G. Beister, W. Sieber, G. Schirmer and E. Hacker, Influence of deposition parameters on the optical and structural properties of TiO_2 films produced by reactive d.c. plasmatron sputtering / Thin Solid Films – 1981 – Vol. 83, № 2 – P. 239-245.
12. D. Hocine, M. S. Belkaid, M. Pasquinelli, L. Escoubas, J. J. Simon, G. A. Rivière and A. Moussi. Improved Efficiency of Multicrystalline Silicon Solar Cells by TiO_2 Antireflection Coatings Derived by APCVD Process / Mater. Sci. Semicond. Process. – 2013 – Vol. 16, № 1 – P. 113-117.
13. J. Szlufcik, J. Majewski, A. Buczkowski, J. Radojewski, L. Jędral and E. B. Radojewska. Screen-printed titanium dioxide anti-reflection coating for silicon solar cells / Sol. Energ. Mat. – 1989 – Vol. 18, № 5 – P. 241-252.
14. Lin, Ching-Hsi & Hsu, Shih-Peng & Wei, Hsu. Silicon Solar Cells: Structural Properties of Ag-Contacts/Si-Substrate / Solar Cells: Silicon-Wafer- Base – technologies – 2011 – P. 93-113.
15. A. Kohler, H. Bassler. Electronic processes in organic semiconductors: an introduction / A. Kohler, H. Bassler – M.: John Wiley & Sons, 2015. – 405p.
16. M. Schwoerer, H. C. Wolf Organic molecular solids: a book, Weinheim, Germany : Wiley, 2005. 427 p.
17. Xia Fan, Mingliang Zhang, Xiaodong Wang, Fuhua Yang and Xiangmin Meng. Recent progress in organic-inorganic hybrid solar cells / Journal of Materials Chemistry A. – 2013 – Vol. 1. – P. 8694-8709.
18. J. S. Huang, C. Y. Hsiao, S. J. Syu, J. J. Chao and C. F. Lin. Well-aligned single-crystalline silicon nanowire hybrid solar cells on glass / Sol. Energy Mater. Sol. Cells – 2009 - Vol. 93. - P. 621–624.
19. Wei MK, Lin CW, Yang CC, Kiang YW, Lee JH, Lin HY. Emission characteristics of organic light-emitting diodes and organic thin-films with planar and corrugated structures / Int J Mol Sci. – 2010 – Vol. 11, №4 - P. 1527–1545.
20. Sol-gel process spin coater: website.
URL: https://www.spincoating.com/en/applications/sol-gel-process-spin-coater/208/

21. Three-dimensional simulations for improving complex blade coating process : website. URL: https://www.cadcrowd.com/gallery/project/three-dimensional-simulations-for-improving
22. Caixia Hou et al. Boron-rich layer removal and surface passivation of boron-doped p-n silicon solar cells / J. Semicond. – 2018 Vol. 39, №12.
23. D. Valentine. Replacements for the arsine and phosphine in MOCVD processing / AlP conference proceedings – 2008 – Vol. 166, №1. P. 35-46.
24. S. Avasthi, S. Lee, Y. Loo and J. C. Sturm. Role of Majority and Minority Carrier Barriers Silicon/Organic Hybrid Heterojunction Solar Cells / Adv. Mater – 2011 – Vol. 23. - P. 5762-5766.
25. W. Wang, E. A. Schiff. Polyaniline on crystalline silicon heterojunction solar cells / Appl. Phys. Lett – 2007 – Vol. 91, №13 - 133504.
26. J. J. M. Halls, K. Pichler, R. H. Friend, S. C. Moratti and A. B. Holmes. Exciton diffusion and dissociation in poly(p-phenylenevinylene)/C60 heterojunction photovoltaic cell / Appl. Phys. Lett – 1996 – Vol. 68, №22 - 3120.
27. J. J. M. Halls, K. Pichler, R. H. Friend, S. C. Moratti and A. B. Holmes. Efficient photodiodes from interpenetrating polymer networks / Nature – 1995 – Vol. 376 – P. 498-500.
28. Jeong, Sangmoo Wang, et al. Hybrid Silicon Nanocone-Polymer Solar Cells / Nano Letters – 2012 – Vol. 12, №6 – P. 2971-2976.
29. Zeiss SteREO Discovery v 12: website URL: https://www.zeiss.com/microscopy/int/products/stereo-zoom-microscopes/stereo-discovery-v12.html
30. J. I. Goldstein et al. Scanning electron microscopy and X-Ray microanalysis / J. I. Goldstein et al. - M: Springer Science+Business, 2003 – 690 p.
31. Reflectance, transmittance and absorption: website. URL: https://spie.org/samples/PM229.pdf
32. Hassanien, Ahmed Saeed & Aly, K. & Akl, Alaa. Study of optical properties of thermally evaporated ZnSe thin films annealed at different pulsed laser powers / Journal of Alloys and Compounds – 2016 – Vol. 685 – P. 733-742.

33. Klugmann-Radziemska, E., Ostrowski, P. Chemical treatment of crystalline silicon solar cells as a method of recovering pure silicon from photovoltaic modules / Renew. Energ. – 2016 – Vol. 35 – P. 1751–1759.

APPENDIX

Appendix A

The evolution of organic film depending on the deposition time and composition

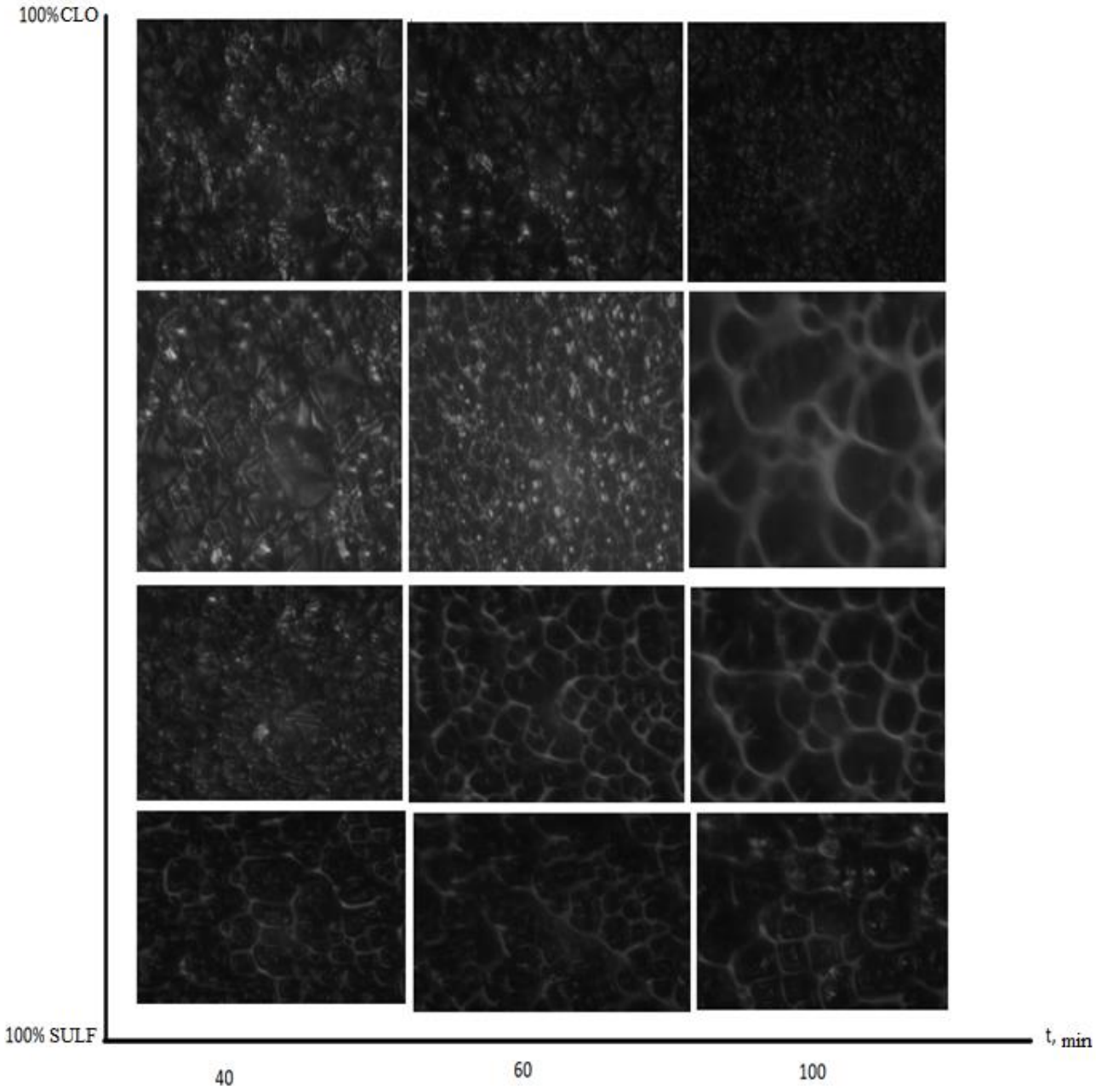

Appendix B

The evolution of the J-V curves depending on the deposition time and composition of the organic film

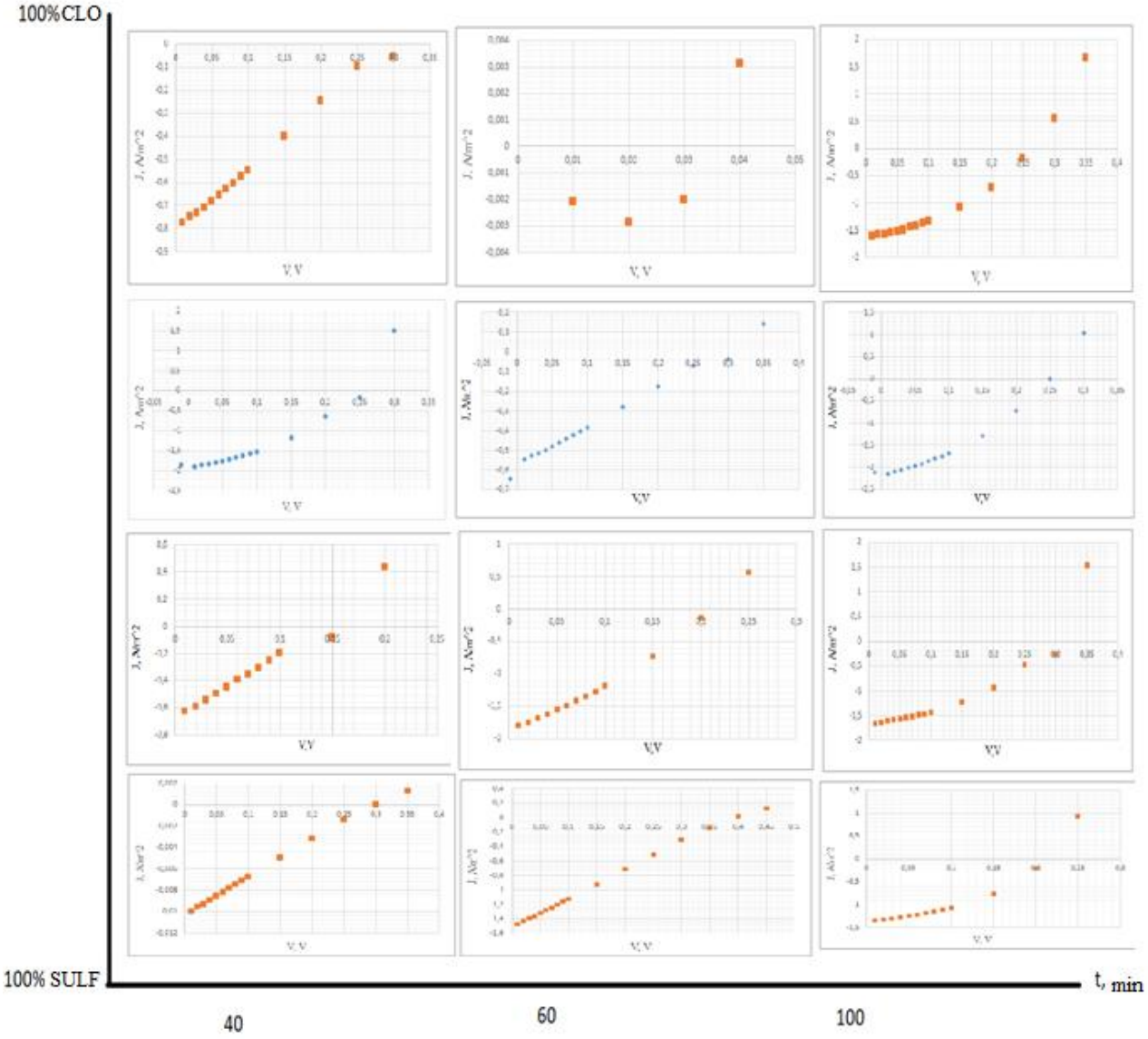

Appendix C

Table of device performances

Parameter/Sample	Clonidine			Sulfacyl			3 CLO/1 SULF			1 CLO/3 SULF		
Depos. time, min	40	60	100	40	60	100	40	60	100	40	60	100
Isc, μA	-	28	137	0,91	17	85	72,3	28	123,2	46	80	106
Voc, V	-	0,30	0,27	0,30	0,38	0,21	0,26	0,30	0,25	0,26	0,21	0,31
FF	-	0,26	0,40	0,25	0,25	0,49	0,36	0,26	0,36	0,15	0,31	0,38
Jsc, A/m^2	-	0,46	1,61	0,01	1,49	1,34	1,89	0,55	2,14	0,64	1,82	1,64
PCE, %	-	0,12	0,56	0,00	0,48	0,46	0,58	0,14	0,64	0,08	0,40	0,65